Master's thesis

NTNU
Norwegian University of Science and Technology
Faculty of Engineering
Department of Civil and Environmental Engineering

Isolde Louise Grønlund Syversen

Deformation properties of hard rock TBM spoil

Large scale oedometer tests on TBM spoil and crushed rock

Master's thesis in Geotechnics and Geohazards
Supervisor: Gustav Grimstad
Co-supervisor: Gunvor Baardvik and Jenny Langford
June 2021

NTNU
Norwegian University of
Science and Technology

Isolde Louise Grønlund Syversen

Deformation properties of hard rock TBM spoil

Large scale oedometer tests on TBM spoil and crushed rock

Master's thesis in Geotechnics and Geohazards
Supervisor: Gustav Grimstad
Co-supervisor: Gunvor Baardvik and Jenny Langford
June 2021

Norwegian University of Science and Technology
Faculty of Engineering
Department of Civil and Environmental Engineering

NTNU
Norwegian University of
Science and Technology

Abstract

Tunnel excavation with tunnel boring machines (TBM) in Norway started in the early 1970s, mostly linked to hydropower tunnels. Since then, over 250 tunnels have been excavated in Norway with TBM. For political reasons the number of hydropower projects were reduced in the late 20th century. Following the number of TBM project were also reduced for a couple of decades, but since 2010 the use of TBM as an excavation method for tunnel excavation increased again. Mostly linked to hydropower projects as Røssåga, railway tunnels as the Ulriken Tunnel and the Follo Line project. Lately the New Water Supply project in Oslo also announced that two of their tunnels will be excavated by three TBMs.

Tunnels are often the solution for urban infrastructure projects with no available space for such constructions on the ground. Thus, the need for utilisation of tunnel spoil is increasing for both environmental and logistic reasons. The European Commission's Circular Economy Action Plan involves legislative proposals on waste, where the long-term aim is to reduce landfilling and increase utilisation of tunnel spoil. In addition, glaciofluvial aggregates for concrete production and backfill material are an unrenewable resource and the gravel- and sand pits near urban areas are experiencing shortage. Oslo, among other cities are no longer able to meet the need of aggregates for construction sites, leading to extended transport and costs.

On the other hand, tunnel excavation generates large quantities of excess spoil, independent of excavation method. The utilisation of tunnel spoil will influence the environmental impact and the economy of the project. The projects in the 20th century were mostly located in rural areas, where the spoil was transported to stockpiles near the construction site, instead of further utilisation. Optimalisation of spoil handling is dependent on extended knowledge of the geotechnical properties of the material. The challenge with utilisation of TBM spoil is linked to the unfavourable grain shape and grain size distribution of the material. However, projects as the Ulriken Tunnel and the Follo Line project have utilised the material with success.

The aim of this thesis is to study the geotechnical properties of hard rock TBM spoil with emphasis on its stiffness properties. Previous investigations have been studied and new laboratory investigations, such as a large scale oedometer test have been conducted. A total of seven incrementally loaded (IL) oedometer tests have been executed, where four of the tests were conducted on TBM spoil and three on crushed rock. The crushed rock is sieved and compiled with a grain size distribution with a maximum grain size comparable to the tested TBM spoil.

The TBM spoil is found to be a well graded material. It is water sensitive and frost susceptible, but do not have enough capillarity for ice lenses to form. The water content of the material is between 5.5 – 6.7 %, where the dry density at the end of the tests variates from 1.93 – 1.96 t/m^3 with a porosity of 26.8 – 28.2 %. The oedometer modulus for the material variated between 9.04 – 9.40 MPa, where the test duration varied from 3.5 – 75 hours. If a 30 metres fill was to be constructed with the material and, a load of 50 kPa was applied at the top of the fill, the results indicates that the fill would settle 22 cm.

Abstract

The TBM spoil produced from hard rock conditions could be utilised with fractionation of coarse gravel for the frost protection layer in a road construction, for construction fills or capping of contaminated sediments on the seabed. Further utilisation could be achieved by crushing the material and/or combining it with other aggregates. Under these preconditions the material could be utilised as concrete aggregates, "pea gravel" for backfilling and in quality construction fills. Previous experience demonstrates that if the spoil characteristics is considered and accounted for, suitable applications can be found, and the material can be utilized. This applies to a range of different applications.

Sammendrag

Bruken av tunnelborremaskiner (TBM) i Norge startet på tidlig 1970-tallet, hovedsakelig knyttet til vannkraftverk. I ettertid har det blitt gravd ut over 250 tunneler i Norge med TBM, store deler knyttet til satsningen på vannkraftverk på 80-tallet. Siden har bruken av TBM blitt redusert, som følge av politiske og miljømessige årsaker. Etter 2010 har bruken av utgravingsmetoden økt, med store prosjekter som vannkraftverkprosjekter som Røssåga, jernbanetunneler som Ulriken tunnelen og Follobaneprosjektet. Nylig har Ny Vannforsyning Oslo prosjektet kunngjort at to av deres tunneler skal utføres med tre TBMer.

Tunneler kan være løsningen for prosjekter lokalisert i urbane strøk med knapphet til arealer over bakkenivå. Behovet for utnyttelsen av overskuddsmasser øker som følge av miljø- og samfunnsmessige årsaker. EUs handlingsplan for en sirkulær økonomi involverer lovgivende forslag om avfall, hvor langtidsmålet er å redusere landfyllinger og øke gjenbruket av masser. Glasifluviale tilslagsmaterialer er en ikkefornybarressurs, der grus- og sandtak nær store byer er i ferd med å tømmes. Hvor blant annet Oslo ikke lenger klarer å imøtekomme behovet for tilslagsmaterialet til byggeprosjekter, noe som fører til økt transport og kostnader. Utgraving av tunneler genererer store mengder med overskuddsmasser, uavhengig av drivemetode.

Utnyttelsen av tunnelmassene påvirker miljøbelastningen og økonomien til et prosjekt. Prosjektene i det forrige århundret var plassert langt fra bebyggelse, hvor overskuddsmassene ble transportert til lagringsplasser nær anleggsplassen og ikke utnyttet ytterligere. Kunnskapen om de geotekniske egenskapene er avgjørende for videre optimalisering av massehåndteringen. Der materialets kornform og kornstørrelsesfordeling fører til utfordringer for videre utnyttelse. Prosjekter som Ulriken tunnelen og Follobaneprosjektet har likevel positive erfaringer med å utnytte overskuddsmassene.

Hensikten med denne masteroppgaven er å undersøke de geotekniske egenskapene til TBM kaks produsert fra norske tunnelprosjekt, med fokus på materialets stivhet. Dette ved å undersøke erfaringer fra tidligere prosjekter og ved å gjennomføre laboratorieundersøkelser, blant annet med et stor skala ødometer. Totalt syv ødometerforsøk med trinnvis belastning (IL) har blitt gjennomført, hvorav fire på TBM kaks og tre på knust stein. Den knuste steinen er skalert til å simulere kornstørrelsesfordelingen til et materiale produsert med boring og sprenging fra liknende geologiske forhold.

Resultatene viser at TBM kaksen er et velgradert materiale som er vannømfintlig og lettere telefarlig, men har ikke nok kapillært sug til å danne islinser. Vanninnholdet i det testede materialet er mellom 5,5 – 6,7 %, hvor tørrdensiteten etter endt forsøk varierer mellom 1,93 – 1,96 t/m^3 med en porøsitet mellom 26,8 – 28,2 %. Ødometer modulusen til TBM kaksen varierer mellom 9,04 – 9,40 MPa, der testenes lenge er mellom 3,5 – 75 timer. Resultatene indikerer at hvis en 30 meter tykk fylling bestående av TBM kaks blir pålastet 50 kPa, vil fyllingen oppnå ca. 22 cm setninger.

TBM kaks fra norske forhold kan utnyttes til en rekke formål. Hvis de største steinene i TBM kaksen blir fjernet, kan materialet bli utnyttet i frostsikringslaget i en

veikonstruksjon, i kvalitetsfyllinger og fyllinger på sjøbunnen. Ytterlige bruksområder kan muliggjøres ved at materialet knuses og/eller tilsettes andre tilslagsmaterialer. Da kan materialet benyttes som tilslag i betong, tilbakefyllingsmateriale i ringspalten og i jernbanekonstruksjonen. Hvis viderebehandling av TBM kaksen er tilpasset de geotekniske og kjemiske egenskapene, viser tidligere erfaringer at materialet kan utnyttes med gode resultater for ulik bruk. Utnyttelsen av materialet har gitt dårlige resultater når egenskapene til den rå TBM kaksen ikke har blitt undersøkt, og materialet har blitt utnyttet uten hensyn og modifikasjoner.

Sammendrag

Preface

This thesis is the final project of my master's degree at the study programme MSc in Geotechnics and Geohazards at the Department of Civil and Environmental Engineering, at the Norwegian University of Science and Technology (NTNU) in Trondheim. The project was proposed by the Norwegian Geotechnical Institute (NGI), where reports and data have been provided from NGI, VAV-Oslo and Bane NOR. The thesis constitutes a workload of 30 SP credits.

The aim of the thesis is to increase the knowledge of the geotechnical properties of spoil produced by a tunnel boring machine (TBM) to both optimise and increase the utilisation of the material. The TBM spoil which has been studied has been excavated by four TBMs linked to the Follo Line Project, located at Åsland south of Oslo. Further laboratory investigation reports referred to in this project is linked to the project New Water Supply Oslo. A specialisation project was accomplished as a preliminary work for this thesis autumn 2020, where some of the work is included.

I am forever grateful for all the help my supervisors at NGI, Jenny Langford and Gunvor Baardvik, have provided the last year. It has been delightful to work with such engagement and expertise, thank you! I would also like to thank Espen Andersen and Karl Ivar Kvisvik at the Geotechnical Laboratory at NTNU for all the help with Anton, as well as my supervisor Gustav Grimstad from the geotechnical division at NTNU. A thank to Marianne Dahl for shearing knowledge about Anton and data from her thesis in 2018. And to my sister, Fredrikke S. G. Syversen, for the encouragement through the years.

A huge thank to Franzefoss, KSR-Maskin and Bane NOR for the supply of test material to the laboratory investigations.

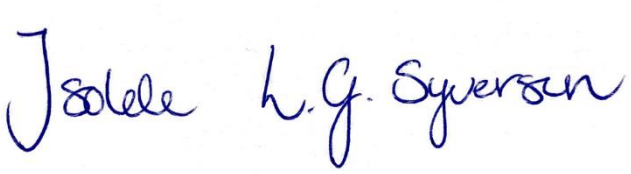

Isolde Louise Grønlund Syversen

Trondheim 08.06.2021

Preface

Table of Content

Figures

Figures

Figures

Figures

Tables

Symbols

a	Attraction	[kPa]
a	Stress exponent	[-]
dε	Change in strain	[%]
dσ′	Change in effective stress	[kPa]
H	Height	[mm]
h_0	Initial height	[mm]
h_s	Height of sample	[m]
m	Modulus number	[-]
M	Oedometer modulus	[kPa]
M	Oedometer modulus	[kPa]
m	Weight of sample	[kg]
m_s	Weight of dry sample	[kg]
n	Number of the current load step	[-]
n	Porosity	[%]
r	Oedometer radius	[m]
R	Time resistance	[-]
r_s	Time resistance number	[-]
V	Volume of sample	[m^3]
V_p	Volume of pores	[m^3]
w	Water content	[%]
δ	Deformation	[mm]
δ_n	Deformation at end of load step	[m]
Δσ′	Change in effective stress	[-]
ε	Strain	[%]
σ'_0	Effective stress	[kPa]
σ'_n	Effective normal stress	[kPa]
σ_a	Reference stress	[kPa]
τ_f	Shear stress	[kPa]
φ	Friction angle	[°]
ρ	Density	[kg/m^3]
ρ_d	Dry density	[kg/m^3]
ρ_s	Density of the grains	[kg/m^3]

Symbols

CR	Crushed rock
D&B	Drill and blast
ISSMGE	International Society for Soil Mechanics and Geotechnical Engineering
ITA	International Tunnelling and Underground Space Association
NFF	The Norwegian Tunnelling Society
NGI	Norwegian Geotechnical Institute
NGU	Geological Survey of Norway
NNRA	Norwegian National Rail Administration
NRPA	Norwegian Public Roads Administration
TBM	Tunnel boring machine

1 Introduction

1.1 Background

The European Commission's Circular Economy Action Plan involves legislative proposals on waste, where the long-term aim is to reduce landfilling and increase utilisation. The Action Plan's goal is to achieve 70 % utilisation of waste materials in buildings and construction projects in Europe. A society with an additional circular economy is beneficial for lowering energy consumption and carbon dioxide emission levels (European Commission, 2017).

Increasing excess of excavation materials from tunnelling projects is a great challenge that must be handled. Landfills and deposit areas are increasing, at the same time as the available areas for this purpose is decreasing. Consequently, new solutions are essential to handle this issue, by reduce landfills, increase recycling and utilisation of material (Glosli, 2020).

Tunnel excavation generates large quantities of excess spoil, independent of excavation method. In the period between 2015 – 2020 an average of approximately 6 million m^3 tunnel spoil was produced each year in Norway (NFF, 2021). The utilisation of spoil will influence the environmental impact and the economy of the project. The geotechnical properties of TBM spoil are dependent on the geology, cutter spacing and machine operation. Thus, challenges in utilisation of the material are linked to unfavourable grain size distribution, grain shape and geology. However, it shall be emphasised that unfavourable geological conditions will result in challenges related to the spoil properties, regardless of the excavation methods.

To be able to utilise a material, it is necessary to investigate its geotechnical and chemical properties. This to be able to evaluate the range of applications, since some application areas demands specific properties and handling. Lack of preliminary investigations might result in unfavourable utilisation. The material might show unexpected behaviour e.g., contamination of gasses, weathering and decreasing strength over time or poor compaction. Extended knowledge of the geotechnical properties of the material facilitates optimised handling in terms of grading, compaction etc.

The focus on utilisation of TBM spoil has increased because of both increased sustainability focus and extended use of TBM as excavation method in urban areas. Large TBM projects executed in urban areas result in more challenges regarding spoil handling than the hydropower projects executed by Statkraft in Norway during the 1980s. In these projects the spoil was transported to stockpiles close to the construction site, and not utilised much further. A reason for this can be linked to the cost of transportation and no limitation for the use of space.

In addition, most of the projects were excavated in micaceous rocks. These geological conditions are not favourable to construction fills. Several laboratory investigations were conducted for the material from dam projects and compared in reports by NGI and NTNU.

Since then, TBMs have had limited use in Norway compared to the number of tunnel projects in total. The number of hydropower projects were reduced in the late 20th century, due to political and environmental reasons. TBMs are efficient for such projects since the tunnels are long with small cross-sectional area and the TBM-tunnel walls should have low friction. Conventional drill and blast are unfavourable for such conditions, because of the impassable terrain, cross cuts and the need for temporary road for construction purposes. The tunnel walls will have a less smooth surface, more friction and loss of hydro power energy.

Although, the previous ten years the use of TBM has increased with large projects like the Ulriken Tunnel, The Follo Line project and the upcoming New Water Supply project in Oslo. The environmental impact and the financial cost of these projects are dependent of the utilisation of the TBM spoil, since such projects produce large amounts of material. For these projects the geological conditions are favourable for further utilisation of the produced spoil, since the TBMs have excavated in hard rock conditions. The knowledge of the geotechnical properties for the TBM spoil is decisive for the further utilisation of the material.

1.2 Problem formulation

This thesis is a research study on the geotechnical properties of hard rock TBM spoil. The thesis will focus especially on the stiffness properties of the TBM spoil. This is achieved by laboratory investigations consisting of seven oedometer tests, four tests on TBM spoil from the Follo Line Project and three on crushed rock from similar geological conditions. The crushed rock is of the same bedrock type (granitic gneiss) as the investigates TBM-spoil from the Follo line. The maximum grain size of the crushed rock used in the laboratory tests is chosen similarly to the maximum grain size of the TBM spoil.

1.3 Objective

The objective of this master thesis is to investigate TBM spoil's geotechnical properties with an emphasis on its stiffness parameters. The overall goal is to achieve consistent laboratory results, in a such way that further utilisation of the material can be optimised. In addition, the results from the tests on TBM spoil are compared to the results from the tests on crushed rock, to compare the stiffness properties of the two materials.

Marianne Dahl accomplished several giant oedometer tests on TBM spoil for her master thesis in 2018 (Dahl, 2018). Her recommendations for further work were to test scaled spoil and to investigate the effect of higher loads and long-time increments to study the creep effect. This is considered and included in the thesis.

1.4 Limitations

The geotechnical properties of TBM spoil are influenced by the geological conditions along the tunnel alignment, as well as the TBM operation. This thesis will focus on spoil produced from hard rock conditions, since this reflects the Norwegian rock conditions. The geological aspects will be further discussed.

1.5 Approach

The approach of this study is to present relevant literature regarding the topic, and then compare the findings from the literature to the results from laboratory investigations. The relevant literature is from different time periods and countries, but primarily from publications related to Norwegian conditions. Several figures included in the study are translated to English and some of them are modified. Those figures are marked with "translated" and/or "modified".

The literature collocated are from project reports, journal paper and scientific papers. Some of the main papers used in the literature survey are dated to the 20st century. The results from thee papers are compared with the results from projects accomplishes in the 80s. Publications compiling experience from different TBM projects during the 21st century are also included.

Chapter 1.1, 2.1, 2.2 and some text from 2.3 is from the report for TBA4510 Geotechnical Engineering, specialisation project, dated 19.12.2020 (Syversen, 2020), with some modification of the text. The specialisation project was preliminary work for this study, some laboratory investigations were conducted, and one of the oedometer tests is included in appendix A.1. The project thesis is not openly published but is attached as a digital appendix.

1.6 Structure of the report

A total of five chapters are included in this thesis. Chapter 1 is included to explain the basis of the study. Chapter 2 is a literature survey and a summary of relevant publications regarding the topic of this study. The principles of a TBM, geotechnical properties of the TBM spoil and previous spoil utilisation are included. In addition, a chapter regarding the drill and blast method and some index properties of blasted rock is included to compare the two types of materials. Chapter 3 includes the methodology of the laboratory investigations (oedometer tests, sieving analysis and water content samples), a description of the material tested and the test results. Chapter 4 contains discussion of the geotechnical properties introduced in chapter 2 and further evaluation of material properties. Chapter 5 summarises and conclude upon the study presented.

2 Literature survey and theory

2.1 The principles of a tunnel boring machine

The method for full face tunnel boring was established in 1850, but it was not until in the middle of the 20th century that a TBM for harder rock conditions was developed by James S. Robbins in USA. The use of TBM in Norway started in the early 1970s with excavation of hydro plant tunnels. Over 250 tunnels have been excavated with TBM in Norway, mostly linked to the hydropower tunnels excavated in the 80s (Hansen *et al.*, 1998). The use of TBM as excavation method has increased since 2010. The increase is linked to more amounts of hydropower projects as Røssåga and railway tunnels as the Ulriken Tunnel and the Follo Line project. Lately the New Water Supply project in Oslo also announced that two of their tunnels will be excavated by three TBMs.

A TBM is utilised to excavate a complete and tight tunnel with circular cross section (Nilsen and Tidemann, 1993). The machine is moving forward contemporary as the cutter head is rotating, forcing the cutter discs to penetrate and break the rock. The trust force is achieved by hydraulic cylinders behind the cutter head. The excavated rock is collected by buckets on the head, slid down inside the cutter head and transported backwards on a conveyor, see Figure 2.1. Shielded TBMs can install a concrete segmental lining continuously as the TBM excavates. As long as the machine is tailormade for the geological conditions it can excavate in bedrock ranging from hard to soft rock and even in soil. TBMs are generally used for excavating tunnels longer than 5 km (Macias and Bruland, 2014). There are different types of TBM that are used for various rock conditions.

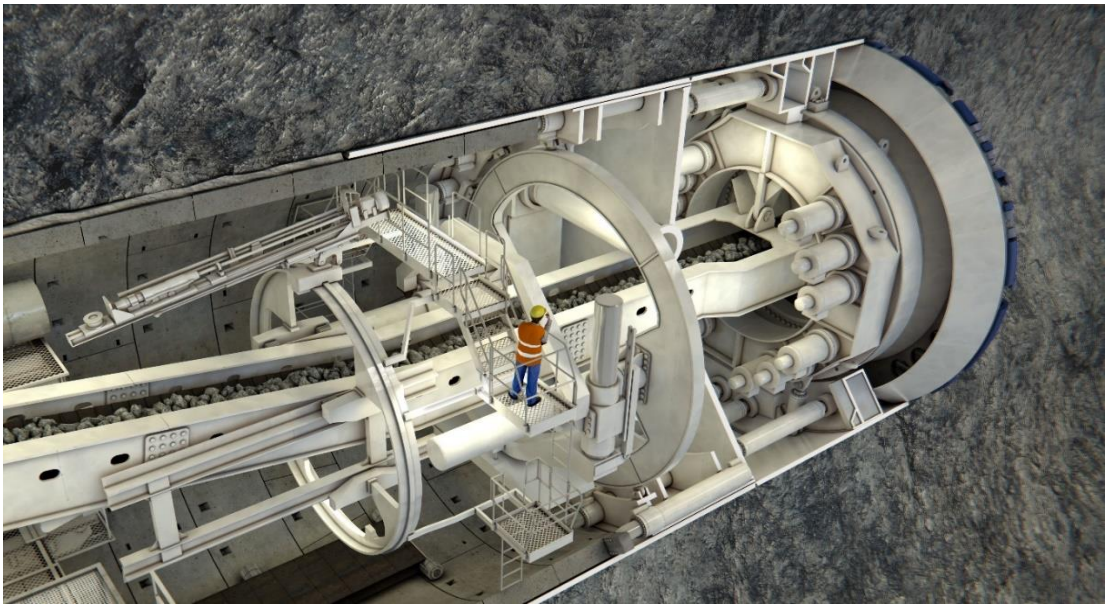

Figure 2.1 TBM principle, cutter head showed from behind (AGJV, 2020)

Pre-grouting can be applied ahead of the tunnel to ensure maintenance of the pore pressure above the tunnel. In hard rock conditions the pre-grouting is also applied to increase control of water inflow and reduce the impact of the groundwater lowering on surrounding areas. Pre-grouting is applied by drilling of grouting holes followed by injection of grout material by use of high pressures until the termination criteria is reached (Nilsen and Tidemann, 1993).

The principle of the mechanical breaking elements of hard rock is shown in Figure 2.2. The cutter discs penetrate a small distance into the rock face due to the high thrust. The penetrating depth varies from 1 mm and up to 15 mm per cutterhead revolution. Penetration depths depends on the rock character and irregularities caused by inhomogeneity and discontinuity. The high thrust cause spalling and chipping of rock flakes in front of the cutter head, as shown in Figure 2.2. The chipping is caused by tensile stresses which are induced perpendicular to the free face (Bruland and Johannesen, 1991).

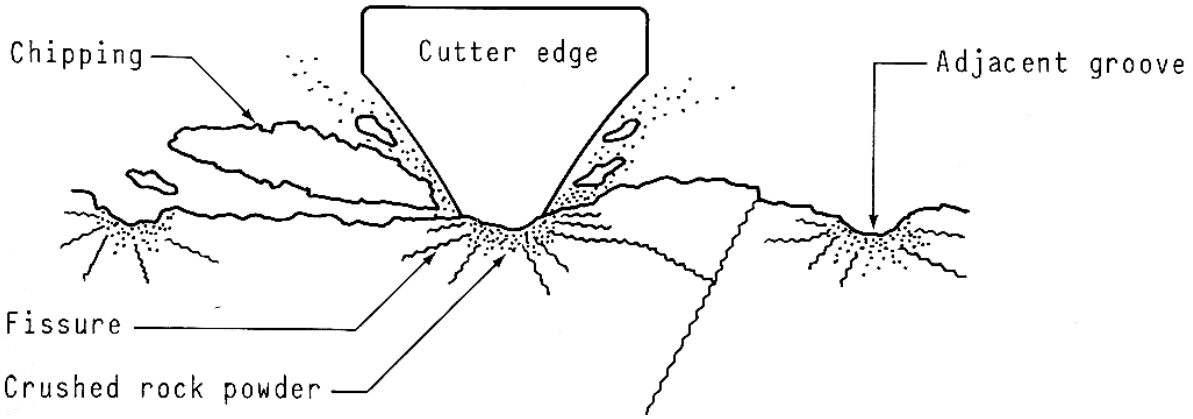

Figure 2.2 The chipping mechanism (Bruland and Johannesen, 1991)

The performance of the boring depends on multiple factors. The factors can be classified into three groups: rock, rock mass and TBM. The properties of the rock that is excavated is influencing the penetration, abrasion and spoil composition. These properties consist of the rock type, mineral composition, rock strength, compression and shear. The rock mass texture, like bedding and clearage to boring axis, jointing and presence of formation water, are influencing the penetration, abrasion and spoil grading. While the TBM's design affect the penetration, stability of the tunnel and chip size (Maidl *et al.*, 2008).

2.1.1 Environmental impact

There are multiple environmental advantages with excavating with TBM compared to controversial drill and blast method. According to Macias and Bruland the average advance rate is in most cases higher for a TBM than for the drill and blast method. The exact ratio would be defined by the local conditions but could vary between one to six times faster. The advance rate for a TBM is among other things dependent on rock quality, machine operation and need for pregrouting. Use of TBM will also reduce the impact and exposure for residents or citizens near the tunnel alignment, due to higher progress, less vibration and lower vibrational noise than conventional drill and blast (Macias and Bruland, 2014).

When a tunnel is excavated with a TBM, the environmental impact of the project could be reduced, since the TBM is driven by electricity. The excavated material is normally transported by a conveyor belt from the head and to the construction site. Thus, reducing the need of fuel driven machines inside the tunnel (Dahlstrøm *et al.*, 2014). Since the TBM is using thrust force and cutters to excavate the tunnel, the TBM spoil will not contain any residues from explosives and other material, such as plastic. The material will contain heavy metals connected to the mineralogical composition in the rock that is excavated, but this is a result of the natural quantity (Ofstad *et al.*, 2018).

One of the factors that has a major influence of a project's environmental impact when using a TBM, is how the excavated material (TBM spoil) is utilised. The impact will be of a greater value if the excavated material must be transported a longer distance to be utilised. The most favourable would be to utilise the spoil locally, or as close to the construction site as possible. In a project it is vital that the utilisation of the spoil is considered early in the planning phase. This allows the project to both schedule temporary storage of the material and to investigate if the project can utilise the material or sell it (Dahlstrøm *et al.*, 2014).

2.2 Geotechnical properties of TBM spoil

In the early 90s, Bruland and Johannesen composed a report linked to a project series discussing D&B and TBM tunnelling. The report concluded that geotechnical properties of TBM spoil are dependent on the geology of rock that is excavated as well as the TBM. The rock parameters that have the largest influence, are the brittleness number, flakiness, compressive strength, hardness, mineral composition, and the jointing of the rock. The principal TBM parameters are the thrust force, cutter distance, cutter diameter, cutter type, water flushing and the buckets collecting the material at the face (Bruland and Johannesen, 1991).

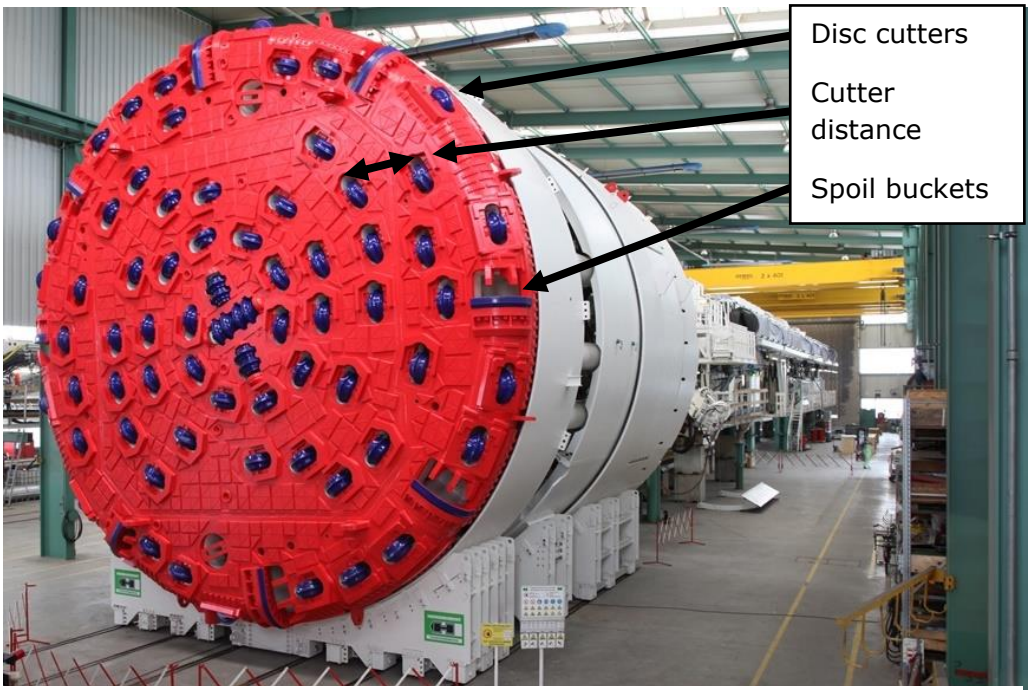

Figure 2.3 The TBM head (Herrenknecht, 2016) (Modified)

Very brittle rocks have more fissures and scaling around the cutters. The spoil produced in these conditions are not suitable for further crushing and are more challenging to utilise. Rocks with low to average brittleness generate thicker and more concave spoil, which are more suited for utilisation. Spoil produced from such rock is more favourable to crush for further use (Bruland and Johannesen, 1991).

Excavating in hard rock without sufficient thrust force will produce thin and long chips. Softer rock conditions will produce relatively thick and rectangular spoil, but with a higher unit of fines. These rocks are weak, and the spoil will have limited applications. Excavating in jointed rock will be more favourable, since the spoil produced will have a cubic shape, and will be more functional (Bruland and Johannesen, 1991).

TBM parameters will also impact the properties of the spoil. The cutter size will impact the coarseness of the spoil and the cutter distance will determine the largest grain sizes. An increase of the thrust force will increase the penetration depth and lead to larger grains. Water flushing will impact the content of fines because the water will flush the fines and it will not be transported from the head. The water flushing will impact the quantity of fines more than the thrust force, pull, brittleness and drillability. The size of the buckets collecting

the spoil at the head of the TBM will affect the coarseness. Smaller buckets will reduce the coarseness since the capacity is smaller and coarser grains will fall downwards and shatter (Bruland and Johannesen, 1991).

2.2.1 Grain shape

When excavating with a TBM the thrust force from the cutter head will break the rock face to thin chips and crushed rock powder. The shape, the composition and characteristics of the cuttings depend upon the rock and TBM parameters. The grain shapes of the cuttings are more dependent on geological conditions. The largest grains are determined by the distance between the cutters on the TBM (Bruland and Johannesen, 1991).

In general, the larger cuttings are flakier and more elongated than the smaller fractions that are more cubic and lined. Especially when the rock is hard, the grain shape will be elongated and flaky. Softer rock will produce more fines and the spoil with grater size will be more rectangular and thicker (Bruland and Johannesen, 1991).

The shape of the TBM spoil is characterised as long and flaky, this is unfavourable for the material's mechanical qualities and compaction will be more challenging. Elongated and flaky grains have reduced resistance towards crushing and produces more fines when the material is compacted. A cubic shape is more favourable for the mechanical shape and compaction properties (ITA, 2019). An example of grain shape is shown in Figure 2.5 with sieved and washed material from the Follo Line Project. Where the elongation index variates between 2.5 to 4, and the flakiness index variates between 1.45 to 2.

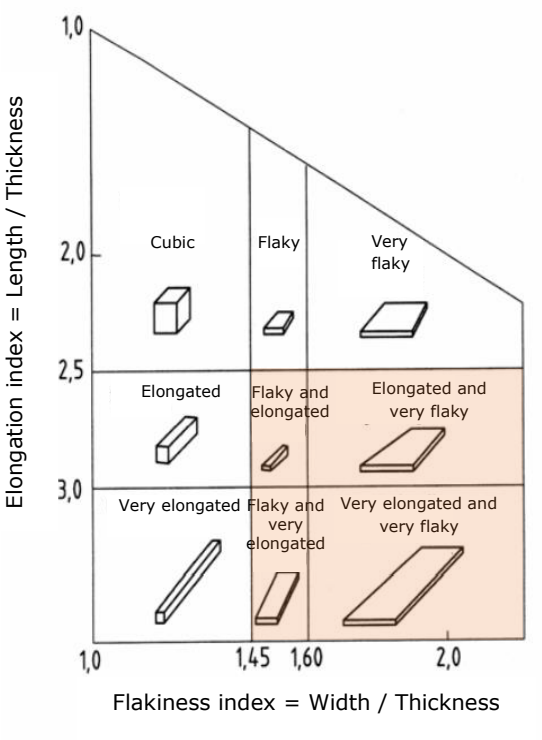

Figure 2.4 Grain shape conditions, relation between length and flakiness (NPRA, 2014) (translated)

Figure 2.5 Sieved and washed TBM spoil from the Follo Line Project (NGI, 2019a)

2.2.2 Grain size distribution

In 1986 NGI published a report containing investigations of 11 soil samples from 1985. The tests contained TBM spoil from different projects in Norway with different geological characteristics. The tests contained different types of rock, cross section area and TBM models, where the represented varieties of rock where schist, mica schist, granitic rock, greenstone, granodiorite, granitic gneiss, phyllite, hornblende schist, limestone and slate (NGI, 1986).

The grading curves for the different tests are uniform, with small differences dependent on the rock conditions. With exception of the tests containing phyllite and mica schist that had a higher content of fines. Beyond that, factors like the rock, rock conditions, cross section and TBM model, had minor impact on the grain size distribution. The variations in grading curves are shown in Figure 2.8 as dashed lines.

In master thesis completed in 2018, Marianne Dahl, investigated TBM spoil for the Follo line project located south of Oslo, and found similar grading curves for granitic gneiss, see Figure 2.8 (Dahl, 2018). Most of the grain size distribution curves completed are in the range of the tests completed by NGI in 1985. The average of the tests shows that the TBM spoil is characterised as a sandy, silty gravel, where 50 % to 70 % of the spoil is gravel. The content of fines, that are defined by the grain size smaller than 63 µm, varies between 10 % to 18 %. Coefficient of uniformity $C_u=d_{60}/d_{10} > 15$ for most of the test, the spoil is considered as a well graded material. This is ideal since the smaller fraction will fill the voids of the larger fractions, and the larger particles will create a stable structure, grain skeleton.

The Ulriken Tunnel, located in Bergen, was excavated in gneiss and limestone. The grading curve for the TBM spoil, Figure 2.7, shows similar distribution as the spoil from the Follo Line Project (COWI, 2015). The International Tunnelling and Underground Space Association (ITA) published a report in 2019, containing data from 59 projects, discussing handling, treatment and disposal of tunnel spoil (ITA, 2019). Figure 2.6 shows grain size distribution for different geological settings from this project. The grain size distributions from the different projects show similar behaviour, with small differences in the content of coarser fractions.

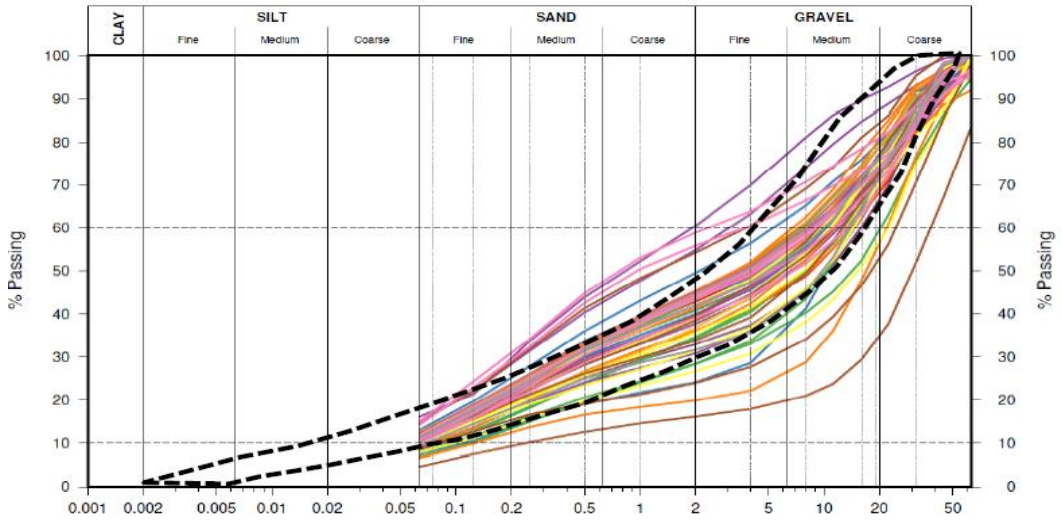

Figure 2.8 The coloured lines are distribution curves from the Follo Line Project, and the dashed lines are the range from the NGI tests from 1985 (Dahl, 2018)

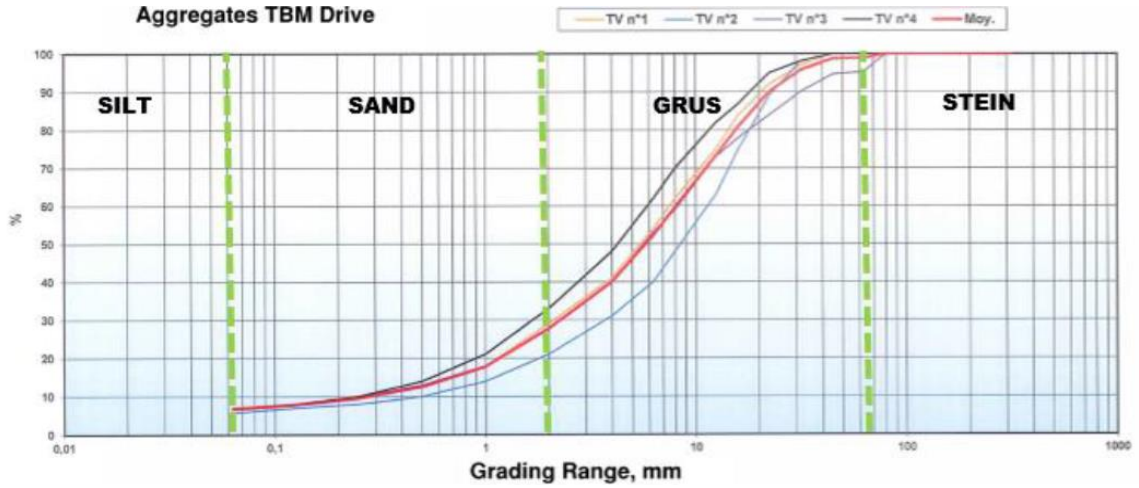

Figure 2.7 Grain size distribution for TBM spoil, Ulriken Tunnel (COWI, 2015)

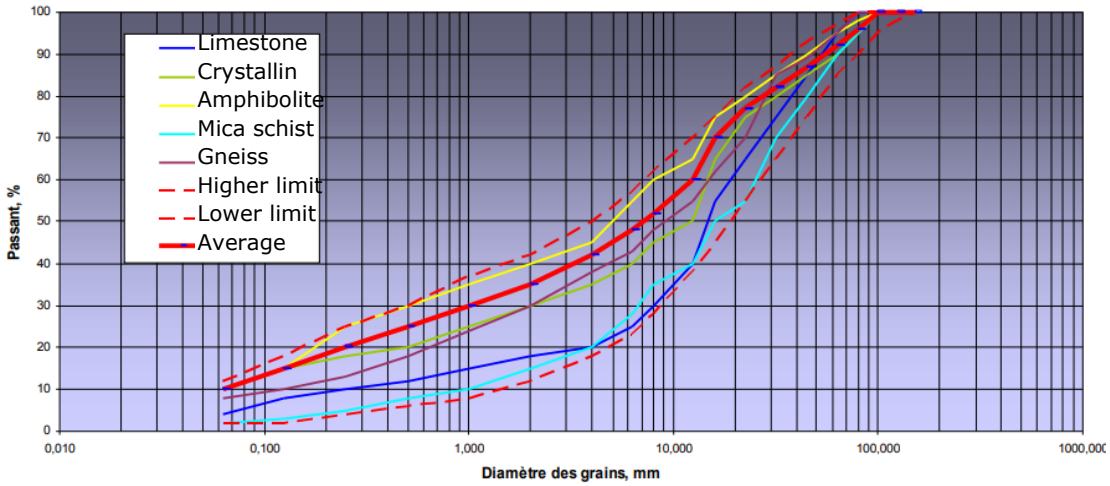

Figure 2.6 Grain size distribution curve for TBM tunnels in different rock conditions (ITA, 2019) (translated)

Gradation method

A challenge with coarse grained materials is attached to characterisation of the geotechnical properties. This due to that the equipment used are adjusted to finer materials, and that the essential size of an equipment investigating coarser materials is larger. There are several techniques for scaling a material sample, but there is no standard on coarse grained materials composed. Several size-scaling techniques are available, where all have their advantages and disadvantages (Dorador and Villalobos, 2020).

The parallel gradation method is the technique utilised in this thesis to investigate the TBM spoil in a giant oedometer. The principle of the method is to scale the grain size distribution for the coarser particles to smaller particles using the same scale ratio for its distribution. Dorador and Villalobos collocated six recommendations for utilisation of the method, where further discussion and arguments for these can be found in their publication (Dorador and Villalobos, 2020):

1. Adopt a maximum of 10 % fines in model graduation samples.
2. Keep parallelism between original and model gradations.
3. Keep similar minimum and maximum density from original to model gradations.
4. Maintain particle shape between original and parallel grain size distribution.
5. Maintain mineralogy and compressive strength on particles.
6. Balance for mixture of particles of different strength on coarse granular materials.

2.2.3 Water sensitivity and frost susceptibility

The water sensitivity and frost susceptibility are vital because of the risk of frost heaving and are dominated by the telemechanism. The telemechanism of a soil body is described by the interaction between capillary water and ice formation. In all soil types there will be absorptive water bound to the soil particles, as well as free water and capillary water in the pores. The free water will freeze first, and then capillary forces will force the water to the crystallised ice when the freezing zone moves downwards in the soil body. The surface tension between the water and the ice will generate a pore suction, in the same way the surface tension between water and air makes a capillary suction in a pore system. This will lead to suction of water from the ground water and ice lenses will form. The properties of the soil, especially the grain size distribution, and distance to the ground water level is decisive for the formation of ice lenses (Aksnes et al., 2016).

The water sensitivity of a material describes the material's ability to maintain bearing capacity when the water content increases. This will mainly be determined by the content of fines in the material. The water content in a material is dependent on different factors, like the type and amount of fines, supply of water from the surface and from the groundwater, as well as the capillary water over the ground water level. A water sensitive material has more than 7 % content of fines smaller than 63 µm (Aksnes et al., 2016).

A material can be water sensitive and not frost susceptible. A material's frost susceptibility describes a material's water suction ability and ability to form ice lenses when freezing. A frost susceptible material will contain more than 3 % of fines smaller than 20 µm. The volume of the frost heaving in a soil body will mainly be determined by the access of water and the content of fines. Ice lenses will only form in the freezing zone if the material is

capable of transporting the water from the groundwater level. If the distance is significant or the permeability and capillary forces in the material to small, the water will not reach the freezing zone (Aksnes et al., 2016).

Problems with frost are dependent on three presumptions: frost, frost susceptible soil and water. When one of these presumptions are removed, the frost problems are reduced. Problems with freezing and melting are mainly connected to the frost depth in the material. The depth of the freezing zone varies with the material and the mean temperature for the specific place. The freeing zone will be terminated by the upper meters in a soil layer. Factors like number of frost days, frost process, the layering in the soil and water access must be considered to determine the frost susceptibility for a soil. The formation of ice lenses is mostly dependent on the capillarity forces in the soil, and the access to free water. This because the water that forms the ice lenses must be transported from underneath the freezing zone, because the free water over this point is frozen and cannot move in the soil body (NRPA, 2018).

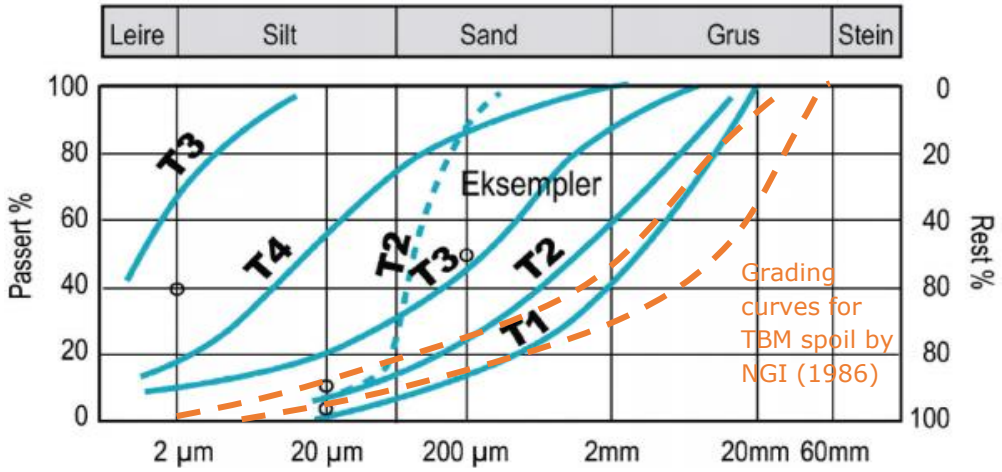

Figure 2.9 Examples of frost susceptibility classification by NPRA (NPRA, 2010) (Modified)

Table 2.1 Frost susceptible classification (NPRA, 2010) (translated)

Frost susceptible group		Material < 22.4 mm		
		Content - %		
		< 2 µm	< 20 µm	< 200 µm
Not frost susceptible	**T1**		< 3	
Little frost susceptible	**T2**		3 – 12	
Medium frost susceptible	**T3**	[1)]	> 12	< 50
Very frost susceptible	**T4**	< 40	> 12	> 50

1) Materials with a content of more than 40 % < 2 µm is considered as medium frost susceptible.

NPRA's handbooks, Norwegian road standards, determines the frost susceptibility for a soil by the grain size distribution, see Table 2.1, this is a simplification and further considerations for the frost situation are needed. The classification exists of four classifications, T1 to T4, where soil classified as T1 is not frost susceptible, and T4 is very frost susceptible, see examples of grading curves and corresponding class in Figure 2.9.

According to this classification, the TBM spoil can be considered little to medium frost susceptible, appurtenant to frost susceptibility class T2 and T3 (NPRA, 2010).

A report published by the International Society for Soil Mechanics and Geotechnical Engineering (ISSMGE) determines the frost susceptibility of soils in two stages. Initially, the frost susceptibility of a material is linked to the soil properties, like capillary forces and content of fines. Then the frost susceptibility is linked to the on-site conditions (Slunga and Saarelainen, 2006). Primarily the properties of various soils are compared with respect to the frost susceptibility. Secondary the geological profile and boundary conditions on the frost heave in a soil layer in-situ are considered, this includes effects of freezing index, the groundwater depth, the stress state and other conditions.

Like the NPRA's handbooks, the ISSMGE recommends that the primary determination of the frost susceptibility is determined by the grain size distribution, but further on the ISSMFE are considering the structure's frost heave tolerance. If the structure tolerates frost heave to a certain extent and/or the work in question concerns big soil masses, primarily the grain size distribution can be considered, and the soil can be considered as frost susceptible or not. The classification recommended by ISSMFE is classified in four levels, see Figure 2.10, where the classification range from 1 to 4:

1. Grain size distributions in this range will always be considered as frost susceptible. In the area of 1L, the frost susceptibility is low.
2. If the grain size distribution falls into 2, 3 or 4, the soil is not frost susceptible.
3. If the grain size distribution curve permanently falls inside the boundary of the finer side, the soil is frost susceptible.
4. Further investigations need to be accomplished to determine the frost susceptibility of the material.

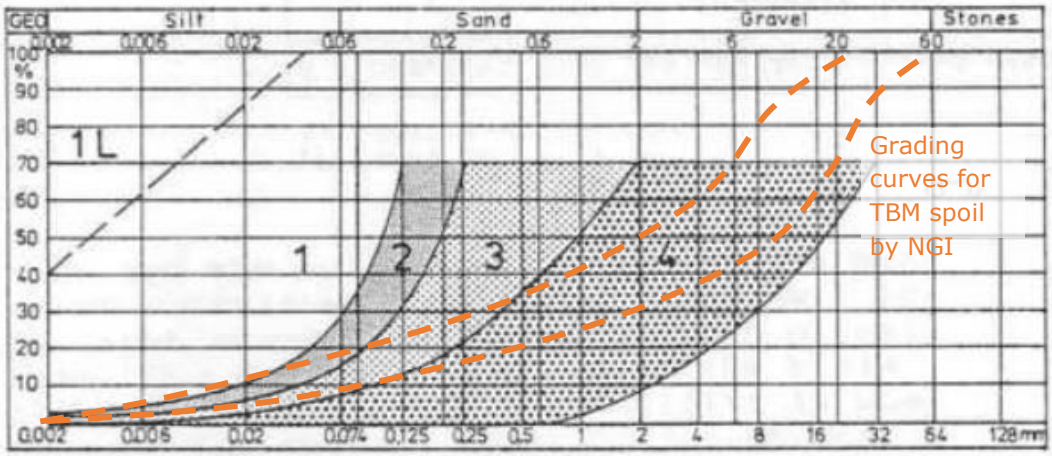

Figure 2.10 Determination of frost susceptibility of a soil based on the grain size distribution in Finland by ISSMFE (Slunga and Saarelainen, 2006) (modified)

When the soil is determined as criterion 4, and needs to be controlled further, the frost susceptibility can be determined by investigations or empirical data. Examples of the investigations can be considering the hight of capillary rise, the content of fines, potential of segregation and frost heave rate. The empirical data consist of frost heave model test for

the determination of segregation potential, or observations in field of the frost heaving, frost depth, temperature and the soil's water content (Slunga and Saarelainen, 2006).

According to the ISSMFE the TBM spoil will be classified as frost susceptibility and a material belonging to class 3, since the grading curve falls inside the boundary of the finer side. The formation of ice lenses will be dependent on the capillary suction in the material and the access of water. NGI carried out laboratory investigations on the material from the Follo Line project, where the freezing and thawing properties of the spoil was tested. NGI concluded that the TBM spoil tested was not frost susceptible, since the material did not have enough capillary suction to form ice lenses (Bane NOR, 2020).

2.2.4 Dry density and optimal water content

Optimal water content is the water content giving the maximum dry density when the material is compacted. The soil's water content has an important impact on the compaction of the material, and it is favourable to compact soil with a water content close to the optimal water content. A Proctor test can be carried out to estimate a relation between the dry unit weight and the optimal water content for a sample. This is done by compacting different samples of the same soil with various water content, then the soil samples are dried, and the dry density is calculated. The water content that result in the highest dry density, will be the optimal water content (NPRA, 2014).

The purpose of compacting a soil, is to increase the strength of the material, this is done by forcing out the trapped air voids in the soil, and therefore increase the unit weight and reduce the porosity. This will also decrease the settlement potential in the soil and reduce the permeability in the soil body, which is important for the further use of the compacted soil (Brown, 2015).

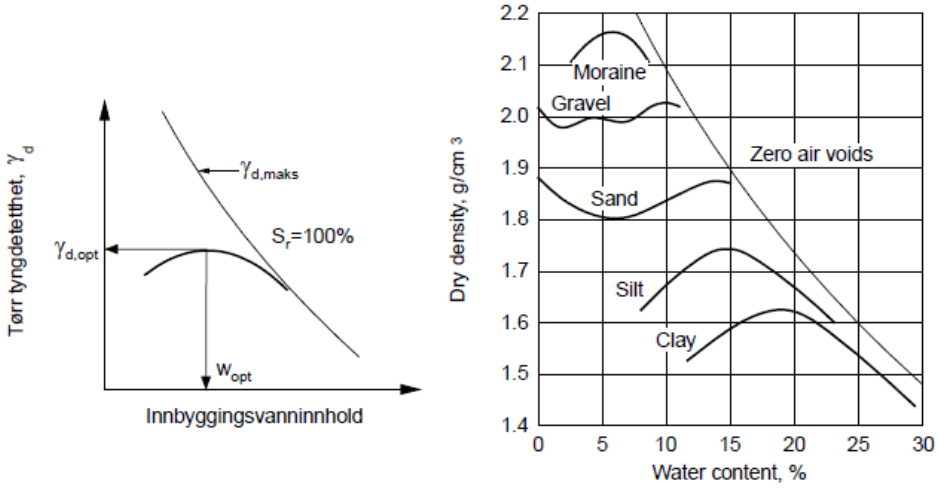

Figure 2.11 Laboratory curves for compaction of different materials (Janbu, 1970)

The reason the water content is relevant for the compaction of a soil, is because a certain water content the water will work as a lubricant and improve the compaction. If the soil is too dry, separate cohesive lumps or large grains can prevent the soil to break and fill voids. When the water content is increased, the soil will behave more plastic and the voids will be reduced during compaction, this will lead to a higher dry density. The dry density will

decrease for water content higher than the optimal water content since the water will saturate the pore volume and resist compaction. The grain size will also effect the level of compaction, and in a well graded material finer grains will fill the voids between the larger units, resulting in a higher density than in a one graded material (Kjærnsli, Valstad and Höeg, 1992).

Results from Standard Proctor test carried out for the Follo Line Project shows that the optimal water content for the TBM spoil ranges from 8 % to 10 %, and the dry density is equal to 2.15 t/m^3 (Dahl, 2018). NGI concluded in 1986 that the optimal water content varies between 6 to 8 %, and the dry density is then between 2.18 and 2.27 t/m^3. The porosity of the spoil when compacted in layers on the construction site variated from 20 – 25 %.

Gertsch et al. published an article in 2000, gathering multiple project data laboratory investigations. Result from Standard and Modified Proctor tests show higher values for optimal water content. Where the Standard Proctor gives an optimal water content of 14.2 % and a dry density of 1.85 t/m^3, the Modified proctor resulted in 1.87 t/m^3 and 13.7 % (Gertsch et al., 2000).

NGI investigated in 2020 the sedimentation of TBM spoil in water, where both the density and porosity properties of TBM spoil was investigated. The investigations were accomplished by pouring spoil into a container with and without water, with a variating salt content and measuring the uncompacted porosity and density. The density of the spoil in water variated between 2.05 – 2.13 t/m^3 in density and 33 – 38 % in porosity. The material without water had a density between 1.71 – 1.72 t/m^3 and 38 – 39 % (NGI, 2020).

2.2.5 Soil stiffness

Soil stiffness is a parameter that describes a material's resistance against deformation. The resistance is a parameter used to calculate the predicted settlements in a material over time. The one-dimensional modulus M, further referred to as the oedometer modulus, is used to define the stiffness of a soil that are fixed ended and exposed for a load (Janbu, 1970):

Equation 1

$$M = \frac{d\sigma'}{d\varepsilon}$$

M – Oedometer modulus [kPa]
dσ' – Change in effective stress [kPa]
dε – Change in strain [%]

Equation 2

$$\varepsilon = \frac{\delta}{h_0}$$

ε – Strain [%]
δ – Deformation [mm]
h_0 – Initial height [mm]

The soil stiffness is most frequently determined by oedometer test in the laboratory. In an oedometer test a soil sample is placed in a cell, where the sample only can deform vertically and are loaded with a known load on the top of the sample. At the top and bottom, a filter is placed, so that the water can drain freely from the sample. In some cases, the water drainage is closed, and the pore pressure is registered. The oedometer cell prevent the sample to deform radial, and this will simulate a one-dimensional deformation, that simplifies the realistic state (NPRA, 2014).

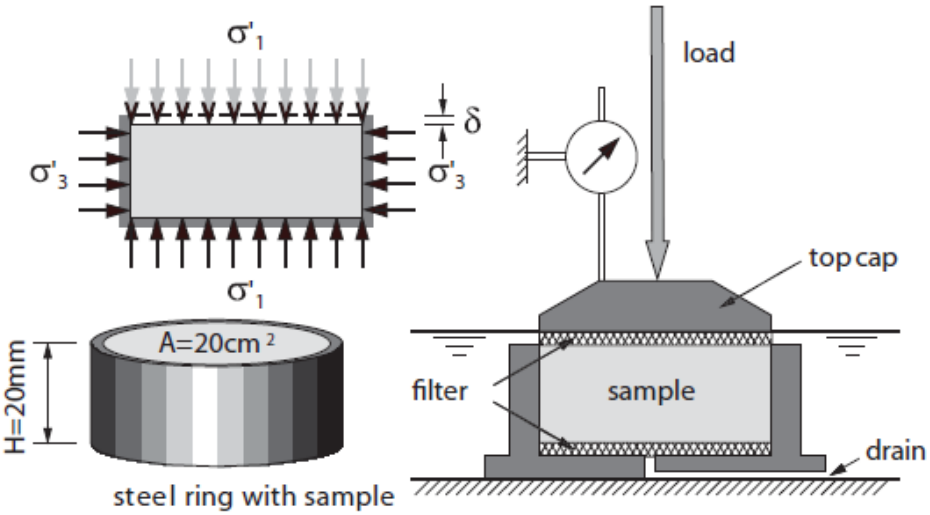

Figure 2.12 Cross-section of an oedometer cell (Emdal, 2014)

When the test is carried out, the soil sample will be built in the cell, and hydromorphic filters will be installed at the top and bottom of the test. The loading can be applied incrementally (IL – incrementally loaded) or constantly (CL – continuously loaded). The load is applied and registered with time, simultaneously as deformation. The loading time of each load step for the IL test, is determined by the consolidation time, meaning that a new load step is applied when the pore pressure has dissipated, or deformation has stopped.

When the particles are loaded and pressed against each other or rotate, sharp edges and corners will break off or be crushed, causing further movement of particles inside the sample. The speed of the deformation in the cell, depends on how the particles can move in relation to each other, and how fast the water can drain from the sample. Air filled voids will not affect the compression of the sample considerable because air is highly compressible. For materials with a higher content of fines, like clay and moraine, the deformation time will be determined by the permeability of the sample. Examples of this principle are shown in Figure 2.13 (Kjærnsli, Valstad and Höeg, 1992).

The initial compression is the immediate settlements that occur when the load is applied. The primary consolidation is caused by an increase in vertical effective stress initiated by dissipation of excess pore pressure over time. Resulting in that the loads transfers from the water to the soil skeleton. The secondary consolidation is the time dependent increase in strain during constant vertical effective stress. The deformation in the material is caused by that the particles are rearranging or some crushing. The boundaries between these different parts is difficult to determine, and is often overlapping between different settlement contributions (Sandven *et al.*, 2017).

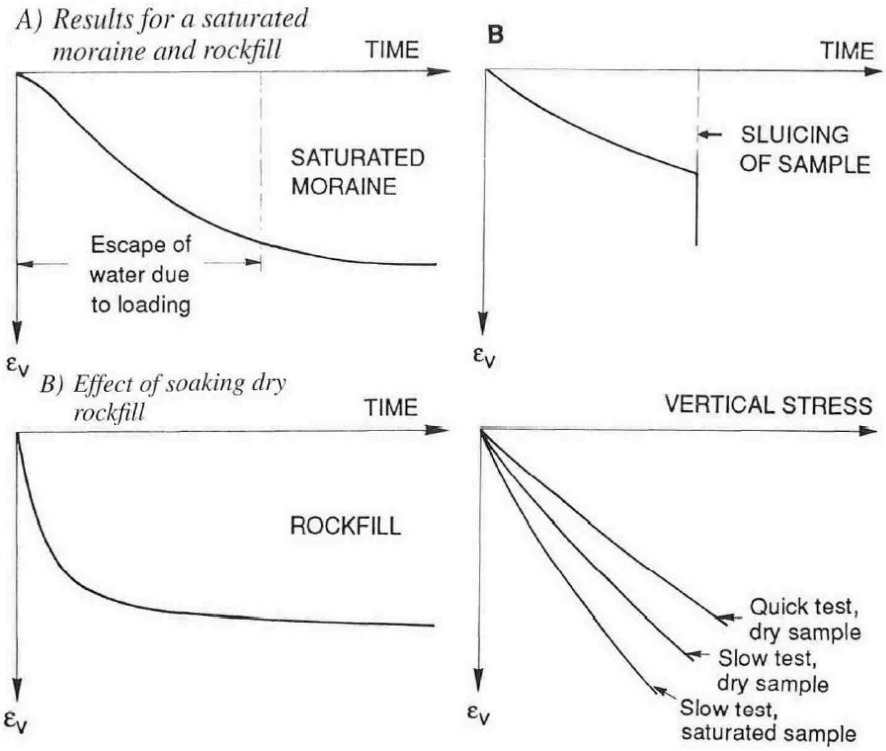

Figure 2.13 Time-compression curves and effect of soaking (Kjærnsli, Valstad and Höeg, 1992)

When testing materials with larger grains, like TBM spoil, a large scale oedometer should be used. Then the sample must be built inside the oedometer cell. This will require multiple layers of soil and compaction of each layer. The type of compaction of the material will be of high importance of the material, where vibratory compaction is more favourable than compaction by static loading. The vibratory compaction will result in a more stable structure because the particles will be shaken into contact, rather than squeezed. When the material is compacted during the oedometer test, this will cause structural change and local crushing. The compressibility of a material is dependent of the grading and the grain shape, where a well graded material with rounded edges will reach less compaction than a flaky homogeneous material (Kjærnsli, Valstad and Höeg, 1992).

Kjærnsli, Valstad and Höeg investigated crushed syenite with a large scale oedometer with a diameter of 600 mm in 1992 (Kjærnsli, Valstad and Höeg, 1992). The tests were carried out on crushed syenite with varying porosity and grain size distribution. The results indicates that the resistance to compression is higher when the material is well graded and compacted, than uniformly graded and loose, see Figure 2.14. The conclusion was that the structure of compacted fills is dependent on the grain size distribution and the shape of the material as well as how the material is placed and compacted.

The results from Figure 2.14 shows the oedometer modulus increase with increasing load. The modulus is greatest for the well graded and compacted moraine, graph 20, since the material has a larger resistance to strain than the other materials. Where the loose and uniformly graded material has the lowest resistance. The conclusion from the oedometer tests is that a material with a flaky and sharp-edged shape is more compressible, than a material that has a rounded shape and is well graded.

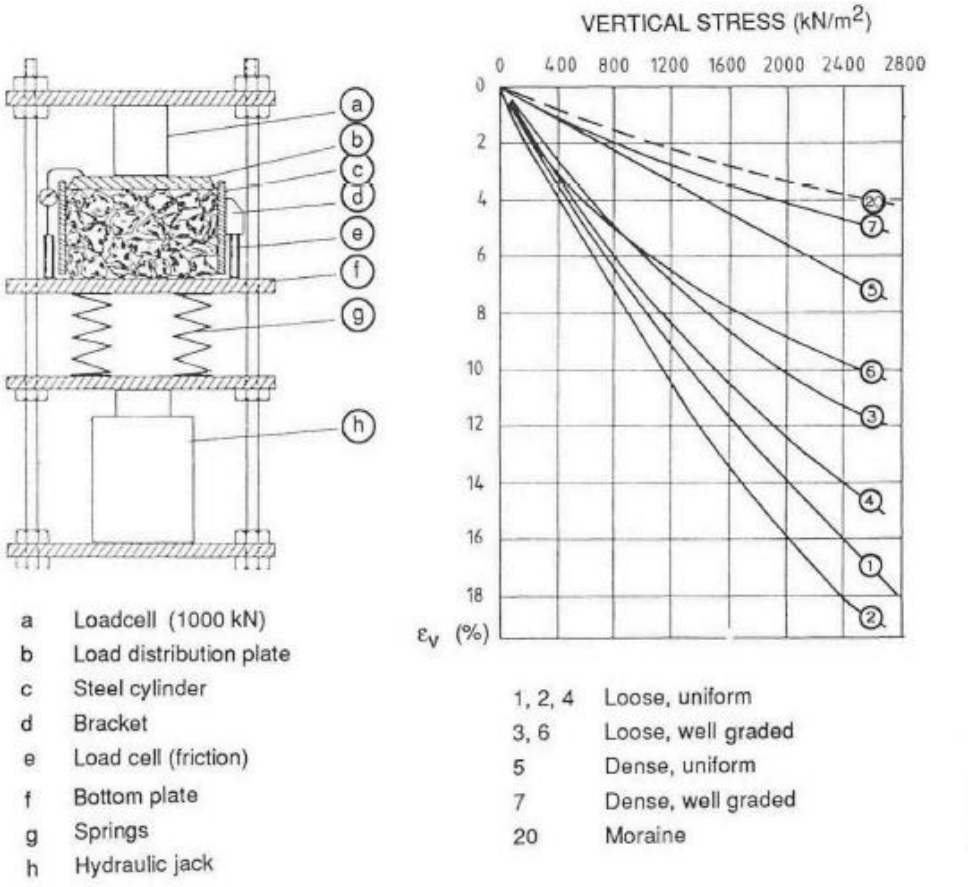

Figure 2.14 Schematic drawing of an oedometer and results of test on crushed syenite (Kjærnsli, Valstad and Höeg, 1992)

From Publication nr. 73 by NGI, Kjærnsli presents oedometer results of crushed rock gravel and moraine, materials suitable as filling material, see Figure 2.16. These results indicates that a dense, well graded gravel and a thin moraine have essential higher oedometer modulus than loose, uniform rock (Kjærnsli, 1968). Where the material with sharp edges and uniform grading is more compressive than rounded well graded material.

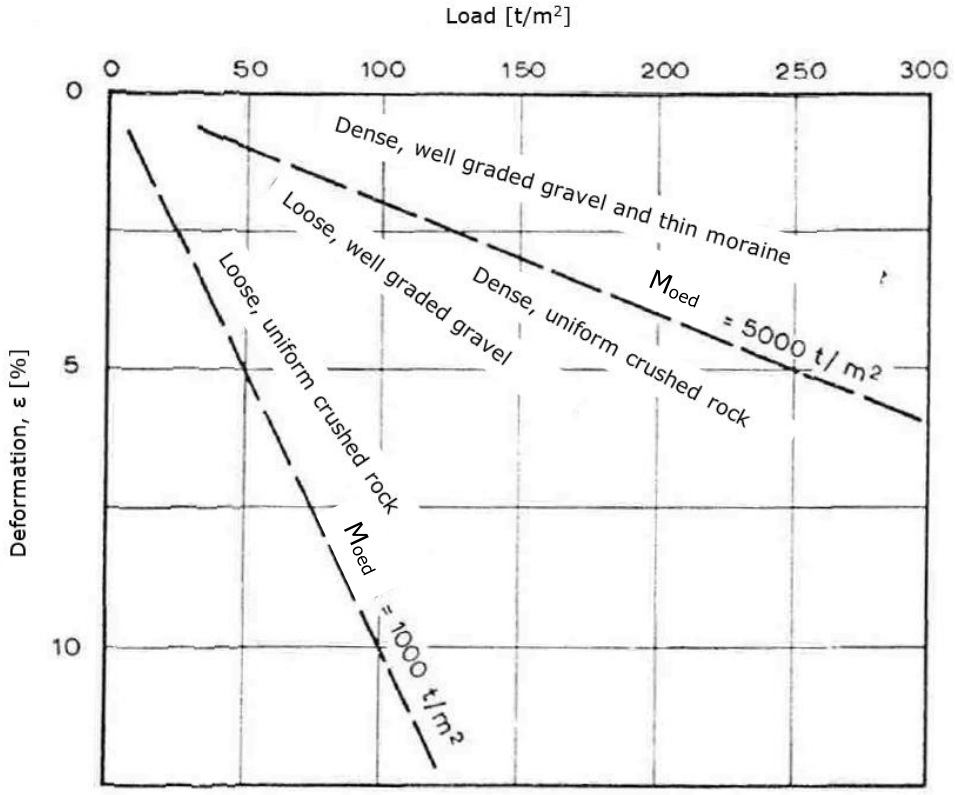

Figure 2.16 Oedometer results for different materials (Kjærnsli, 1968) (translated)

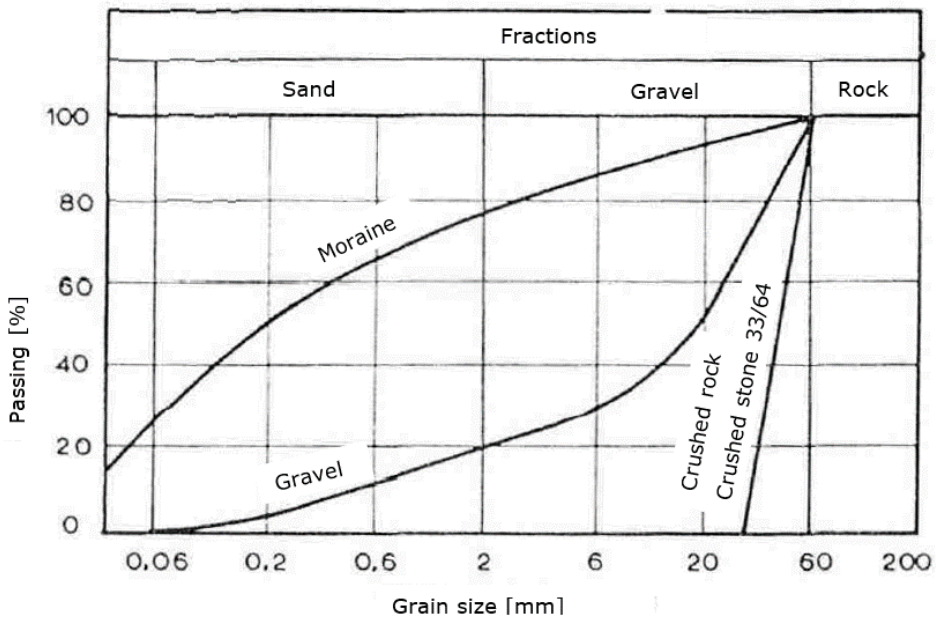

Figure 2.15 The grain size distributions for the materials tested in oedometer in Figure 2.16 (translated)

An ordinary oedometer test with fine graded material is carried out on a soil sample with 50 mm diameter and 20 mm height, Figure 2.12. The oedometer cell K/Ø[1] Anton is used in this project to carry out oedometer tests in larger scale. The equipment has an inner diameter of 49.9 cm and height of 57.7 cm. The method used is further explained in Chapter 3.

The European Standard regarding geotechnical investigation and testing for IL oedometer test (*NS-EN ISO 17892-5:2017*), declare the dimension for an oedometer test (Standard Norge, 2017). The diameter should not be less than 6 multiplied with the largest grain size and the required diameter and height relationship should not be less than 2.5. This is equal to a height of 50 cm and a diameter of 1.2 meter.

The Anton oedometer has a diameter and height relationship smaller than 1.0. This is a disadvantage since the comparisons with other test results can give a wrong impression. The different in scaling should be considered when comparing results from Anton with results from other equipment. Additionally, the side friction in the cell can also lead to a higher value for stiffness, since the high friction can cause a larger load to compress the sample.

[1] K/Ø – Giant Oedometer

Marianne Dahls results

From Dahl's oedometer tests carried out in 2018, see Table 2.2, the oedometer modulus increase when the dry density increases. Test 2 shows the best results, in terms of best compaction and small value in strain, but this test contains a saturated sample that impersonate a stronger material. The dry density in this test is favourable considering the Proctor tests carried out for the same project. The water content in test 2 has a higher value than the same Proctor test, but corresponds to the results from Gertsch et al. In general Dahl's results correspond to the range of the mentioned tests, that had a range in dry density between 1.85 to 2.27 t/m^3.

Table 2.2 Summary of oedometer test results done by Marianne Dahl (Dahl, 2018)

Test	Dry density [t/m^3]	Water content [%]	Modulus number [MPa]	Strain [%]	Increments [min]	Comments
1	1.69 -1.83	10.2	11	8.3	30	Thicker layers
2	2.2 – 2.27	13	23	3.5	20	Leakage of water
3	1.71 – 1.90	6.2	6	10	15	Terminated at 360 kPa
4	1.94 – 2.04	7.6	11	4.9	15	
Average		9.25	12.8	6.68		

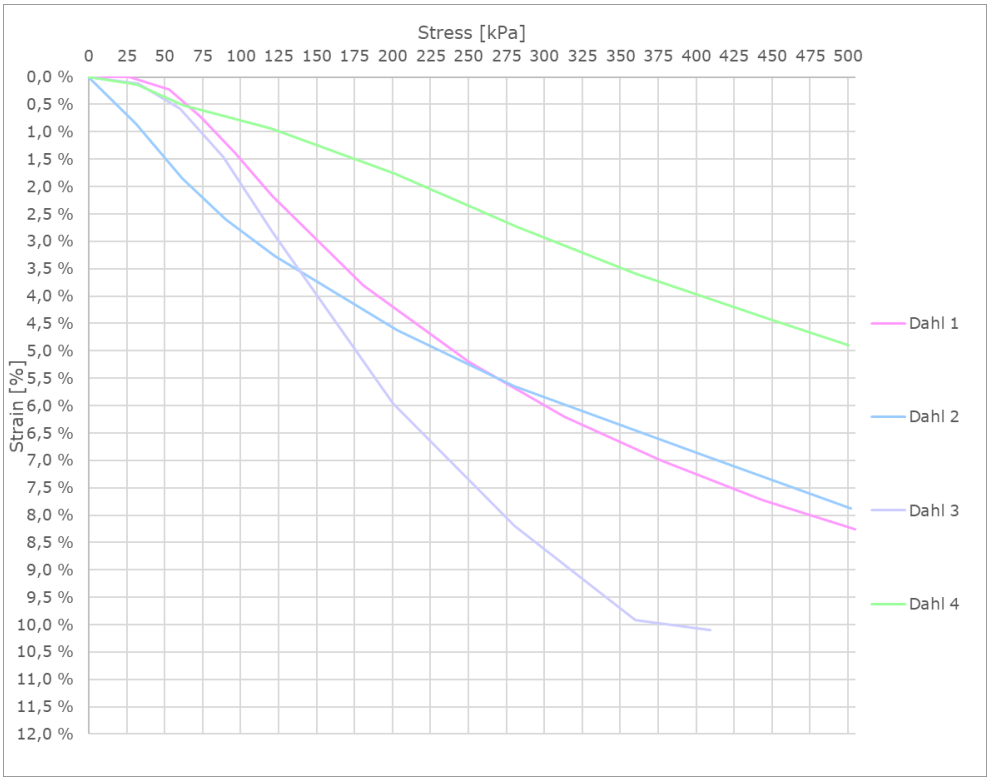

Figure 2.17 Stress - strain results from Dahl's oedometer tests (Dahl, 2018)

Figure 2.17 indicates the difference in strain values for the four tests. Dahl experienced difference in the soil samples due to splitting of material in the barrels used for storage. The water content in the spoil had variations, as indicated in Table 2.2. Test 3 was the sample with lowest water content and the largest strain and was ended at 360 kPa.

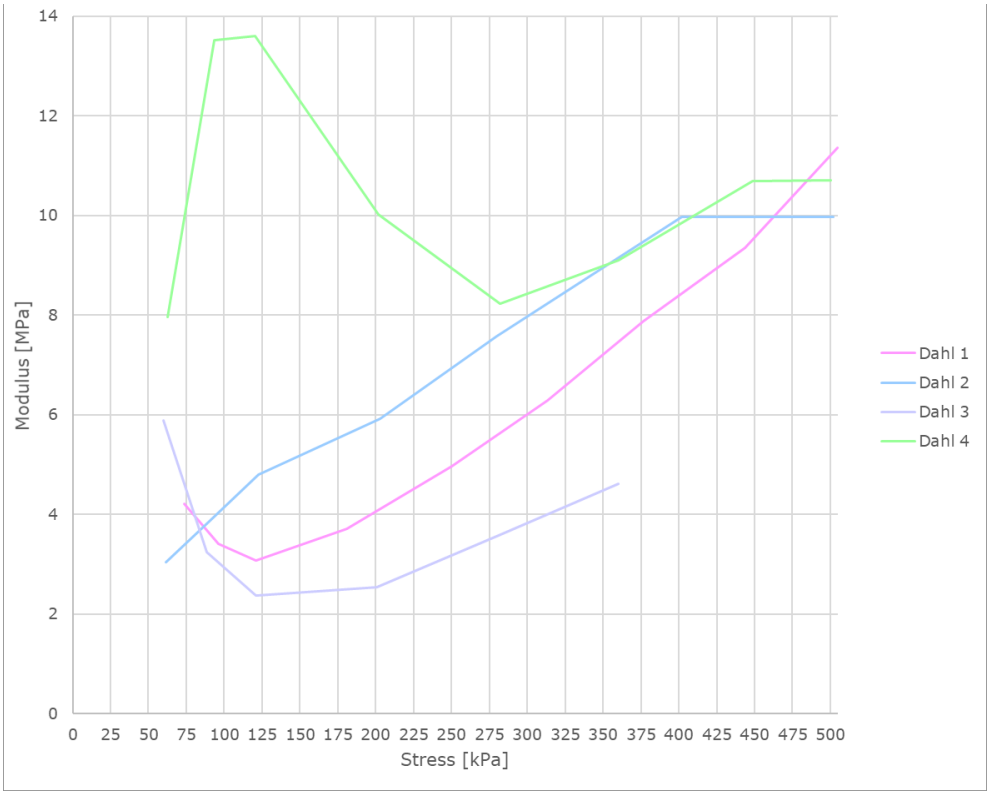

Figure 2.18 Stress - modulus curves from Dahl's oedometer tests (Dahl, 2018)

Figure 2.18 includes the stress and oedometer modulus for Dahl's results, these curves indicates that the spoil have both plastic and brittle properties. The brittle behaviour is expected due to its flaky shape and is more sensitive for crushing. Some of the tests show a sensitive behaviour due to this property because the material can be crushed into a more stable state. Some of the tests show a linear increase in oedometer modulus until the modulus stabilises and then reach a more plastic behaviour. The tests resulting in the highest resistance correspond to a loose, uniform crushed rock compared to the results provided by Kjærnsli, Valstad and Höeg in 1992.

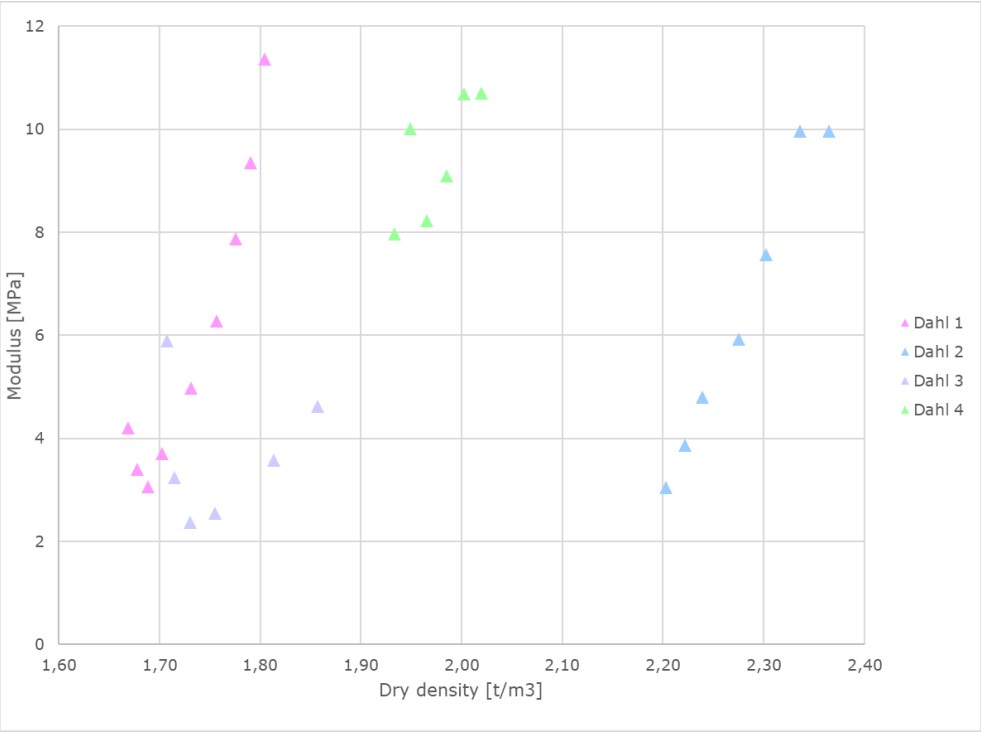

Figure 2.19 Dry density - modulus results from Dahl's oedometer tests (Dahl, 2018)

From Dahl's results in Figure 2.19, there is a tendency of less strain with higher achieved dry density, meaning that the material achieve improved compaction for higher stresses (Dahl, 2018). Test 2 was most likely saturated since the density values are closer to rock than to spoil. The Anton oedometer do not measure pore pressure, and therefore the pore pressure is not divided from pressure between the grains. This must be included in the consideration of this test for further discussion.

2.2.6 Shear strength

The shear strength is determined by the friction angle in the material, that is the angle a natural slope if the material is stable, and the effective stress level. The friction angle for a soil is a parameter derived from the Mohr-Coulomb failure criterion. The Mohr-Coulomb criteria describes how the maximal shear force on a failure plane varies in the soil with the normal stress to the plane. This is given by the equation:

Equation 3

$$\tau_f = (\sigma'_n + a)tan\varphi$$

τ_f	– Shear stress	[kPa]
σ'_n	– Effective normal stress	[kPa]
a	– Attraction	[kPa]
φ	– Friction angle	[°]

The friction angle of a coarse material depends on the grain size distribution, grain shape and the porosity, see Figure 2.20. A well graded material has a higher friction between the grains, than a uniform graded material. A material with sharp edges will have a higher friction angle, than a material with rounded grains. When a material is compacted, the friction angle will increase, because the grains are packed together. The friction angle will be dependent on the stress level, and can vary in a material, where the angle will decrease with increasing effective stress (Kjærnsli, Valstad and Höeg, 1992).

The shear strength of a material is normally determined in a triaxial test. The equipment is adapted to the material tested. This will depend on if the material is a cohesive material like clay, or a free draining material like sand or gravel. For sand, gravel and stones the triaxial test are performed in vacuum-triaxial equipment. The sample is loaded until failure by increasing the vertical load. Continuously during the vertical stress, under pressure inside the sample, vertical deformation and volume change is recorded (Kjærnsli, Valstad and Höeg, 1992).

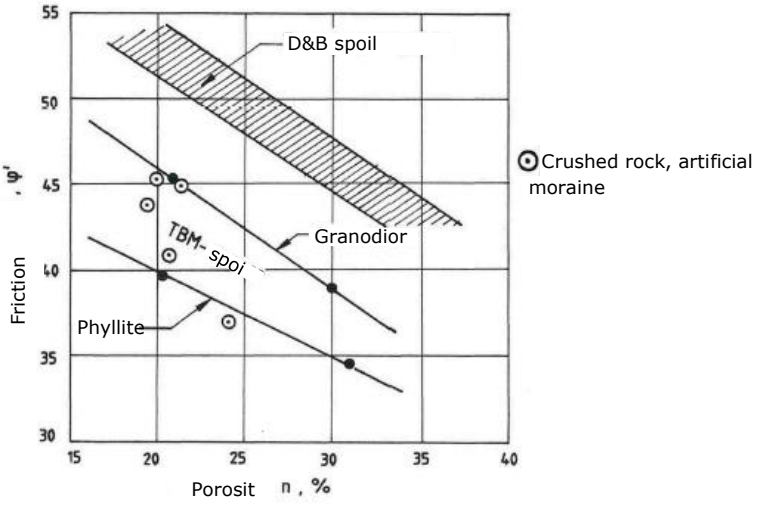

Figure 2.20 Friction angle and porosity (NGI, 1986) (translated)

NGI executed triaxial tests for the TBM spoil in 1986, these results are shown in Figure 2.20. The friction angle for the different samples varies from 40° to 50°, around 9° to 10° less than spoil from D&B with same porosity.

T. M. Leps carried out a large number of triaxial tests on different rock fills in 1970, where the results are shown in Figure 2.21 (Leps, 1970). The results show the difference in friction angle and normal stress, dependent on the compaction, grading and particle strength. Leps' results show the correlation is favourable for the friction angel to have a well compacted, well graded material existing of strong particles.

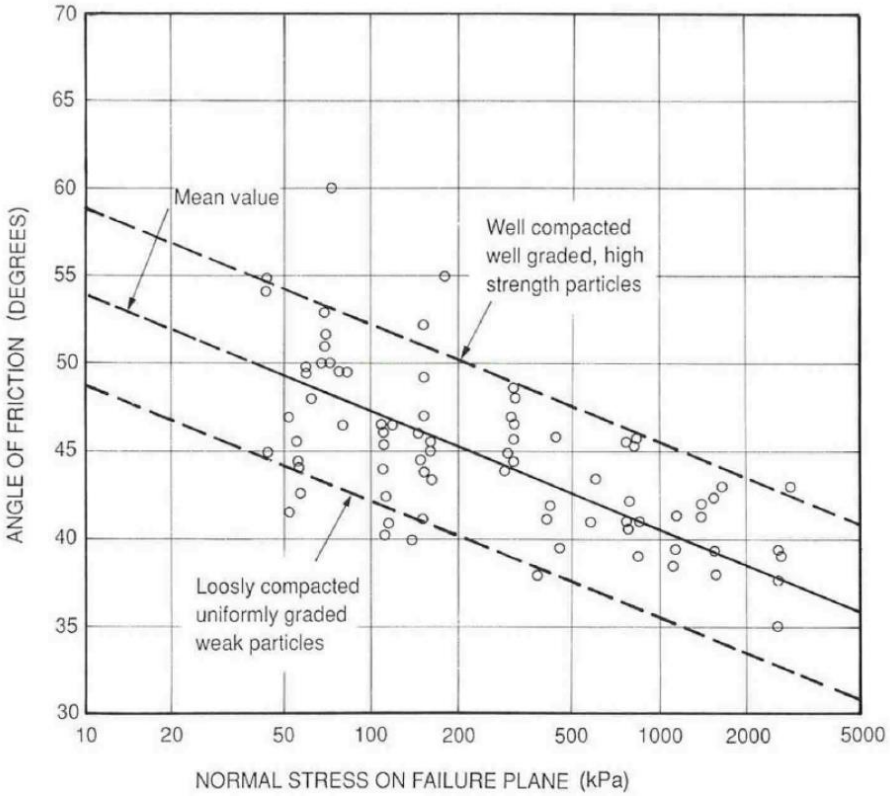

Figure 2.21 The friction angle and corresponding effective stress on the failure plane (Leps, 1970)

2.3 Utilisation of TBM spoil

Aggregates, in conformity with oil and gas, are an unrenewable resource, where the gravel- and sand pits near urban areas are experiencing shortage. Where Oslo, among other cities are no longer able to meet the need of aggregates for construction sites, leading to extended transport and costs (Mathiesen, 2020). The shortage of resources and areas for stockpiles result in a need of improved utilisation of the material produced by tunnel excavation.

Utilisation of the TBM spoil must be planned for each project since the quality of the material is varying accordingly and dependently on the rock quality and the TBM parameters. Measures to achieve the required geotechnical parameters for each project should also be planned for and tailormade prior to project execution. Normal utilisation of crushed rock is in road or rail constructions, aggregate in concrete, coverage for polluted material, fillings on land and in sea, berms, and noise barrier. Where the properties of the spoil need to be investigated for some of the range of applications (NGI, 2019a).

Gertsch et al. collected experienced data of TBM spoil from hard rock in a study published in 2000. The article concluded that the TBM spoil can be successfully utilised and that it can in many cases reduce costs and/or increase revenues for a tunnel project. With proviso that knowledge of characteristics of the spoil and of the requirements of the construction aggregate for which it will be used (Gertsch *et al.*, 2000). Although they remark that very few TBM spoils are suitable for direct use without modification. This modification can consist of processing plant that is designed to separate the material into multiple size classes. These operations will have an economical cost, that must be weighted by the further utilisation.

The Follo Line project and the Ulriken Tunnel utilised the majority of the TBM spoil produced. The spoil from the Ulriken Tunnel was used to cover a polluted seabed in Puddefjorden (PEAB, 2018). The spoil produced for the Follo Line project was utilised as landfill in a ravine valley near the construction site. The thickness of the landfill is up to 27-metres. The landfill will be a part of a future neighbourhood belonging to the city of Oslo (NGI, 2019a).

The upcoming New Water Supply project located near Oslo are planning to utilise the spoil as a filling on the seabed. Preliminary laboratory investigations have been carried out on the spoil from the Follo Line project, where the turbidity and porosity have been tested in water. The test results indicates that the material has good qualities for covering polluted sediments (NGI, 2020).

The aim of the DRAGON project (Development of Resource-efficient and Advances Underground Technologies) was to improve the resource efficiency in tunnelling and other underground construction processes. This by developing a system for the automated bypass analysis, online classification and in-stream sorting of excavated material (Erben and Galler, 2014). It is recommended that the spoil is used directly on site during the construction phase of the project if the material meets the requirements for the purpose. If the aggregates production is larger than the internal demand, the material should be marketed to local producers and processors of raw materials can be tested. Erben and Galler composed a possible utilisation hierarchy in Table 2.3, where the quality of the spoil can be sorted by classes. The quality is reduced by each class.

Table 2.3 Utilization of excavated material (Erben and Galler, 2014)

Class 1	Utilization as construction raw material on site (aggregates for inner lining and segment concrete, shotcrete, annular gap grout, load-bearing layers, asphalt mixes etc.)
Class 1a	Utilization as construction raw material outside the site (railway ballast etc.)
Class 2	Utilization as an industrial raw material – corresponding to a requirement catalogue of the mineral raw materials industry (gypsum, brick, cement, glass, abrasives, chemical industries etc.)
Class 3	No higher-quality utilization
Class 3a	Material for landscaping: embankment fill, backfilling, road sub-base, filling on seabed etc.
Class 3b	Landfill

2.4 Drill and blast

2.4.1 Principles of drill and blast

Drill and blast, further referred to as D&B, is a more conventional excavational method than the TBM. The principle of this method is a circle of operations that consists of drilling, loading, blasting and several other operations indicated in Figure 2.22. The operations are repeated until the total length of the tunnel is excavated. Pre-grouting is applied ahead of the blasting to control the stability of the tunnel, the pore pressure and the water inflow. Pre-grouting follows the same principles as described for TBM (Nilsen and Tidemann, 1993).

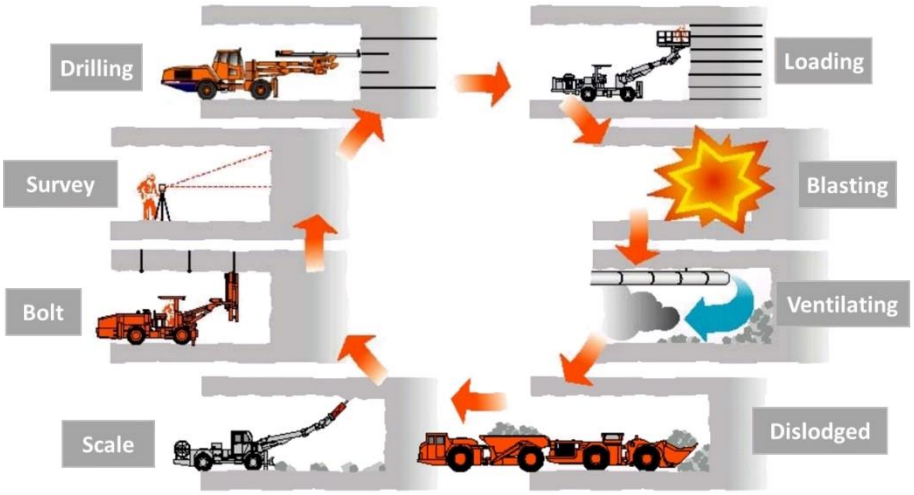

Figure 2.22 The Drill and Blast operation circle (railsystem.net, 2015)

The D&B method is the most traditional excavation method used for medium to hard rock conditions. Some advantages with D&B compared to TBM, is the flexibility, the short mobilisation time and versatile equipment that have relative low costs. The method has some weaknesses in urban areas due to the blast vibration and noise. Another disadvantage is linked to the required work site organisation, due to the need of different specialists in each operation. Continuously in the excavation circle the drilling pattern, injections, the quantity of explosives and the need of support must be investigated. This is due to the variation of the mechanical condition of the rock mass (Nilsen and Tidemann, 1993).

The result of a blast will depend on different factors, including type of cut, drill hole pattern, type of explosives, detonators along with the geological parameters. The mechanical strength of the rock, the degree of jointing, the density of the rock mass and the anisotropy of the rock mass are the geological parameters that will influence the blastability. The net advance rate of a blast will in normal conditions be in order between 90 – 95 % of the drilled length, but will be considerably lower for more challenging conditions When the advance rate is lower, the effectivity of tunnelling is reduced (Nilsen and Tidemann, 1993).

The net advance rate of a blast is higher for a rock with characteristics like low moderate anisotropy, moderate mechanical strength and low density. Rocks with these qualities are typical coarse grained granites, syenites and quartzites (Nilsen and Tidemann, 1993).

2.4.2 Environmental impact

The environmental pollution from D&B are linked to the emissions from the machines used in the excavation. A project excavating with D&B are dependent on several number of fossil fuel vehicles. This is caused by the operation circle, where all the operations are dependent of machines to operate (Dahlstrøm *et al.*, 2014).

Compared to the TBM method, the tunnel spoil will be more polluted from concrete from injections, explosives and plastic from the cartridges. The machines used in the operation is also causing pollution from engine oil. For further use of the tunnel spoil, the pollution must be removed from the spoil (Dahlstrøm *et al.*, 2014). Experiences from Norwegian tunnelling projects shows that it is challenging to remove the plastic from the excavated spoil (Miljødirektoratet, 2018). The removal has proven to be very difficult due to the need of space, time, costs and occupational health and safety (OH&S) of the workers. This pollution will cause problems if the plastic is free, meaning that the plastic inside the material will be protected from erosion.

The sources of the plastic in the excavated masses are the detonators, and the casing, but mostly from the concrete reinforcement. The plastic in the reinforcement can often be exchanged with steel. There are three detonators used when blasting: electronic, electric and blast wave. The plastic used in detonators can be reduced by 30 % if electronic or electric detonators are used instead of blast wave detonators. The casing used as hole cursor must be removed from the face before blasting (Miljødirektoratet, 2018).

The utilisation of the tunnel spoil is in some cases a challenge due to the variation in quality and grain size for each blast. For optimal use it is essential that the spoil is sorted and crushed soon after it is excavated. It is favourable that the spoil is utilised at the construction site as aggregate in cement, asphalt or in the road construction. This will reduce the need of transportation and the probability of utilisation will increase (Dahlstrøm *et al.*, 2014).

Often tunnel spoil is utilised as landfills in the ocean or lakes to expand land areas. This is problematic since the spoil often contain large quantities of plastic. The decomposition of plastic is slow in marine environment, and after a long period microplastic is produced. This is a challenge for the organisms in the sea, due to the confusion of food (Miljødirektoratet, 2018).

2.5 Geotechnical properties of blasted rock

2.5.1 Grain shape and grain size distribution

NGI investigated basted gneiss from Akershusstranda in 2020 where the grain size distribution is shown in Figure 2.25. The D&B method will generally produce a material with more cubic shape and a smaller content of fines compared to TBM. The grain shape of the material had a large variation in grain shape, where half of the grains was near cubic, and the remaining variated from elongated to flaky, to very elongated and very flaky. The largest grains had a variation from cubic to flaky. The smaller grains had a tendency to have a more elongated and flaky shape (NGI, 2020).

Figure 2.23 24 Sieved and washed D&B spoil from Akershusstranda (NGI, 2020)

The geology conditions will have a major impact on the grain shape of the particle. New boring- and explosive dust will have sharp edges, dependent on mineralogy and handling, the particles will be smaller and more cubic with time (NRPA, 2015). If the material is treated further in a crushing mill, the material properties will be refined by a more optimal grain shape (Alnæs *et al.*, 2019).

The geotechnical properties for blasted rock, as for the TBM spoil, will be dependent on the rock quality and the performance of the excavation. The blasting pattern and the use of explosives among others, will affect the grading curve, the fine content and the shape of the material (Alnæs *et al.*, 2019). When comparing blasted rock from tunnels and day zone with the same mineralogy, the material from tunnels will have a higher content of fines. This is caused by the available machinery inside the tunnels, where smaller machinery requires smaller fractions, and that a larger amount of explosives is used. Predrilling holes for the injection of explosives will also produce a large amount of chipping cuttings, in addition to the fines produced by the blast (NFF, 2009; NRPA, 2015). Most of the fine content will be released in receiving waters, but not the total content.

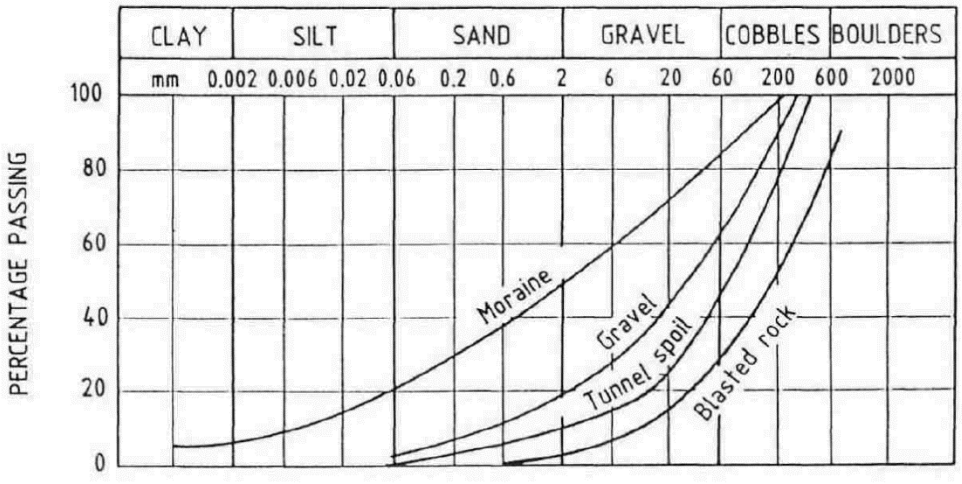

Figure 2.26 Typical grain size distribution for blasted rock among others (Kjærnsli, Valstad and Höeg, 1992)

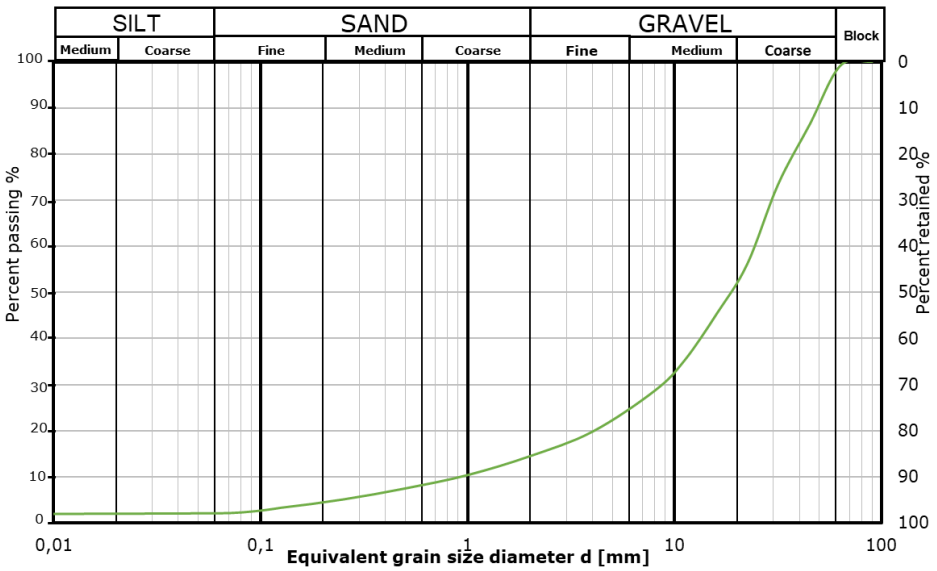

Figure 2.25 Grain size distribution of blasted gneiss from Akershusstranda (NGI, 2020)

Production of gravel by blasting and crushing rock will produce up to 20 – 25 % content ≤4 mm, or higher. The fines are produced by the blasting and the further crushing (Nielsen, Hansen and Myrvang, 1994). Ouchterlony et al. investigated the production of particles <35 and 40 mm from blasting and crushing (Ouchterlony *et al.*, 2006). The result from these investigations indicates that blasting produces 10 – 22 % of these fractions, and further crushing increased the content to 25 – 30 %.

2.5.2 Water sensitivity and frost susceptibiliy

The blasted rock will in most cases contain less than 7 % fines smaller than 63 µm and less than 3 % smaller than 20 µm. Thus, the blasted rock is not water and frost susceptible. According to NRPA's classification of frost susceptibility, the blasted rock will be appurtenant class T1, not frost susceptible, see Figure 2.27. The material will be appurtenant to class 4 in Finland's classification, where further investigations on the local site are needed, see Figure 2.28.

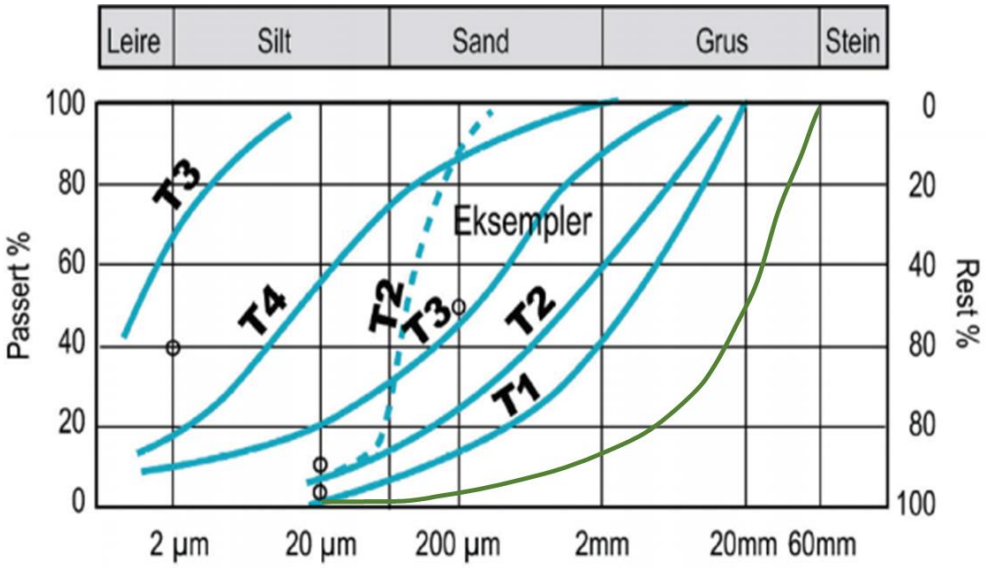

Figure 2.27 Examples of frost susceptibility classification by NPRA (NPRA, 2010) (Modified)

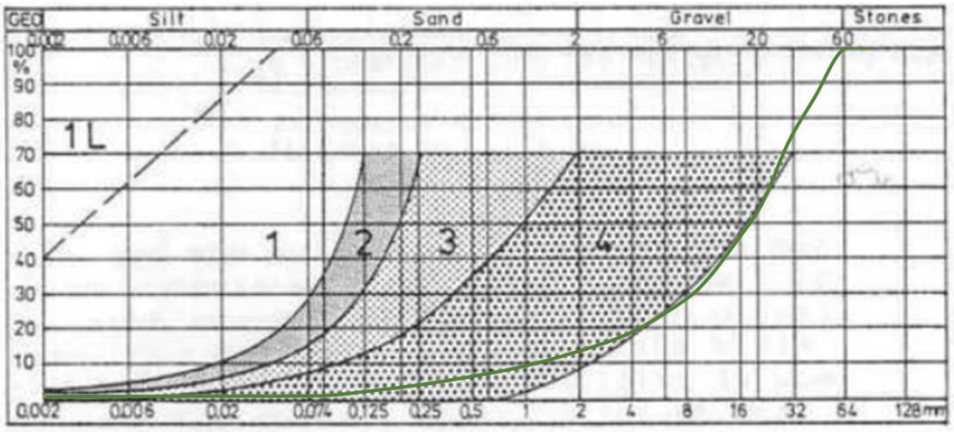

Figure 2.28 Determination of frost susceptibility of a soil based on grain size distribution in Finland by ISSMFE (Slunga and Saarelainen, 2006) (modified)

The challenge regarding utilisation of the blasted rock on site regarding frost, will be the frost depth of the material. Since the material has a coarser grain size distribution and smaller water content, the frost penetrates deeper in the blasted rock than finer materials, see Figure 2.29.

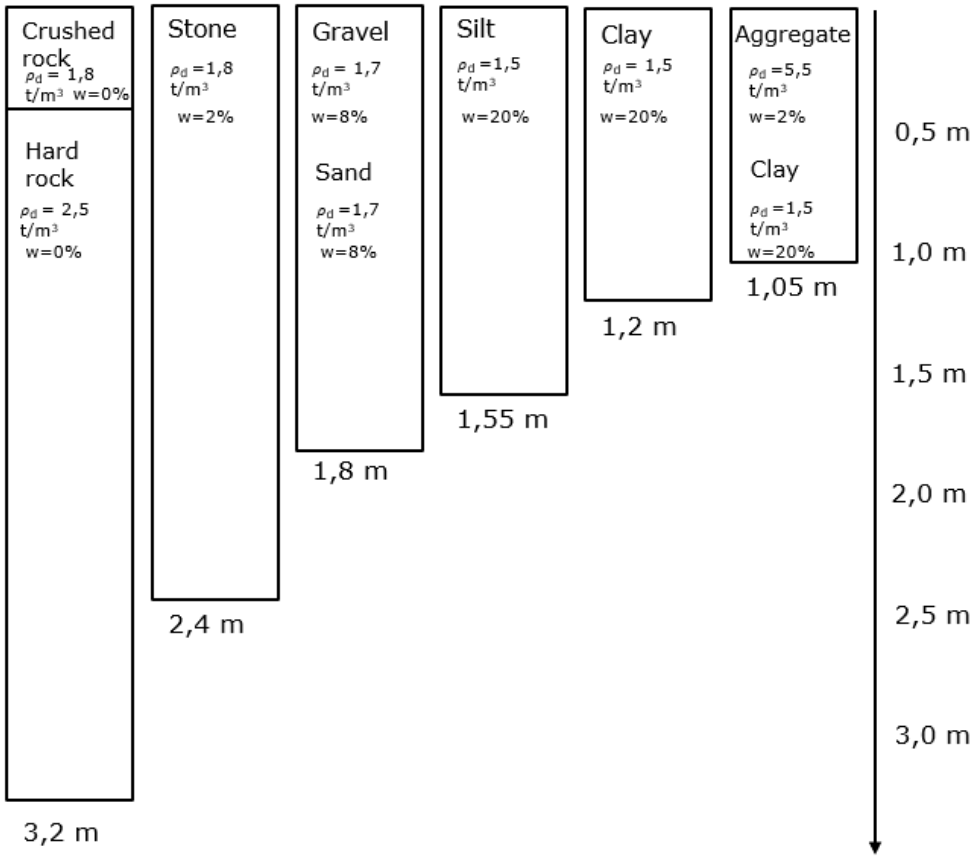

Figure 2.29 Calculated frost depth for different materials. Frost index 25 000h°C and mean year temperature 5.0 °C (The Royal Norwegian Council for Scientific and Industrial Research and The Public Roads Administration's Committee, 1973) (modified and translated)

3 Laboratory investigations

3.1 Methodology

3.1.1 Large scale oedometer - K/Ø Anton

The laboratory investigations are carried out at the Geotechnical Laboratory at NTNU in Trondheim. The equipment used is a large scale oedometer cell, K/Ø Anton, with an inner diameter of 49.9 cm and inner height of 57.7 cm, see Figure 3.3 (Dahl, 2018). Six holes are placed in the bottom of the cell to allow the water in the sample to drain. The drained water and the pore pressure in the cell are not measured. A lid is placed on top of the cell. The load is applied by a plate pressed down by air pressure and the maximum applied load is 700 kPa. The soil samples are built in the cell by layers compacted by a vibrating compaction plate designed for Anton, with a diameter of 49.7 cm and a weight of 13.8 kg, see Figure 3.1.

According to the standard "Geotechnical investigation and testing - Laboratory testing of soil - Part 5: Incremental loading oedometer test" (*NS-EN ISO 17892-5:2017*) the diameter/height ratio should not be less than 2.5 (Standard Norge, 2017). The ratio for Anton is diverging from this with a value of 0.9. The reason for this ratio is due to the large forces needed to maintain the pressure in the cell, these forces would be much larger for the dimension required for a larger apparatus.

The standard indicates that the largest particle size in an oedometer should not be larger than 1/5 of the oedometer ring. The favourable oedometer testing TBM spoil should have a minimum height of 48 cm and a minimum diameter of 125 cm, if the largest grain size is 80 mm. With these dimensions the needed load for the oedometer test consist of several tons. K/Ø Anton does not fulfil these requirements. Thus, because of the challenging dimensions and loading procedure, the tested material in this thesis is therefore sieved and scaled. This to ensure the removal of larger particles than the standard recommends for the height of Anton. The process is further discussed in Chapter 3.2.1.

Figure 3.2 Setup of the oedometer equipment

Figure 3.1 Compaction of material

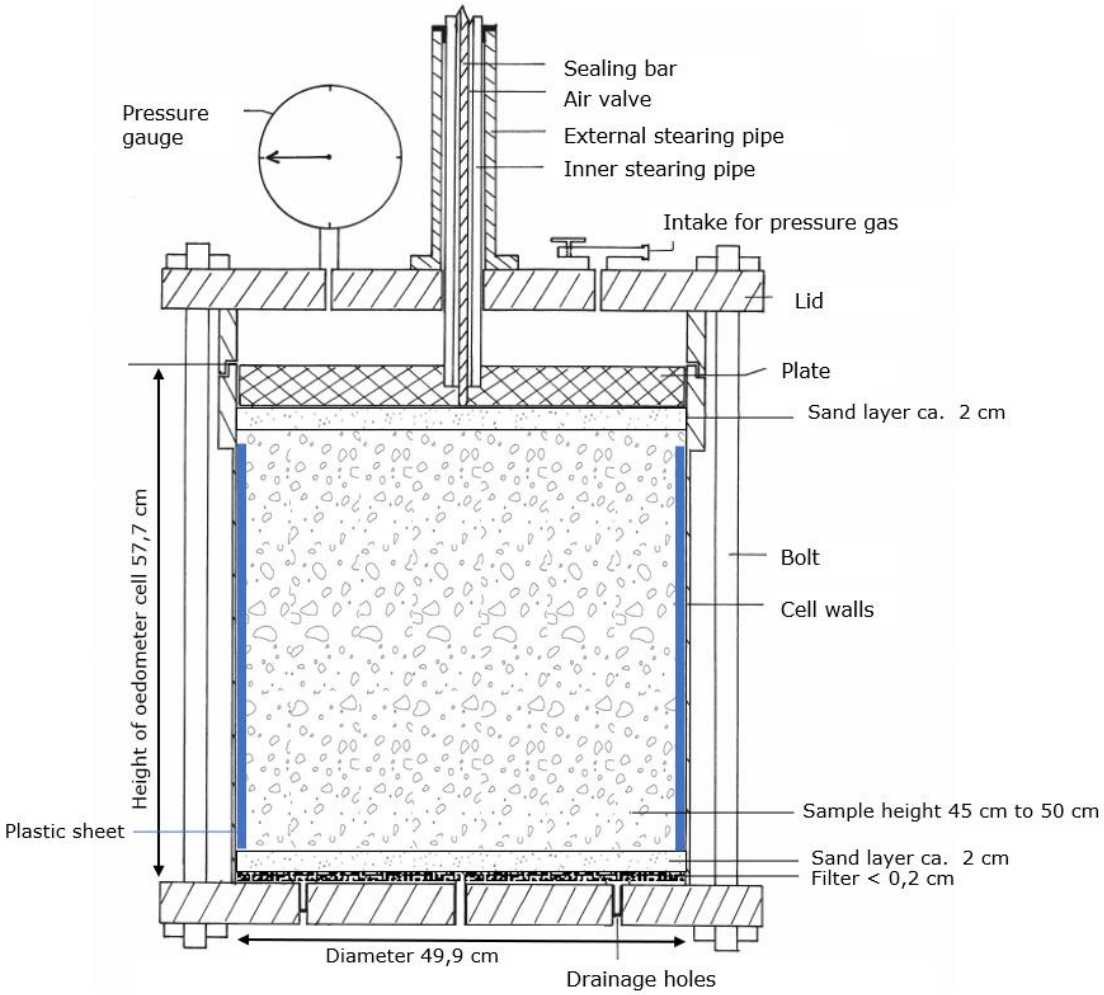

Figure 3.3 Illustration of the Anton oedometer (Motzfeldt, 1975) (modified and translated)

The walls in the oedometer are covered with a grease layer and a plastic sheet to reduce wall friction. The plastic sheet is cut 10 cm from the top before the test is started. This to prevent the air from escaping between the sheet and the walls of the cell. A filter is placed in the bottom of the cell to prevent the material from leaking out of the drainage holes. The filter consists of a woven geotextile of plastic. A layer of sand is placed in the top and bottom of the cell to counteract crushing between the steel and the material. In a field investigation this crushing would occur in a smaller scale, since the crushing would occur mostly between grains.

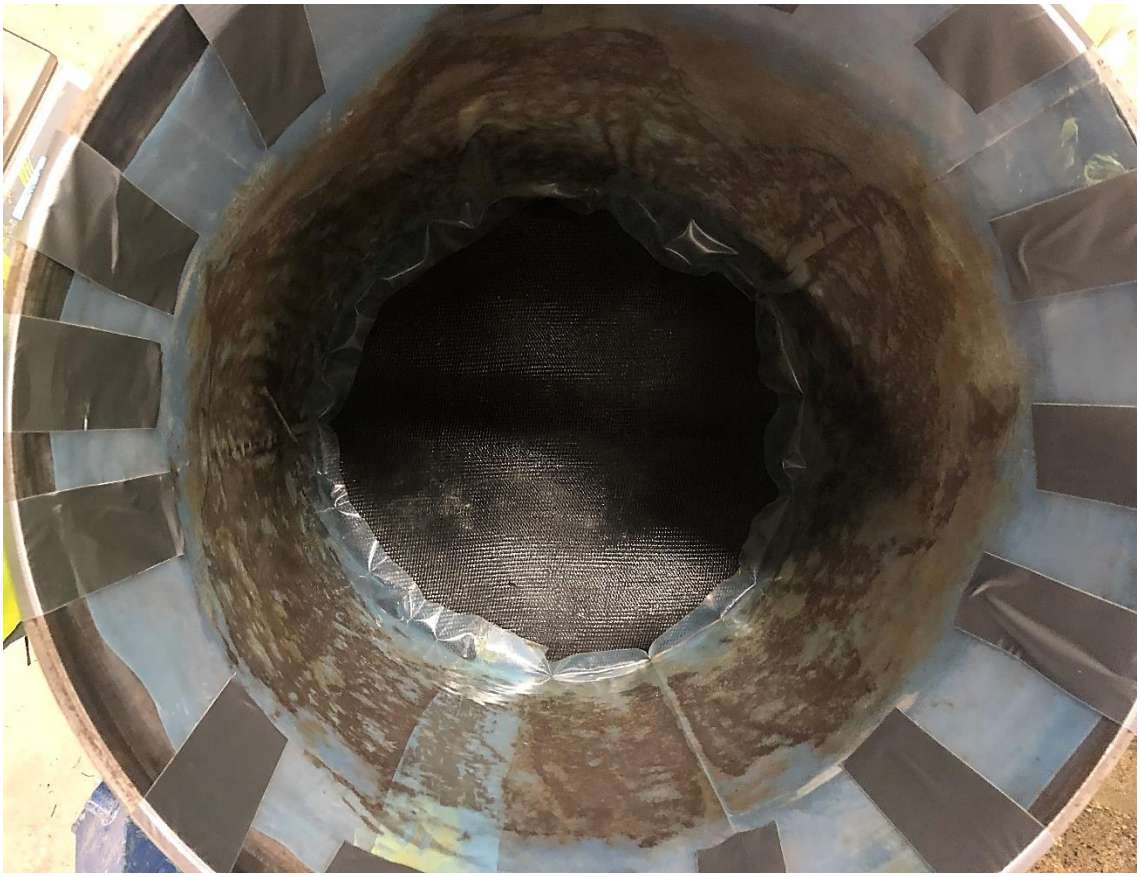

Figure 3.4 Inside the cell, filter and plastic sheet

The load is applied by rotating a pressure wheel, the application of load lasts for approximately 30 to 40 seconds. The pressure wheel is sensitive and has a delay of a few seconds. Thus, some applications can be uneven in the stress-strain curves shown in the results. Regarding *NS-EN ISO 17892-5:2017* the required load should be applied without jolting within a period of two seconds, this criterion is challenging to achieve with this equipment.

The oedometer test is an IL-test with 13 load steps, se Table 0.2 and Table 0.4 in Appendix A: Results from laboratory investigations, for further details. The time of the load steps are based on the results from Dahl and the preliminary specialisation project. The increment time was initially set to 15 minutes but then increased for larger load steps, since the creep settlements did not stabilise during this period. Test 2 and 3 with TBM spoil and test 2 with crushed rock, had a 70-hour increment time at 350 kPa to investigate the "short-long time" effect of the creep settlements.

The deformation in the material is continuously logged by LabView software, logging the deformations in a given time interval, Figure 3.5. The time interval between each logging is set to 2 or 3 seconds when the load is applied for 15 – 30 minutes, and to 30 seconds when the application lasts over 70 hours. Figure 3.5 is a print screen of the software used during the tests. The example is taken from the long-time interval for test 2 with TBM spoil. When the load is applied, the pressure value shown in the software is used to adjust the load step. The graphs in the software does not have the correct values on the axis, but the scale is correct. The sample height in the cell must be measured to calculate the strain values. The accuracy of this is ±5 mm due to uneven surface of the sample.

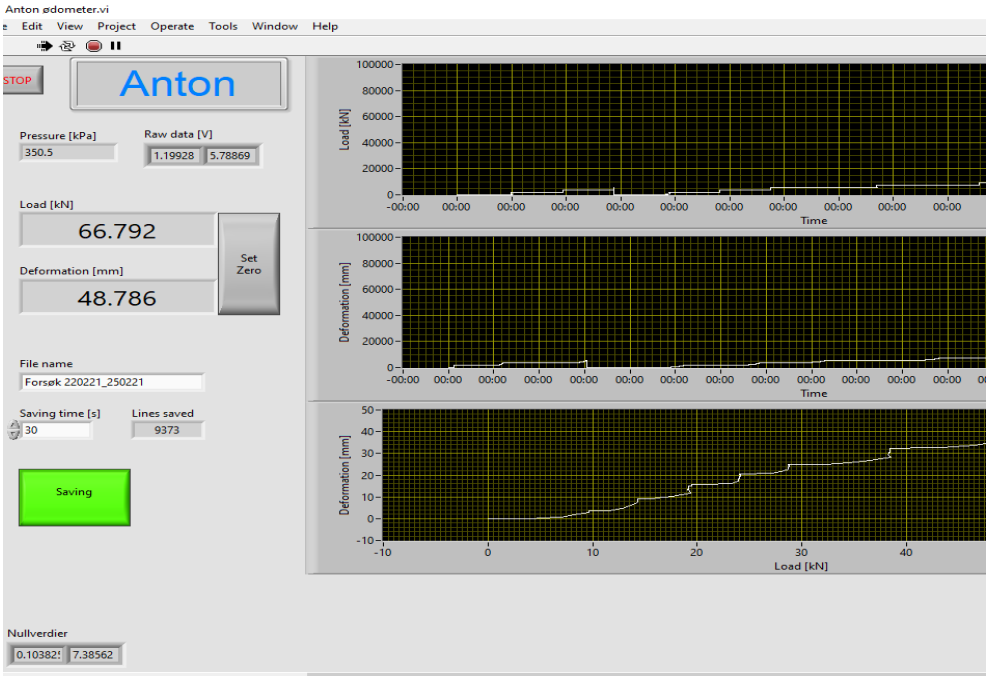

Figure 3.5 LabView software used during testing

The tests are built by hand, where the material from the crushed rock is manually excavated from a 0.6-ton bag, see Figure 3.6, into buckets that were weighted and lifted in to the oedometer cell. The TBM spoil are delivered in buckets that weighed between 16 to 20 kg.

To ensure that the water content is uniform in the buckets, they were turned upside down two days before the tests were built. The layers of crushed rock were laid in approximately same amount as the spoil, with two buckets of 16 – 17 kg each layer that was compacted for 60 seconds.

The total time spent on building, running and emptying a short time test, with load steps lasting for 20-30 minutes, are approximately 8 hours. Test 2 and 3 with TBM spoil and test 2 with crushed rock are tested over several days, from Monday morning to Thursday afternoon. The total time used on one test is approximately 80 hours.

Figure 3.6 The material from the stone crushing plant, Franzefoss

Figure 3.7 To the left: The content in the TBM spoil buckets. To the right: The amount of two tests. Pictures taken by KSR-Maskin.

The tests are built with the intention to be as equal as possible. However, variation in layers occurred since the material filled in the buckets varied in weight. Each layer consisted of two buckets of material that are compacted for 60 seconds. Some of the tests consisted of a sixth layer with one bucket of material. This because the height needed adjustment for the plate to function. The height needed to be at least 42 cm, since the upper 15.7 cm is polished to reduce the friction for the plate.

The tests containing the crushed rock from the rock crushing plant had a larger variation in test height and weight, caused by separation of material in the material bag. Meaning that the grain size distribution variates from the given distribution through the bag. Thus, the different layers in the cell would variate in coarseness, and the height in the cell needed further adjustment than the TBM spoil.

Table 3.1 The weight of each test

Test number	TBM 1	TBM 2	TBM 3	TBM 4	CR 1	CR 2	CR 3
Layer 1	33.0	33.2	38.0	34.2	34.8	32.0	32.0
Layer 2	35.2	35.9	39.1	36.6	34.5	32.0	32.0
Layer 3	32.2	36.0	38.9	33.9	34.5	32.0	32.0
Layer 4	33.6	35.4	39.3	36.2	34.7	32.0	32.0
Layer 5	32.5	35.8	39.7	35.8	17.0	32.0	32.0
Layer 6	17.0	13.2	-	17.4	-	26	24.8
Sand layers	8	8	-	8	8	8.6	8.2
Weight of buckets	4.8	4.3	4.2	4.8	-	-	-
Total weight of test [kg]	186.74	193.18	190.78	197.35	163.5	194.6	195

The tests of the TBM spoil were built by first weighing the buckets with material, see Figure 3.7, before they were emptied in the cell and compacted. When the total height of the test was built, the buckets were stacked and weighed. This to subtract the weight of the buckets from the total weight, to further calculate the total weight of the material. Not performing this would impact the density calculations.

Whilst building the test with crushed rock, the material was taken from the bag into a bucket placed on a scale. Since the same bucket was used continuously during the building, the scale was tared when the bucket was placed on it. A standard weight was calculated from the first test with crushed rock. Thus, test 2 and 3 were built with the exact same weight of each layer. These two tests needed more sand to the top layer to straighten the surface.

Test 1 of crushed rock was the first test accomplished for this thesis. This to ensure that the equipment was functioning. After test 1 of crushed rock, all the tests of TBM spoil were accomplished before test 2 and 3 with crushed rock. The length of the load steps was adjusted during some of the tests, since the material had a larger strain than expected.

Progress of method

The method used for the oedometer tests in this thesis is a collocation of experiences from previous tests carried out in 2018 by Marianne Dahl and for the preliminary specialisation project in 2020.The intention of the tests performed in 2020 was to test drive the equipment and method as a preliminary work for this master thesis. The main experiences from these tests are listed below:

Sieved and split material in buckets

The tests in 2018 and 2020 were both accomplished with TBM spoil delivered in 660 litres barrels. The experience with this is that the material is splitting in the barrel, meaning that the grain size distribution was varying from layer to layer in the oedometer cell. The same experience as for the bag with crushed rock. Large blocks were also removed from the sample. To comply with the requirements in *NS-EN ISO 17892-5:2017* for this thesis, the TBM spoil and crushed rock was sieved to a distribution adjusted to the size of Anton. The TBM spoil was additionally split and portioned in buckets to reduce the chance of splitting. The experience with this was positive.

Height

The upper 15.7 cm of the cell has a polished surface to reduce the friction between the walls and the plate. In the first tests in 2020 the height was not adjusted accordingly. It is advantageous that the thickness of the layers is adjusted such that the upper surface is placed in the polished area, with a margin of the expected deformations. This can be challenging due to some differences in material.

Plastic sheet

The plastic sheet is placed in the oedometer cell to reduce the friction from the walls. The tests in 2018 was completed successfully with the plastic sheet covering the entire height of the cell, held up by duct tape. This did not succeed in the test in 2020, since the plate got jammed in the duct tape and then loosened, resulting in false deformation. For the next test the plastic sheet was cut in line with the surface of the sample in the cell, resulting in that air escaped between the wall and the plastic sheet at 250 kPa, and no increase in pressure/load. For the tests in this thesis the plastic sheet was cut approximately 10 cm from the top of the cell, to prevent these challenges. It was cut before the final bucket of material was applied. This method was successful for the seven tests accomplished for this thesis.

Water content

The water content in the tests in 2018 was up to 13 %, the experience was that an excess pore pressure in the cell appeared. Making it difficult for the equipment to function. It was considered in this thesis to add water to the TBM spoil, so that that the water content was close to the optimal water content. This was not carried out in concern of experiencing the same challenges as Dahl in 2018. There have not been any problems with excessive pore pressure in the cell during the tests for this thesis.

Time interval of the loggings

The time interval must be defined in the software, meaning how often the deformation is logged during the test. This value is set to 2 – 3 seconds for a test lasting under 8 hours. For the time steps lasting for minimum 70 hours, the time interval is set to 30 seconds due to the size of the text file generated. For test 2 with TBM spoil the first 24 hours had a time interval of 2 seconds, making the calculations difficult, since Microsoft Excel struggles to handle the amount of data generated.

3.1.2 Water content

Samples from the tests are collected to inspect the water content. From the buckets with TBM spoil, one sample from each test is collected ahead of the test. Samples from test 2, 3 and 4 are collected from the top, middle and bottom of the cell when the material is removed from the cell. Two water content samples are collected from the crushed rock, one from the bag and one from test 2. No further samples are collected due to the small water content of the material, less than 0.5 %. The water contents are listed in Table 3.4 on page 53.

3.1.3 Sieving analysis

Four samples of TBM spoil are collected for a tentative sieving analysis. Two samples are collected from test 2 and two from test 3. Those samples are collected from the top and the bottom from the cell. The intention is to investigate if it occurred crushing of material in the contact zones in the top and bottom of the cell. It is expected that a larger amount of material will be crushed in an oedometer cell, than if the material was loaded in a construction situation.

From test 2, the sand layer was removed carefully, and a sample was collected from the top, then a sample was collected from the bottom of the test, by collecting the sample before entering the sand layer. Test 3 had no sand layer, hence it was the upper and lower layer in contact with the steel that were collected. The collected samples were dried for 24-hours before the sieving analysis.

For test 2, 4.4 and 4.5 kg of material were collected from the top and bottom of the cell. For test 3, 14.8 and 16 kg were collected. According to *NS-EN 933-1:2012* when testing material with aggregate size 32 mm, at least 10 kg of material should be sieved (Standard Norge, 2012). Consequently, the sieving analysis accomplished for test 2 is not according to the standard.

The sieving tests are carried out at the Pavement Technology Laboratory at NTNU. The equipment used is a Havier EML digital PLUS, with a time of 3 minutes, 4 intervals and a 1.2 amplitude. The sieving is carried out in two parts; first the material is sieved trough sieves from 22.4 mm to 4 mm. Further on the retaining materiel smaller than 4 mm was collected and sieved further from 2 mm to 63 µm, see Table 3.2. For the material from test 3, the collected sample is distributed over two sieving analyses. This to not overload the equipment.

Table 3.2 Sieving sizes [mm]

First sieving						Second sieving					
22.4	19	16	11.2	8	4	2	1	0.5	0.25	0.125	0.063

Figure 3.8 Sieving equipment

KSR-Maskin accomplished sieving of the spoil when the material was collected from the field site at Åsland and split for the oedometer tests with Anton. Wet screening was achieved, where a sample of 21 to 22 kg of material was collected, then sieved at 22.4, 31.5, 45, 63 and 90 mm. The content of fines is investigated by sieving 5 to 6 kg of the sample with a grain size smaller than 22.4 mm. Then these 5 to 6 kg are washed with a 63 µm sieve, and the material smaller than 63 µm is dried and sieved. The content of fines that is washed off is collected and weighed. Then the grain size distribution is collocated.

The sieving analysis accomplished in this thesis will only be used as a tentative analysis. Since the analysis carried out does not utterly follow the procedure of *NS-EN 933-1:2012* and the method carried out by KRS-Maskin. According to Roberston *et. al.* a wet sieving will result in a higher content of particles <63 µm (Robertson *et al.*, 1984). Consequently, the dry sieving will represent a coarser material. This is unfavourable when the importance of the investigation is to examine if the content of fines increases due to crushing in contact with steel during the oedometer tests.

3.1.4 Calculations

The data provided by the oedometer is the time, deformation and stress, further calculations are needed for the end results. Calculations for the thesis are executed in Microsoft Excel.

The strain is calculated by Equation 2 in chapter 2.2.5:

Equation 2

$$\varepsilon = \frac{\delta}{h_0}$$

ε – Strain [%]
δ – Deformation [mm]
h_0 – Initial height [mm]

The initial height is the height of the sample in the odometer, calculated by subtracting the given height in the oedometer cell, by the measured distance from the sample to the top of the cell. The strain is calculated for each deformation value. The strain is further potted during time or stress.

The stiffness is calculated by Equation 1 in chapter 2.2.5:

Equation 1

$$M = \frac{d\sigma'}{d\varepsilon}$$

M – Oedometer modulus [kPa]
dσ' – Change in effective stress [kPa]
dε – Change in strain [%]

The oedometer modulus is calculated at the end of each load step. 13 load steps are used for the oedometer tests in this thesis, from step 1 at 25 kPa to load step 13 at 500 kPa. Each load step can be seen in Appendix A: Results from laboratory investigations. The change in effective stress and strain is calculated by subtracting the values at the end of each load step:

Equation 4

$$M = \frac{\sigma'_{n+1} - \sigma'_n}{\varepsilon_{n+1} - \varepsilon_n}$$

n – The number of the current load step [-]
σ'_n – The effective stress at the end of load step n [kPa]
ε_n – The strain at the end of load step n [%]

The oedometer modulus in this thesis is given in MPa = 10^{-3} kPa and plotted during stress and dry density.

The time resistance is calculated for the long load increment at 350 kPa for TBM 2, TBM 3 and CR 2. This is accomplished by calculating the ratio for the difference in time and strain at the beginning and end at the increment (Janbu, 1970):

Equation 5

$$R = \frac{dt}{d\varepsilon}$$

R – Time resistance [-]
dt – Change in time [min]

The time resistance number r_s is the slope between the two points:

Equation 6

$$r_s = \frac{dR}{d\varepsilon}$$

dR – Change in time resistance [-]

The dry density is given by the equations (Janbu, 1970):

Equation 7

$$\rho_d = \frac{m_s}{V}$$

ρ_d - Dry density [kg/m^3]
m_s - Weight of dry sample [kg]
V - Volume of sample [m^3]

The dry density is calculated at the end of each load step.

Equation 8

$$m_s = m * (1 - w)$$

m_s - Weight of dry sample [kg]
m - Weight of sample [kg]
w - Water content [%]

The porosity of the material is calculate by the equations (Janbu, 1970):

Equation 9

$$V = \pi r^2 (h_s - \delta_n)$$

r - Oedometer radius [m]
h_s - Height of sample [m]
δ_n - Deformation at end of load step [m]

The porosity is calculated at the beginning and at the end of the tests. The density of the

Equation 10

$$n = \frac{V_p}{V} = 1 - \frac{\rho}{\rho_s(1+w)} * 100\ \%$$

n - Porosity [%]
V_p - Volume of pores [m^3]
ρ - Density [kg/m^3]
ρ_s - Density of the grains [kg/m^3]

grains for TBM spoil and crushed rock is provided by a pycnometer test performed by NGI, ρ_s = 2.69 kg/m^3 (Dahl, 2018). The materials are produced from rock with the same geological conditions, and the same grain density is presumed for the materials.

The modulus number is a parameter that describes the increase in the oedometer modulus with stress. The modulus number is found by contemplate the slope of the trendline of the stress-modulus curve (Janbu, 1970).

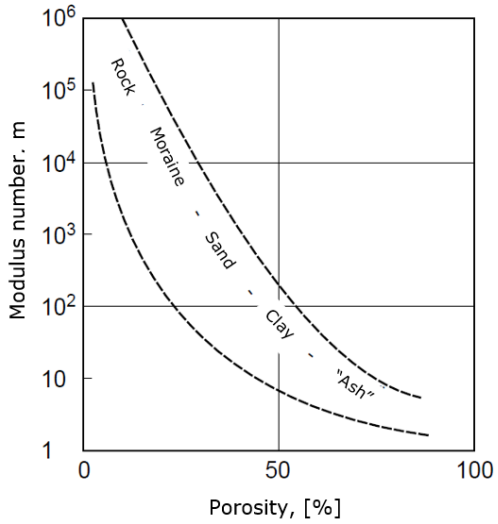

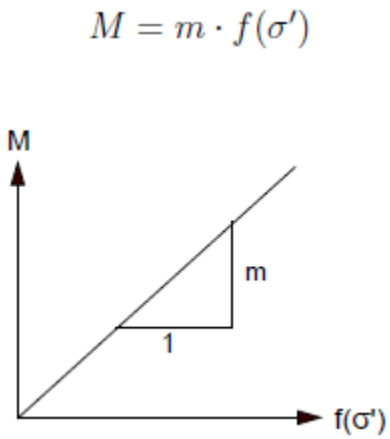

Figure 3.10 Modulus number

Figure 3.11 Empirical values of

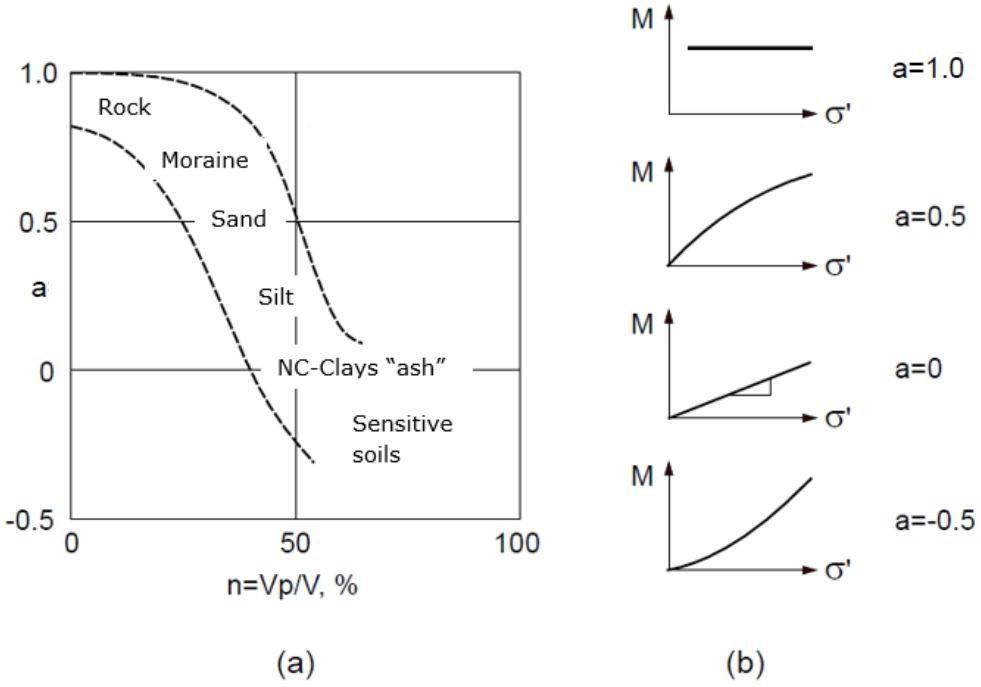

Figure 3.9 (a) Empirical values for the stress exponent (Janbu, 1970) (translated). (b) Different curve shapes for the stress exponent

The stress exponent is given by the shape of the modulus curve, since the shape of the curve gives an indication of the material properties and the character (Janbu, 1970). For granular materials the curve will typically follow the exponential a=0.5. The stress exponent will variate between 0 and 1.0 since the materials experience a parabolic increase in

stiffness with increased stress (Janbu, 1970). The stress exponent and modulus number for the different tests are found by the least squares method in Microsoft Excel.

The stress exponent and modulus number are then utilised to estimate the materials' deformation for an estimated load. Calculated by the equations (Janbu, 1970):

Equation 12

$$M = m\sigma_a \left(\frac{\sigma'_0}{\sigma_a}\right)^{1-a}$$

m - Modulus number [-]
a - Stress exponent [-]
σ_a - Reference stress [kPa]
σ'_0 - Effective stress [kPa]

Equation 11

$$\delta = \varepsilon * H = \frac{\Delta\sigma'}{\mathrm{M}} H$$

H - Height
Δσ' - Change in effective stress [-]

3.1.5 Source of errors

Several factors might have an influence on the results that is represented in this thesis, both attached to human errors and equipment errors. Errors related to human errors are measurements, calculations and choice of method. The measurements of the height of the sample in the oedometer cell is a mean value, the height of the sample could vary up to 1 cm in the same test. The height measurements influence the strain, density and oedometer modulus results.

These results are also influenced by the amount of material in the cell. However, the tests are built with the intention to be as equal as possible. This might be challenging to carry out with large amounts of material, where small variations in the material can have an impact on the height of the test. This can lead to the need of an extra layer, existing of 15 kg of material that is compacted. This in turn can make the material appear stiffer, since the upper layer is compacted better than the other layers.

Logging during the tests generates large amounts of data. During the tests time, load and deformation are logged continuously. This resulted in a total of approx. 144 000 loggings for each parameter for the seven tests. Small errors in equation formulations and selection of values might also have a large impact on the results.

The accuracy of the oedometer is essential for the reliability of the results of this thesis. The equipment was calibrated before the tests were performed. The accuracy of the deformation values in the oedometer is ± 0.07 %. The accuracy of the strain values is dependent on the manual measurement of the height.

The water content in the material is an average value from multiple water content samples. One sample from one of the buckets from each test with TBM spoil was collected before the oedometer tests were started. After the tests was finished some samples was collected from different heights in the cell. The number of water content samples varies from test to test.

For the TBM spoil the most accuracy would be to take samples from each delivered bucket. This was not achieved, since the water content values had small variations. The crushed rock had minor variation in water content, and therefore few samples were collected. The accuracy of these values could be more precise if several samples were collected before and after the oedometer tests.

The TBM spoil is collected at the field site at Åsland, split into different sieving sizes and then portioned to fit the scaled grain size distribution. The placement of the collected material could have an impact of the material since the material could be more crushed in the upper layer of the filling. This can impact the mechanical propertied of the material. The scaled material could also depart from the original material.

The sieving analysis performed is a dry sieving, where two of the sieving samples did not fulfil the requirements of the standards regarding weight. The sieving analysis accomplished is a tentative analysis. A dry sieving will result in a sieving curve with a reduced amount of fines < 63 µm (Robertson *et al.*, 1984). The initial sieving curves for the TBM spoil utilised is carried out by KSR-Maskin with a wet sieving. These curves will have a larger amount of fines, and the spoil that is dry sieved could appear as a coarser material.

3.2 Material tested

The standard *NS-EN ISO 17892-5:2017* requires that the mean diameter of the largest particle in a material tested in an oedometer should not exceed 1/5 of the oedometer ring (Standard Norge, 2017). The TBM spoil tested by Dahl and in November 2020 had particles up to 100 mm, shown as "complete sieve analysis" in Figure 3.12. To comply with the standard for this thesis the TBM spoil and the crushed rock is scaled by size. This is done by the parallel gradation method, this size-scaling technique consists in scaling coarse particles to smaller particles, by using the same scale ratio for all particle sizes. The intention with the method is to reproduce the original geotechnical properties of the material (Dorador and Villalobos, 2020).

3.2.1 TBM spoil

The spoil is collected from the field site at Åsland, from the Follo Line Project south of Oslo, see Chapter 2.2 for further details about the properties of the material. KSR – Maskin have collected, split the material to different fractions and sieved the material, then distributed the material in buckets of 12.5 litres. The grain size that exceeds 31.5 mm are removed due to the diameter and height relation in the oedometer. The grain size distribution for the complete analysis and the downscaling for Anton is shown in Figure 3.12.

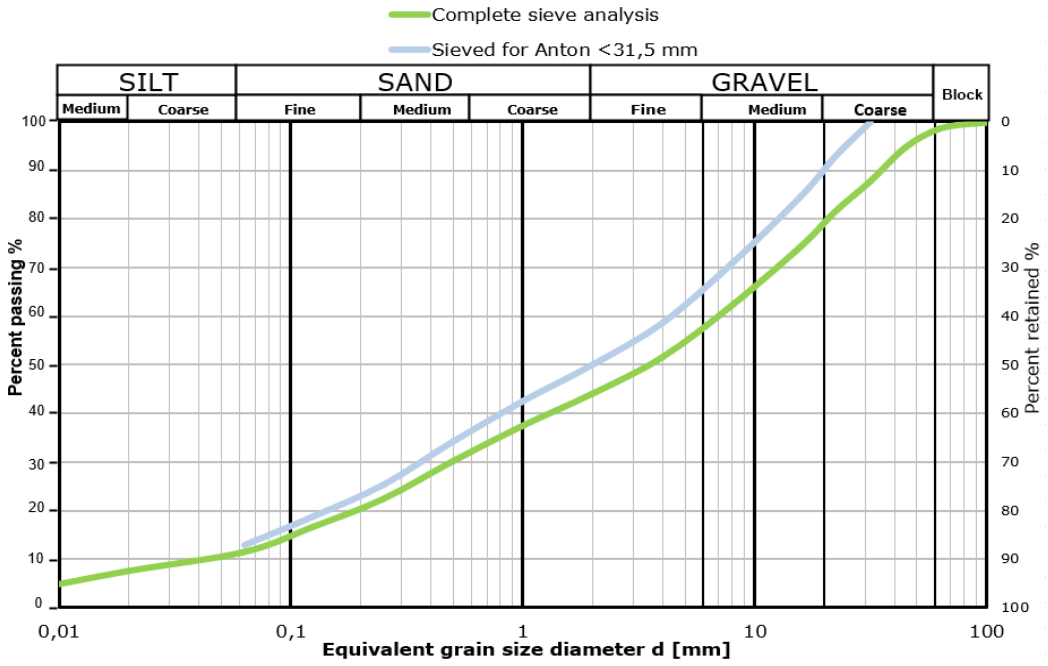

Figure 3.12 Sieving analysis of TBM spoil, accomplished by KSR Maskin

Figure 3.13 TBM spoil in the delivered buckets

3.2.2 Crushed rock

The crushed rock (CR) is produced and delivered by Franzefoss rock-crushing plant. Franzefoss has sieved and compiled the material to a sieving curve between 0 – 32 mm. This to simulate a grain size distribution with a maximum grain size comparable to the tested TBM spoil, and to adjust to *NS-EN ISO 17892-5:2017*. The geological conditions are similar to the TBM spoil, consisting of gneiss and granite. Figure 3.14 shows the sieving curve for the crushed rock, where the dashed lines are the allowed maximum and minimum contents.

Note that the material is produced by crushing rock blasted in a day zone. This material is excavated from hard rock, produced to have favourable mechanical properties. Materials produced from tunnel excavation is produced as a result of the most cost-efficient excavation, not for its properties. This will affect the excavated material properties as grain shape and content of fines. Thus, the crushed rock from Franzefoss will divide from the blasted rock when it comes to content as grain shape and mechanical properties. The common features will be grain shape distribution and mineralogy.

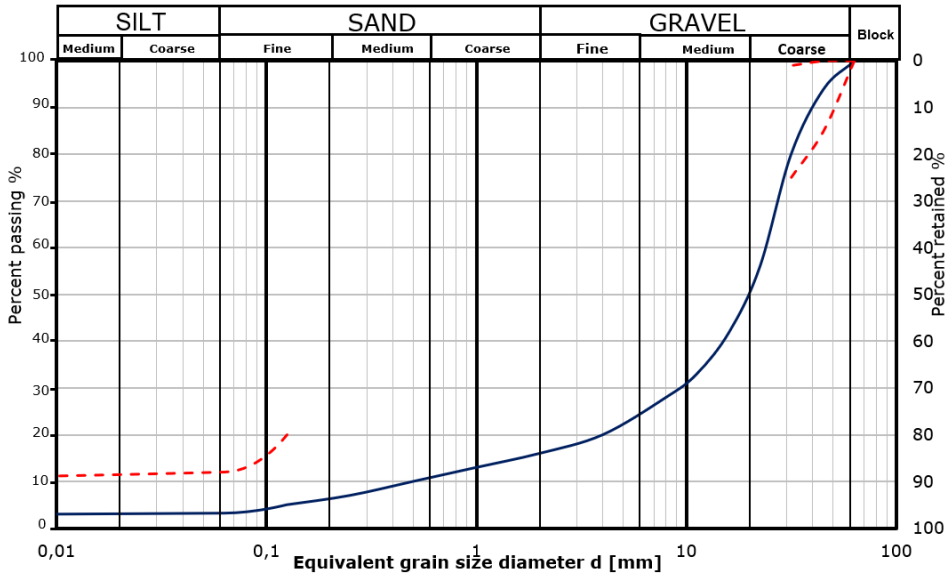

Figure 3.14 Sieving curve of the crushed rock, accomplished by Franzefoss

Figure 3.15 Crushed rock placed in oedometer cell

3.2.3 Sand

The sand utilised for the layers in the top and bottom of the oedometer is from the Stokke gravel pit in Kvål, Melhus municipality. The sand is glaciofluvial deposit and in the 0/2 mm fraction (NGU, 1985). The sand has a water content of approximately 3 – 5 %.

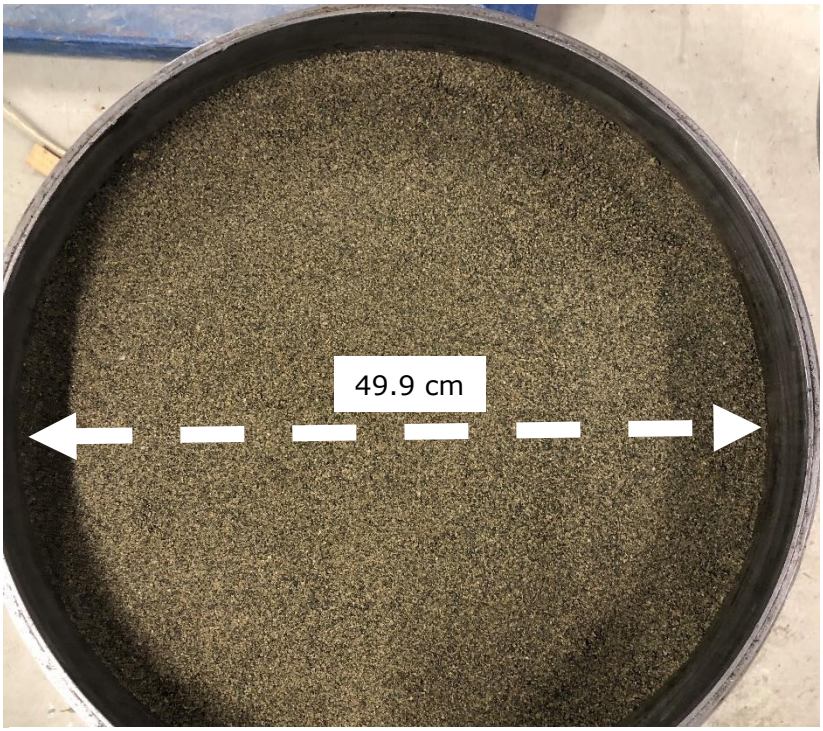

Figure 3.16 Picture of the sand used in the upper and lower layer

3.3 Results of the laboratory investigations

3.3.1 Collocation of tests

Index properties

Table 3.3 and Table 3.4 contain index properties of the materials utilised in the tests, for detailed results see Appendix A: Results from laboratory investigations. The water content for the TBM spoil has small variations for each test, were the total measured values varieties from 4.9 % to 7 %. The values listed in Table 3.4 is an average of multiple water content samples for each test.

Table 3.3 Weight, layers and length of tests

	Test number	Weight [kg]	Number of layers	Test height [cm]	Test length [hours]	Comments
TBM	1	186.7	5.5	51.2	4.3	
	2	193.2	5.5	54.2	75.8	70 hours load increment at 350 kPa.
	3	190.8	5	52.6	76.9	70 hours load increment at 350 kPa. No sand layers.
	4	197.4	5.5	54.0	5.5	
CR	1	163.5	4.5	49.7	3.5	
	2	194.6	6	52.2	75.2	70 hours load increment at 350 kPa.
	3	195.0	6	54.2	5.3	

Table 3.4 Index properties

	Test nr.	Dry density [t/m3]		Water content [%]		Oedometer modulus [MPa]	Strain [%]	Porosity [%]		
				before	at end			before	at end	change
TBM	1	1.74	1.96	6.5 %	6.5 %	9.34	11.01 %	34.9 %	26.8 %	8.1 %
	2	1.70	1.93	6.0 %	6.7 %	9.11	11.70 %	36.5 %	28.1 %	8.4 %
	3	1.75	1.96	5.8 %	5.5 %	9.40	10.79 %	34.6 %	28.2 %	6.4 %
	4	1.76	1.96	6.5 %	6.4 %	9.04	10.70 %	34.5 %	26.9 %	7.6 %
	Average	*1.74*	*1.95*	*6.2 %*	*6.3 %*	*9.23*	*11.05 %*	*35.1 %*	*27.5 %*	*7.6 %*
CR	1	1.68	1.72	0.13 %	-	27.56	2.45 %	37.5 %	36.1 %	1.5 %
	2	1.90	1.94	0.28 %	-	29.94	1.78 %	29.3 %	28.1 %	1.3 %
	3	1.83	1.87	-	-	32.20	1.92 %	31.8 %	30.6 %	1.2 %
	Average	*1.80*	*1.84*	*0.20 %*	*-*	*29.90*	*2.05 %*	*32.9 %*	*31.6 %*	*1.3 %*

The TBM spoil had small variation in total strain, variating with a total of 1 %. Test 1, 2 and 4 had a thinner layer on top due to adjustment of height, the layer consisted of approximately 15 kg of material. This did not seem to have an impact on the results. Test 3 had no sand layer, to investigate if any crushing of material occurred. The strain values did not seem to be affected by this, but the material is stiffer than the other tests and has a smaller change in porosity. Further discussion of the crushing of the material is accomplished under Figure 3.23 at page 59.

The crushed rock has as expected smaller strain, smaller change of porosity and a higher oedometer modulus, caused by more favourable mechanical properties in terms of coarser material. The material has a an average oedometer modulus of 29.9 MPa and an average strain of 2.05 %. The material is three times stiffer than the spoil, with an average of 9.2 MPa and 11.05 %. When the load increments were applied some creaking noises came from the material inside the oedometer. This can indicate that crushing of the material occurred when the load was applied. This did not occur for the TBM spoil.

Oedometer results

In Figure 3.17 the stress during the load steps is shown, the TBM spoil has higher strain values, where test 2 of TBM spoil has the largest strain of the seven tests. Test 2 of crushed rock has the lowest strain values, where small variations are separating test 2 and 3.

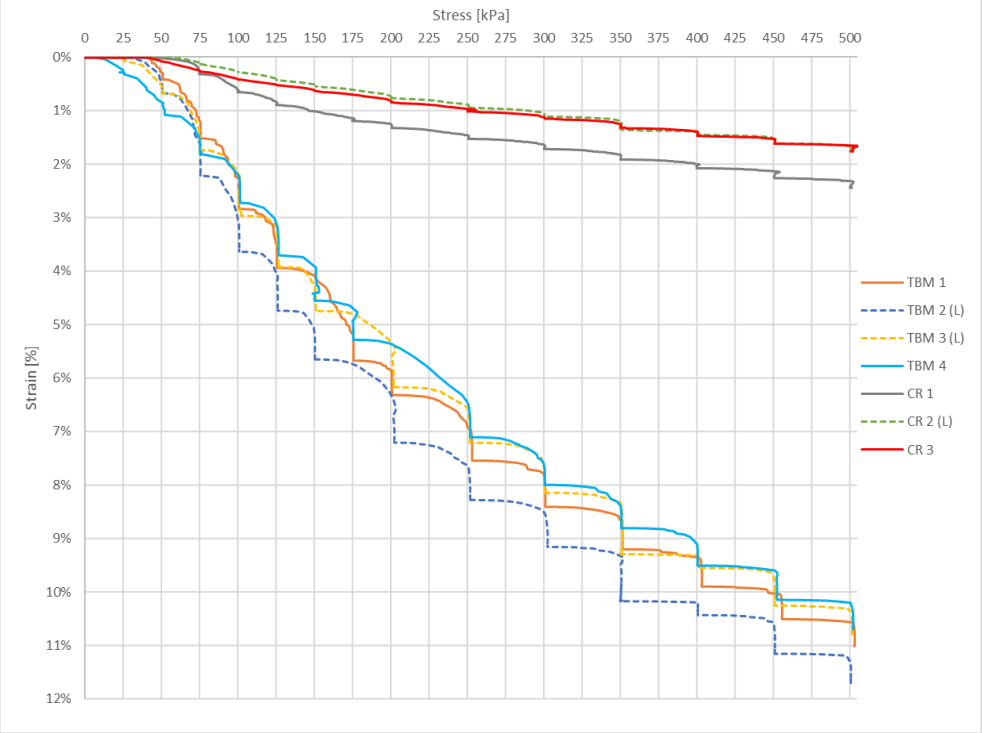

Figure 3.17 Collocation of the results of stress-strain, the tests with 70 hours load step of 350 kPa have dashed lines and are marked with (L)

Figure 3.18 indicates that the primary consolidation is higher for TBM spoil than the crushed rock, since the deformation for the crushed rock does not seem to decline for the period of the load steps. For higher loads a secondary consolidation occur since the deformation requires more time to equalise.

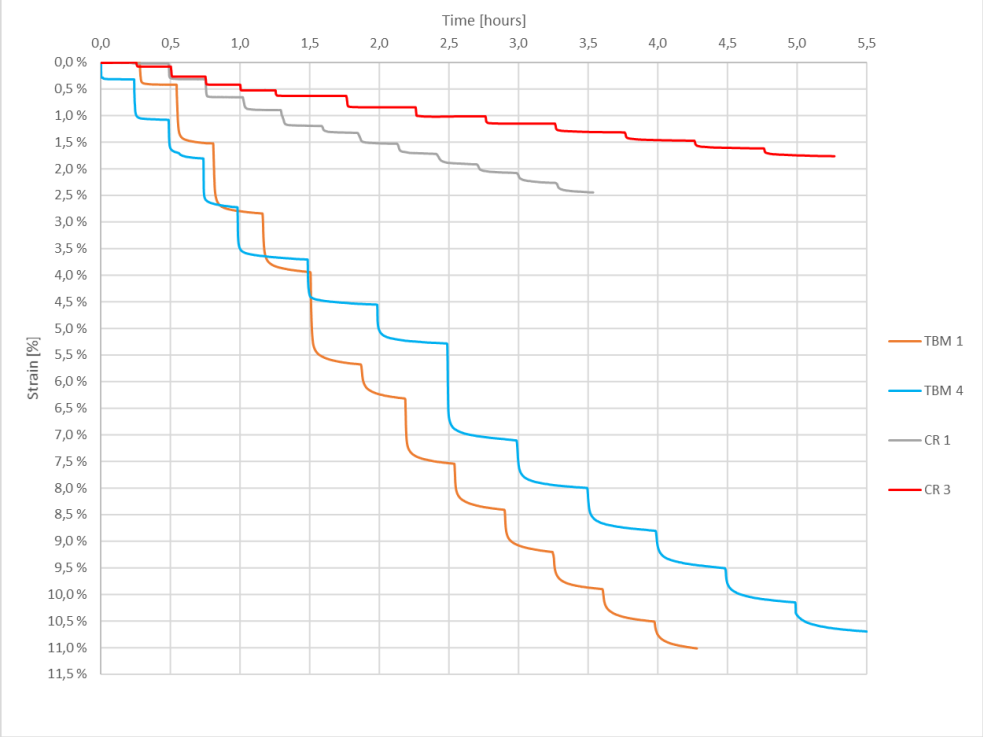

Figure 3.18 Time – stress curves for the tests lasting < 6 hours

Figure 3.18 shows the strain during time, for test 1 and 4 of TBM spoil, and test 1 and 3 of crushed rock. Test 2 and 3 of spoil and 2 of crushed rock is not included. This because these tests lasted for nearly 75 hours, and the inclinations of the short tests would be challenging to interpret. The graphs indicate that the materials are instantly responding when the stress is applied, representing the initial compression of the material. The strain stabilises after a few minutes, but for larger stresses the strain curve does not flatten out. Indicating that the material has some creep settlements for higher load steps. These creep settlements are larger for the TBM spoil than the crushed rock. The creep settlements for the crushed rock appear clearer in Figure 3.35, Figure 3.38 and Figure 3.40.

Figure 3.19 shows the strain at the end of each load step. Note that the correspondence between the tests appears clearer from this figure. Test 1, 3 and 4 of TBM spoil are synchronous with approximately 0.5 % difference in strain throughout the tests. When test 2 is included, the total difference in strain does not exceed 1.5 %. The results of the tests are considered to be reliable and valid. The difference in load step and time for the different tests appear clear in Figure 3.17.

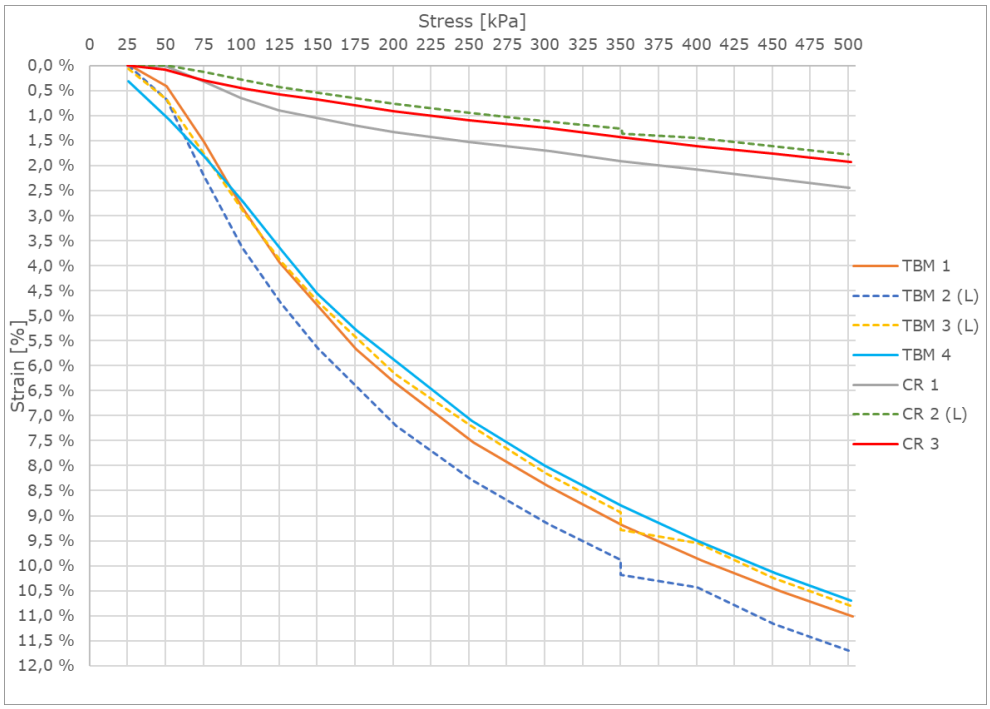

Figure 3.19 Stress – strain at the end of the 13 load steps

The dashed lines in Figure 3.19 are the results from the tests with the 70-hour time steps of 350 kPa. This illustrates that the materials adjust to its initial pathway after the load step. Figure 3.20 shows the strain during time for the 70-hour load step at 350 kPa for test 2 and 3 with TBM spoil. The dart is illustrating when the deformation is flattening out and reaches

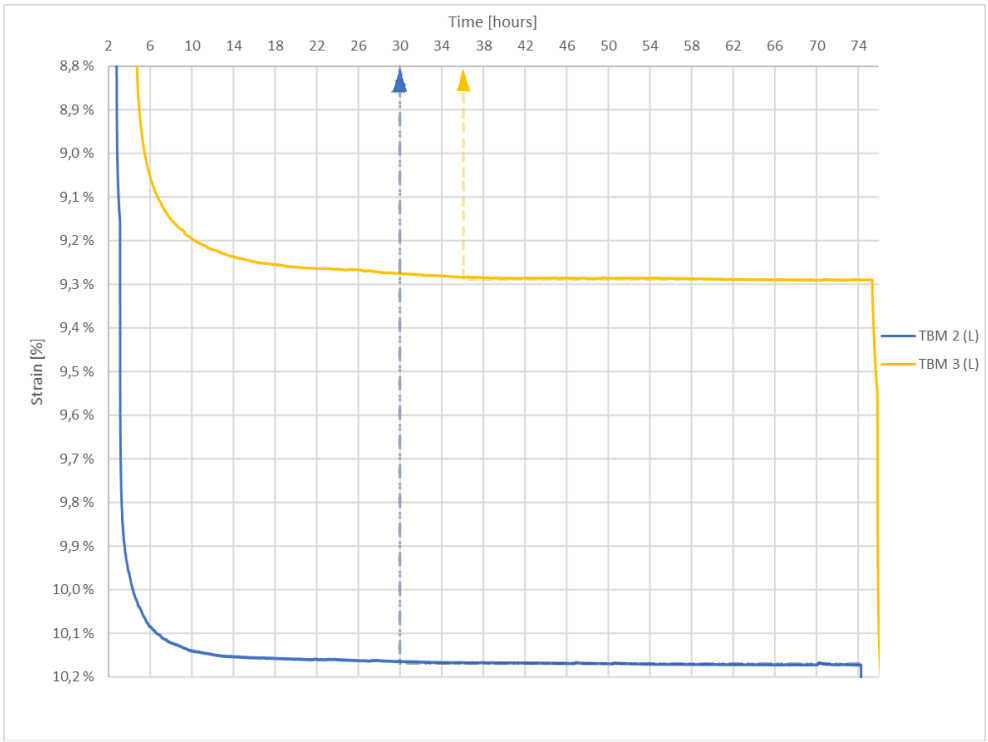

Figure 3.20 Time – stress curves for the long-time increment (350 kPa) for test 2 and 3, the time is given from the start of the test

the end value for the increment. These shows that the strain is equalising after 28 (TBM 2) to 30 (TBM 3) hours after the load step is applied. The time resistance R for TBM 2 is higher (418 828) than for TBM 2 (368 100), with a time resistance number r_s of 98 and 86. In chapter 3.3.3 and 3.3.4 more detailed descriptions of these results are accomplished.

The graphs in Figure 3.21 indicates that the crushed rock has generally 4 to 6 times higher stiffness than the TBM spoil. The variation in the long tests before and after 350 kPa is due to the high difference in strain at that point. The large differences in stiffness for the crushed rock shows the variation of material. This is due to the different grading throughout the bag. The same problem occurred whilst testing TBM spoil delivered in large barrels during the specialisation project for this thesis.

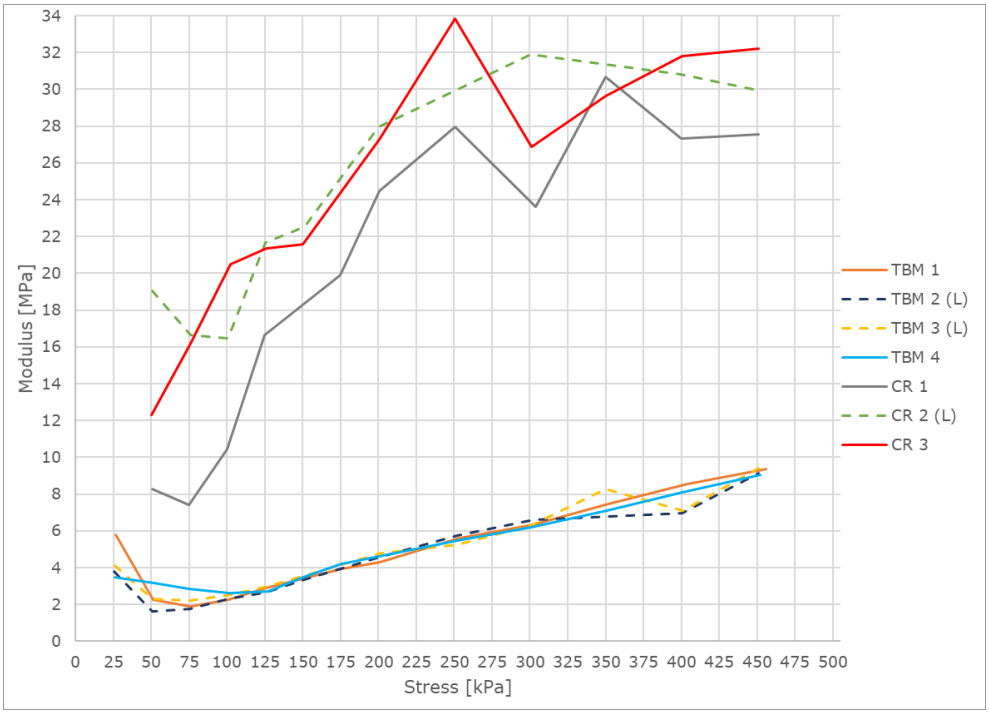

Figure 3.21 Stress – modulus curves

The oedometer modulus is plotted with dry density to investigate the compaction of the material. Where the largest difference is for the crushed rock, where test 1 is the test with poorest compaction. The reason for this is likely due to the coarse grain size distribution compared to the two other tests. When comparing the TBM spoil, test 3 that did not have any sand layers, is generally less stiff than the other test, but has the highest oedometer modulus and density at the end of the test. The material with higher modulus and higher dry density has better compaction.

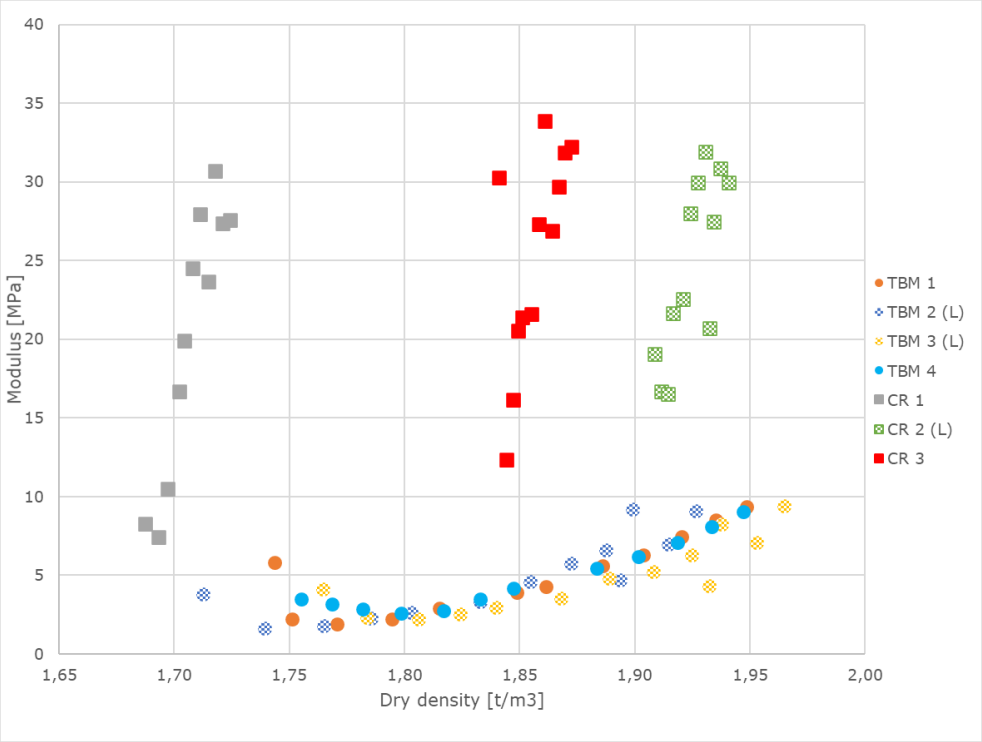

Figure 3.22 Dry density – modulus

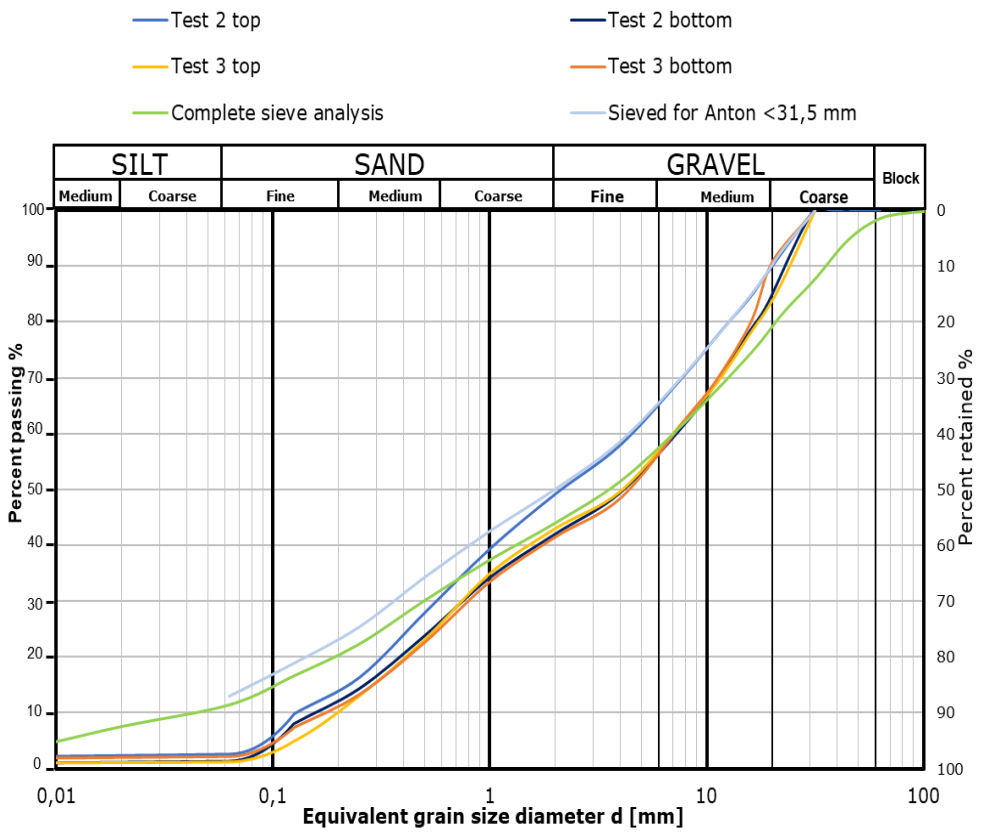

Figure 3.23 Collocation of sieving analysis, material before and after oedometer tests

Material from the top and bottom of the cell was collected from test 2 and 3, with the intention to investigate if any crushing occurred in the cell. In Figure 3.23 the results from the sieving analysis are shown combined with the sieving accomplished by KSR Maskin.

Test 2 had a sand layer in the top and bottom of the cell, test 3 did not have sand layers. The intention of the sand layer was to reduce crushing due to contact with the steel and to levelling out the stress. The sieving curve for test 3 is expected to have a lager content of fines compared to test 2. The collocation of the analysis shows that the material from both tests is generally uniform. The sample from the top of the cell in test 2 have some higher content of fines. This can be caused by that some sand is included in the sample, since the sieving curve has considerable higher values in the 0/2 mm interval. The sample weight from test 3 had a smaller weight than what is required by *NS-EN 933-1:2012*, if a larger sample was collected it could have resulted in a higher content of coarser fractions.

The material from test 3 has the smallest content of fines, contradictory to the expectations from the results. All the samples had a lower content of fines than the sieving curve accomplished by KSR-Maskin, as discussed in Chapter 3.1. Where the samples were uniform to the complete sieve analysis for TBM spoil for coarser sand and gravel. The sample collected from the top of test 2 is more uniform to the material sieved for Anton. The reason for this can be due to the difference in sieving method. Since the total result has a reduced content of fines, this can indicate that the oedometer test does not cause any crushing of the material.

3.3.2 TBM spoil, test 1

The first test with TBM spoil had initially 15 minutes load steps. The time period was based on the tests accomplished in the specialisation project and from the results in Dahl's thesis (Dahl, 2018). When the deformations did not stabilise during the three first load steps, the time increments were extended five minutes. The buckets for this test had a smaller weight than the other tests, and the total weight was lower. The weight of the test does not seem to have a significant impact of the strain values compared to the other tests. A lower weight can impact the strain in terms of lower strain values, since the layers will be thinner and more compacted. However, this is not indicated in Figure 3.22.

The strain was higher than the expected values, where previous oedometer tests with TBM spoil have had between 3.5 to 10 % strain. The water content was taken from one of the buckets ahead of the test and had a value of 6.5 %, which is in the lower range of the material tested by Dahl (6.2 – 10.2 %).

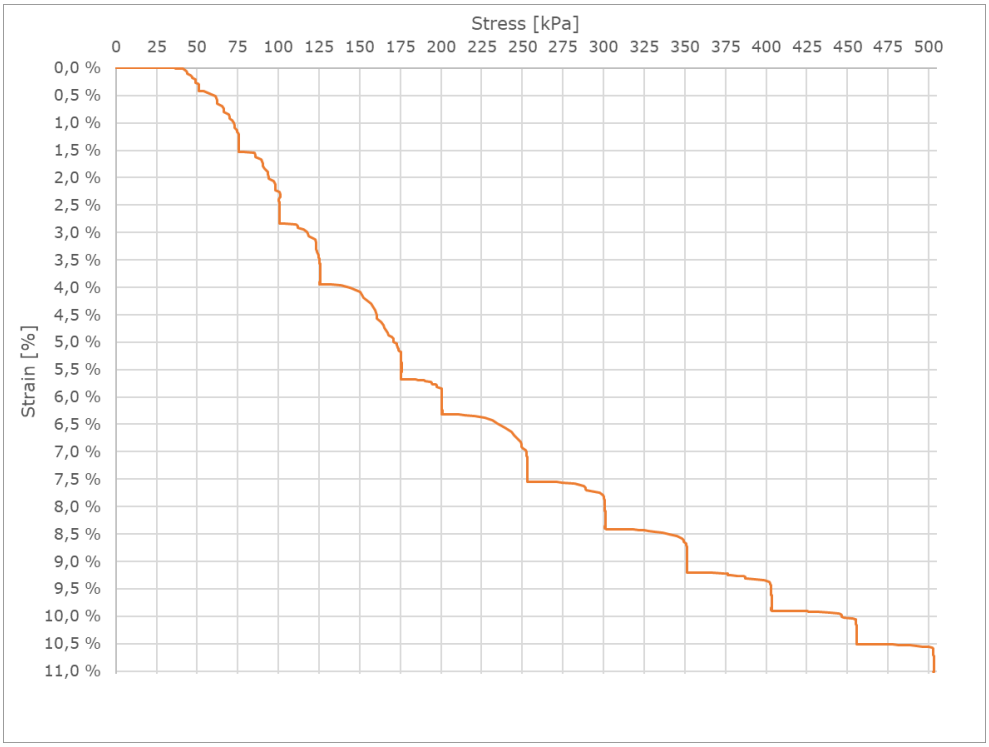

Figure 3.24 Stress – strain for TBM 1

The uneven behaviour of the graph in Figure 3.24 is caused by the delay of the pressure wheel used to increase the stress in the cell, and the load must be applied gradually. The strain caused by the stress have a higher increase for the lower values before the increase of strain is reduced.

Figure 3.25 shows the strain during time. The material is responding instantly when the load is applied, before it is flattening out when the increase of load is stopped. When the load exceeds 100 kPa the creep settlements increase.

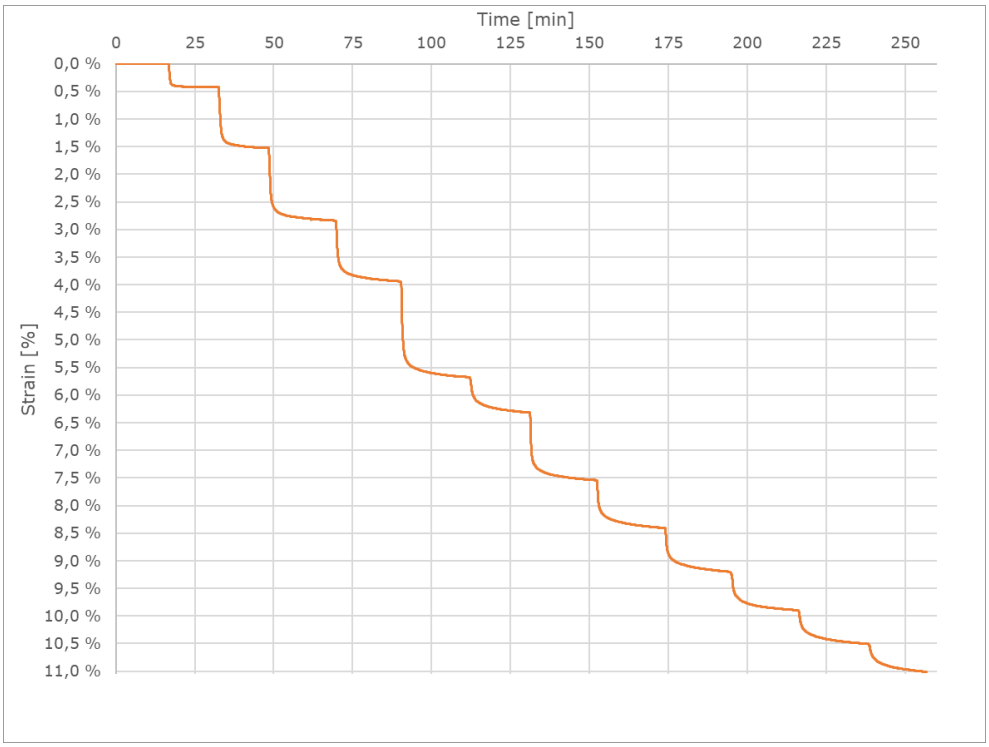

Figure 3.25 Time – strain for TBM 1

3.3.3 TBM spoil, test 2

The load increments for test 2 were longer than for test 1. In particular the increment at 350 kPa that was applied for 71 hours. The intention of the long increment is to investigate the creep settlements over a "short-long term" situation. The long load increment constituted a settlement creep of 0.3 %. The values for water content in the cell indicate higher values for the upper and lower layer. The sand used in the layers was not dried and had a water content of 3 – 5 %.

Table 3.5 Water contents for test 2

Location	Water content
Bucket	6.0 %
Top	6.7 %
Top (sieving)	6.5 %
Middle	6.4 %
Bottom	7.0 %
Bottom (sieving)	6.7 %
Average from cell	6.7 %

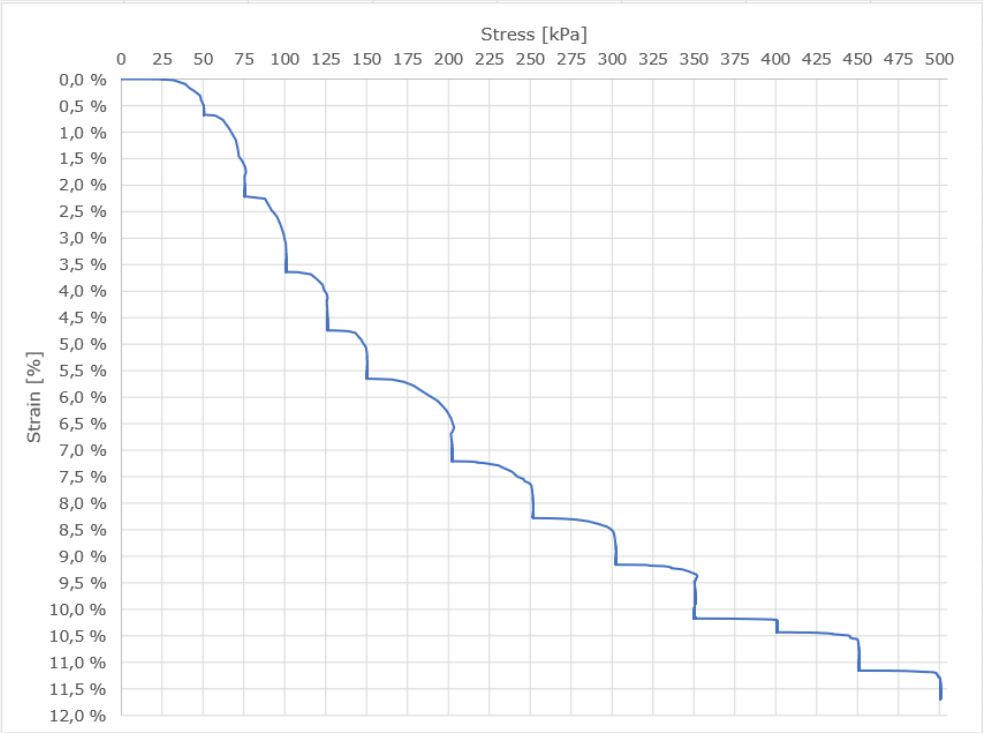

Figure 3.26 Stress – strain for TBM 2

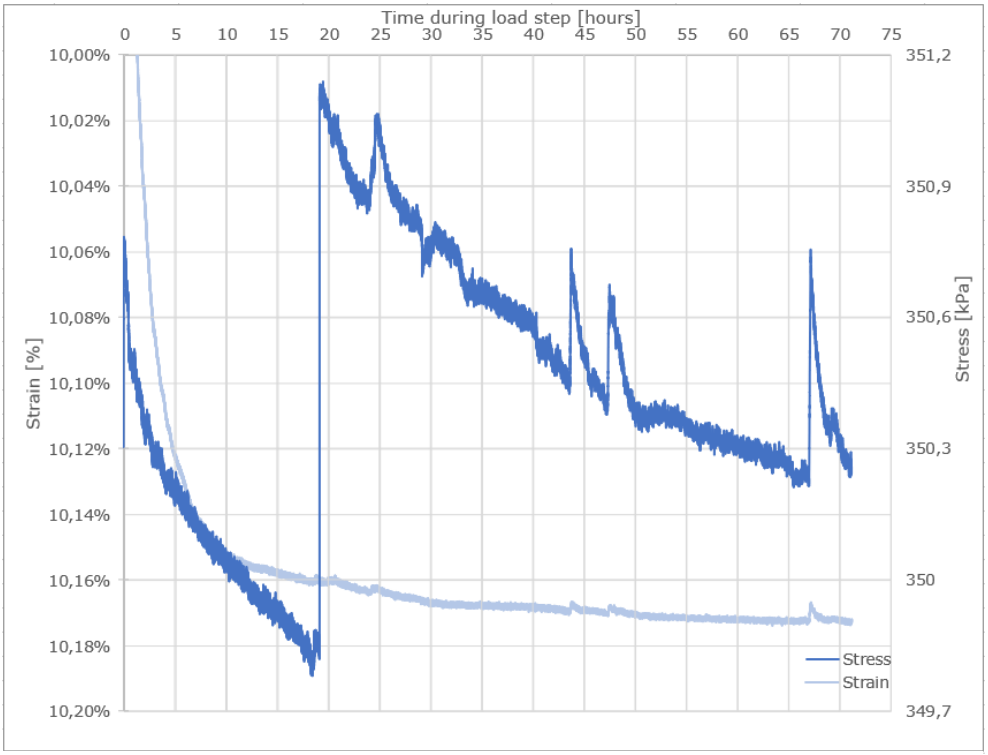

Figure 3.27 Time during the 70-hour load increment – strain and stress for TBM 2

The material used for the test has similar behaviour as test 1, but has some higher strain values, generally 0.5 % above the values for test 1. The load step of 350 kPa is shown in Figure 3.27, where the dark blue line represents the stress during time, and the lighter blue represents the contemporary strain. The strain values can be seen on the left axis, and the stress on the right axis. This graph is included to show the behaviour of the material during the time step, also to indicate when the strain is caused by increase in stress.

The stress in the cell shows a tendency to decrease over a longer period. Consequently, it can be necessary to adjust the stress during the load increment, if the stress decreases under 350 kPa. This can be due to air leakage from the cell. Adjustment of the air pressure has only been necessary for the longer time increments, and not for increments ongoing for 20 – 30 minutes. The equipment used for adjustment of stress is sensitive, and a large leap of stress is seen in the graph when the stress is adjusted.

The strain value is 9.88 % after the first 20 minutes, a normal load increment, after 71 hours the strain increases to 10.17 %, an increase of 0.29 % strain. The strain stabilises at 10.17 % after 28 hours after the load step was applied. The adjustment of load is achieved after 19 hours. The material is not corresponding directly from the increment but has a slow increase in strain. Small increments in stress can be seen with corresponding decrease in strain. A coherence can be that the material is relocating in the cell, and an increase in stress is occurring.

Figure 3.28 shows the strain over time before and after the long increment, the time step of 350 kPa is not included, since the scale made it difficult to see the inclination of the strain. The strain before the 70-hour time step can be seen at the upper axis, 0 to 3.5 hours. The time after can be seen at the lower axis, 72.5 to 76.0 hours.

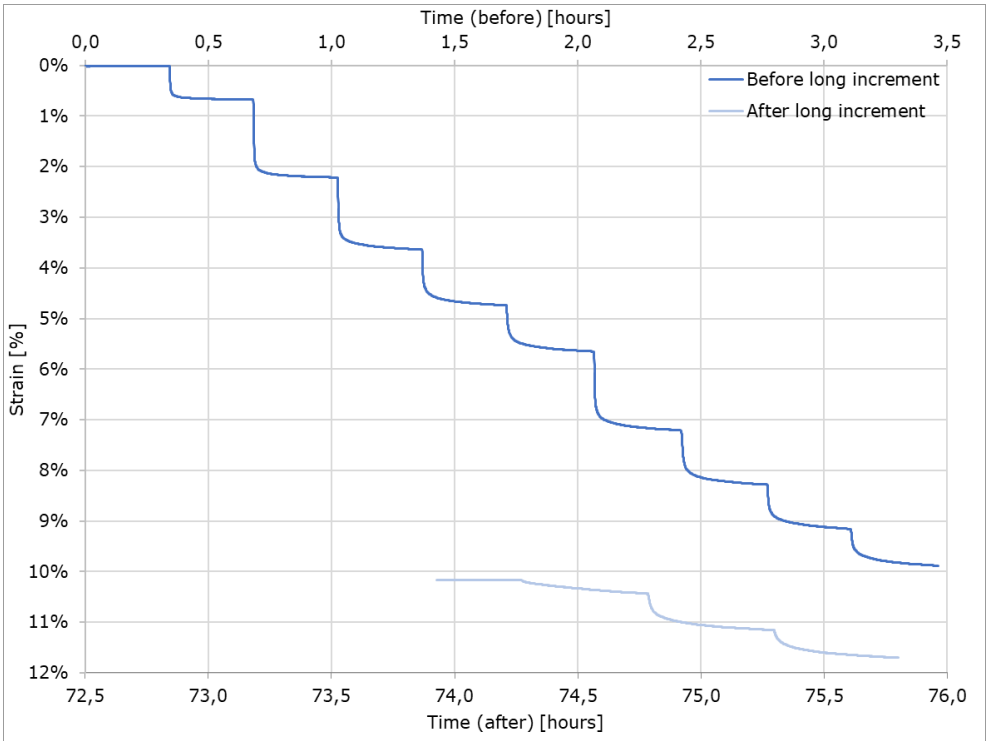

Figure 3.28 Time before long increment (upper x– axis) and after (lower x-axis) – strain for TBM 2

Prior to the long increment, the increments lasted for 20 minutes, followed by 30 minutes. The graph is indicating that the strain curve requires more time to flatten for larger loads than for smaller loads. The load increment 400 kPa has a smaller leap in strain than the other increments. This can be a consequence of step 350 kPa that had a larger increase in strain.

3.3.4 TBM spoil, test 3

To inspect the crushing of material in the contact zones between the top and bottom of the cell and the material, test 3 did not have sand layers. Samples from the upper and lower layer was collected and sieving tests were accomplished, the results of these are shown in Figure 3.23 in chapter 3.3.1. The water content from different locations in the cell, shows the same indication as for test 2, where the water content is higher in the top and bottom of the cell.

Table 3.6 Water contents for test 3

Location	Water content
Random bucket from test	6.0 %
Top	5.6 %
Top (sieving)	5.8 %
Middle	4.9 %
Bottom	6.1 %
Bottom (sieving)	6.1 %
Average from cell	5.7 %

The increment at 350 kPa for this test was maintained for 70 hours. The strain and stress curve in Figure 3.29, has the same indication as for test 2, here the load step at 400 kPa has a lower increase in strain compared to the other stress values. The strain increase for the steps are even over and under 350 and 400 kPa. The strain increment for the long-time step at 350 kPa added with the increase for the 400 kPa step, constitutes a value that is lower

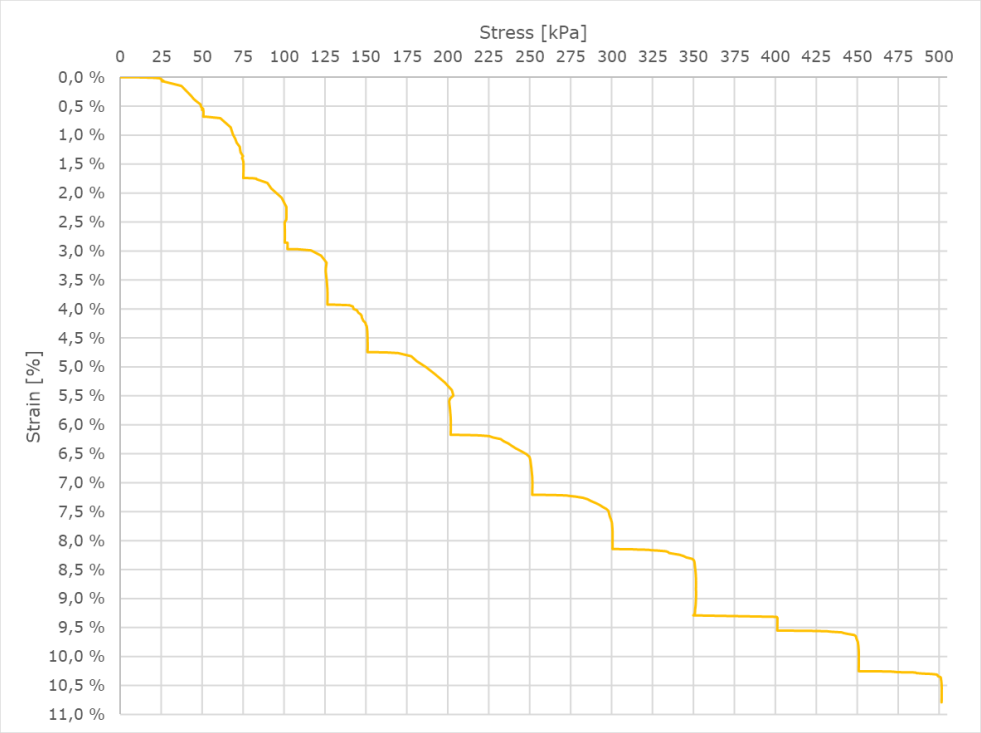

Figure 3.29 Stress – strain for TBM 3

than the average strain increases for the other steps. In total the high strain increment for 350 kPa and the lower increment for 400 kPa equalises. This can be seen clearly in Figure 3.19 in chapter 3.3.1.

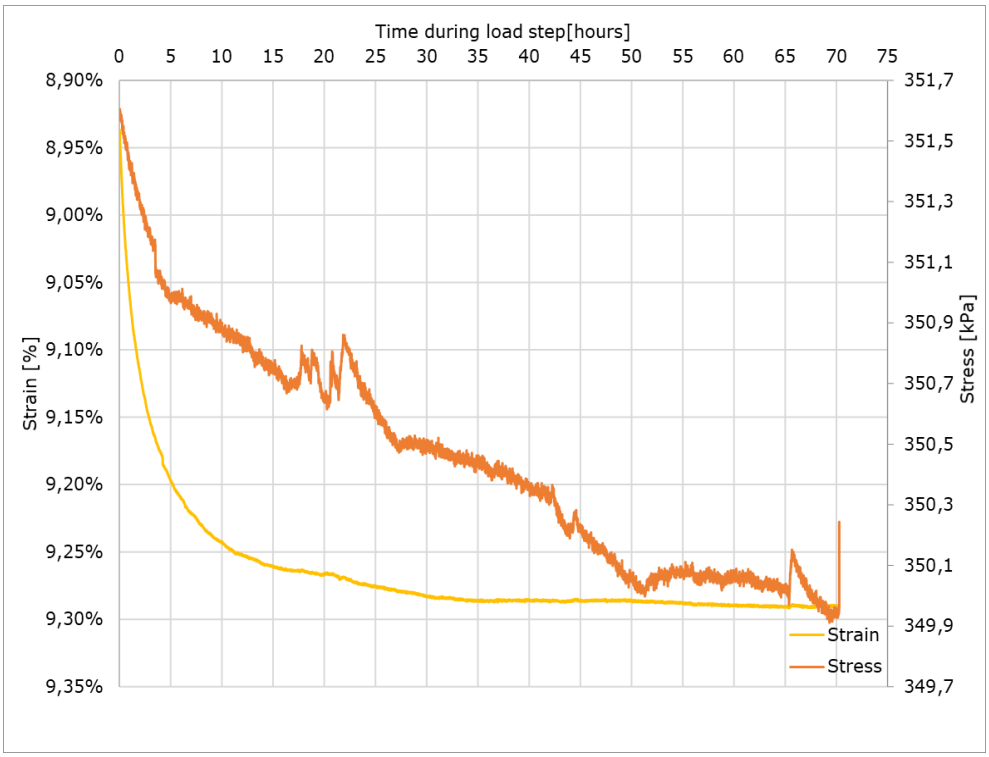

Figure 3.30 Time during the 70-hour load increment – strain and stress for TBM 3

Figure 3.30 shows the strain and stress curves for the load step at 350 kPa over time. The strain values are indicated by the yellow curve, where the appurtenant values are on the left axis. The orange curve is the stress curve, here the values are on the right axis. The stress level in the cell was not increased manually during the load step. The stress in the cell is steadily declining during time but have some increases when the material is settling. The settling is barely seen in the strain curve but are clearly indicated for the stress curve.

Figure 3.31 shows the strain over time before and after the long increment. The time step of 350 kPa is not included, since the scale made it difficult to see the inclination of the strain. The strain before the 70-hour time step can be seen at the upper axis, 0 to 5.5 hours. The time after can be seen at the lower axis, 72.5 to 77.5 hours. The load steps were applied for 30 minutes for each step, except from 350 kPa. The larger load steps from 200 kPa and above have a smaller equalisation during time than the smaller load steps.

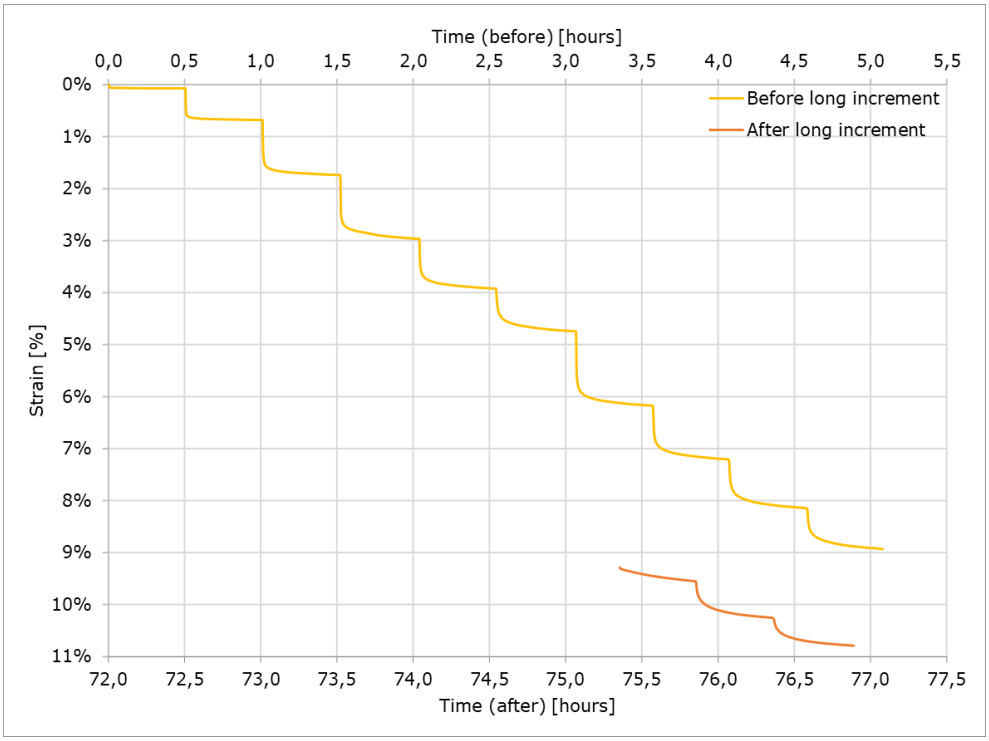

Figure 3.31 Time before long increment (upper x– axis) and after (lower x-axis) – strain for TBM 3

3.3.5 TBM spoil, test 4

Due to limitation of time, test 4 had 15 minutes load increments until 100 kPa, followed by 30 minutes increments. The test had the highest weight of the four test, 10.6 kg heavier than test 1. The water content taken from the cell has in contrast to test 2 and 3 a higher water content in the middle than in the top and bottom.

Table 3.7 Water contents for test 4

Location	Water content
Random bucket from test	5.8 %
Top	6.4 %
Middle	6.8 %
Bottom	6.0 %
Average from cell	6.4 %

An error was made when the load step 175 kPa was applied for 30 minutes instead of 200 kPa. This is shown in Figure 3.32 by the high increase in stress. This error can result in some lower strain values compared to the other tests. The strain values from test 3 and 4 are even, separating the strain with 0.1 %. Test 4 has the highest strain values for load under 50 kPa, but the smallest strain in total of the TBM spoils.

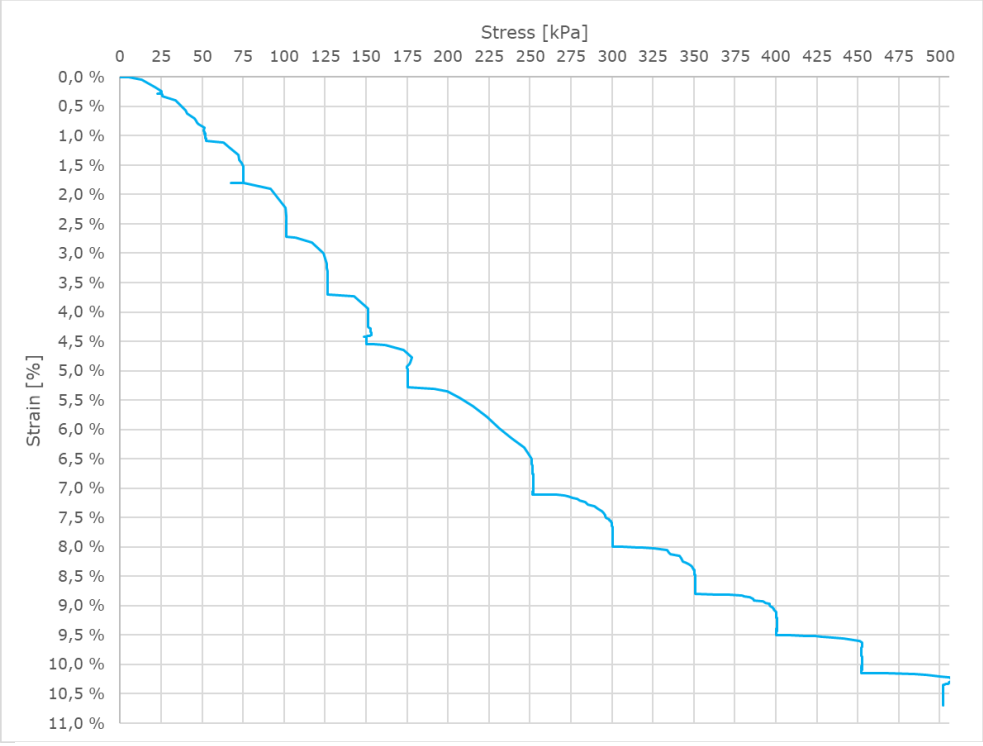

Figure 3.32 Stress – strain for TBM 4

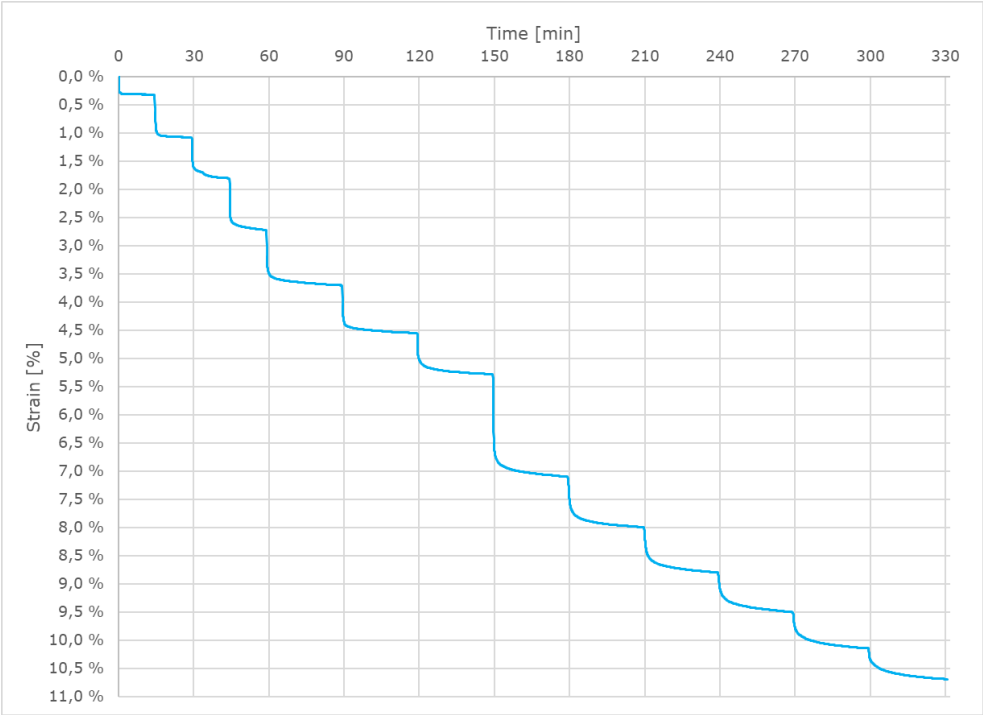

Figure 3.33 Time – strain for TBM 4

Figure 3.33 shows that the strain values do not equalise during the time of the load steps. For this test it could be favourable to extend the time of the load steps further.

3.3.6 Crushed rock, test 1

Test 1 with crushed rock was the first test accomplished for this thesis. The test had the lowest weight in total and had the shortest time increments. One sample from the bag was dried to investigate the water content of the material. No further samples were collected for this test since the water content in the material was comprehended as uniform. A large amount of dust was whirled up when the material was spaded out of the bag into the cell and compacted.

The bag with material was not sealed and the material was in contact with air, and the material appeared as desiccated. The water content for this test was 0.13 %. The sample was taken from the top of the bag and had a small amount of fines compared to the other tests. Larger particles can lead to a larger degree of crushing, since the voids between the large particles are filled with air, and not smaller particles.

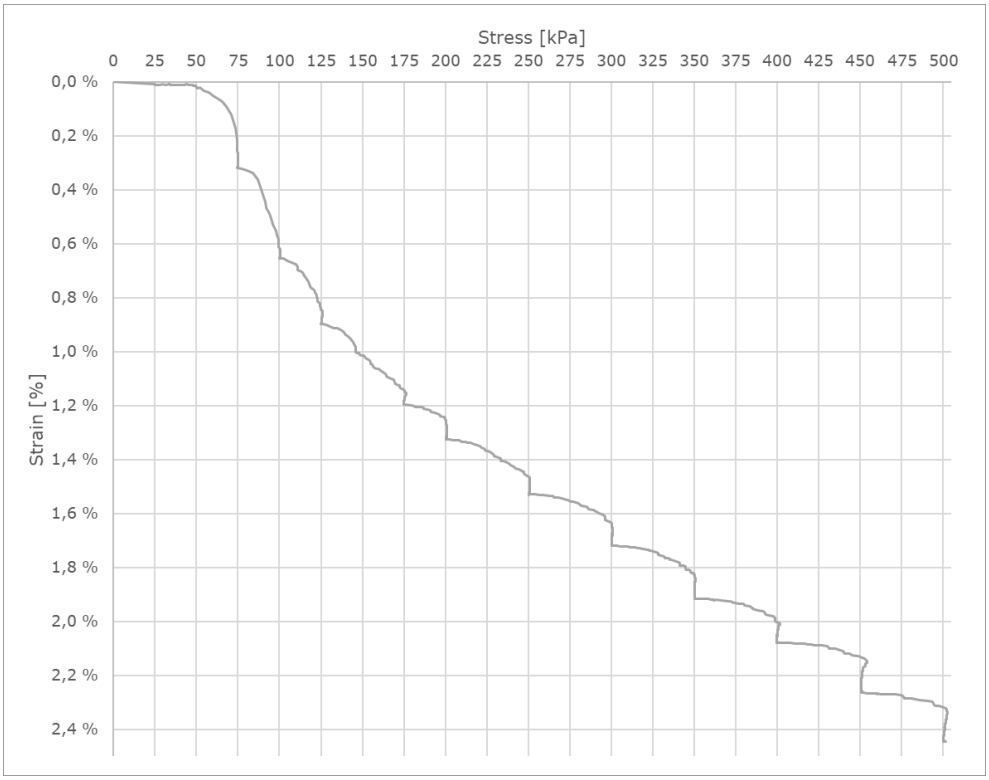

Figure 3.34 Stress – strain for CR 1

Figure 3.34 indicates that the material has small creep settlements until the load step 250 kPa. The material is responding instantly when the load is implemented, with no or little increase in strain during the time of the applied step. For the load step of 250 kPa some creep settlements can be seen in Figure 3.35, from 120 minutes and further.

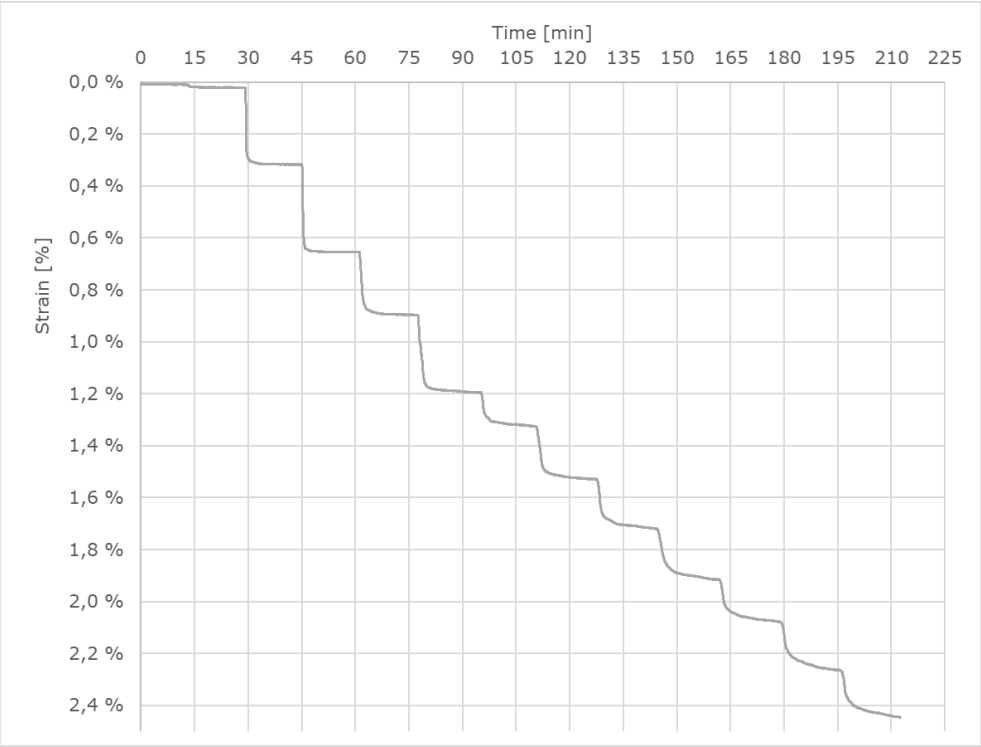

Figure 3.35 Time – strain for CR 1

3.3.7 Crushed rock, test 2

Since this test was collected from a lower location in the bag, a larger content of fines was included. A water content sample was collected with finer particles, and had some higher content of water, 0.28 %. Load step of 350 kPa lasted for 70 hours, like test 2 and 3 with TBM spoil. Small creep strain is indicated in Figure 3.36, until 200 kPa where an increase in strain is seen. A large increase in strain is seen at 350 kPa, that is equalised at load step 400 kPa. The test has the smallest total strain of the three tests of crushed rock.

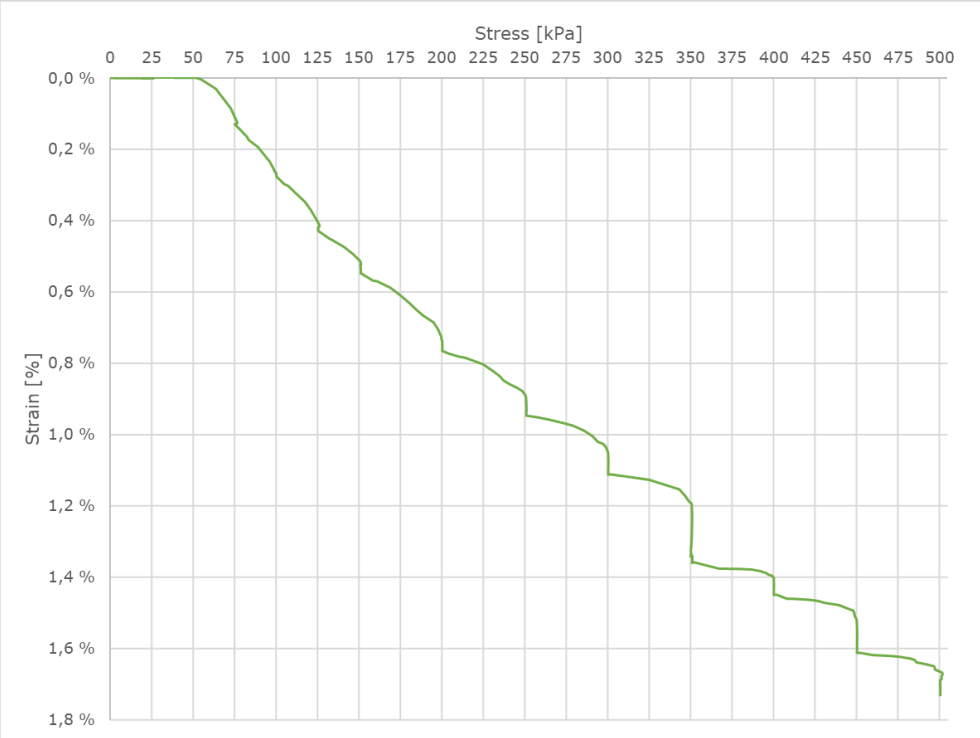

Figure 3.36 Stress – strain for CR 2

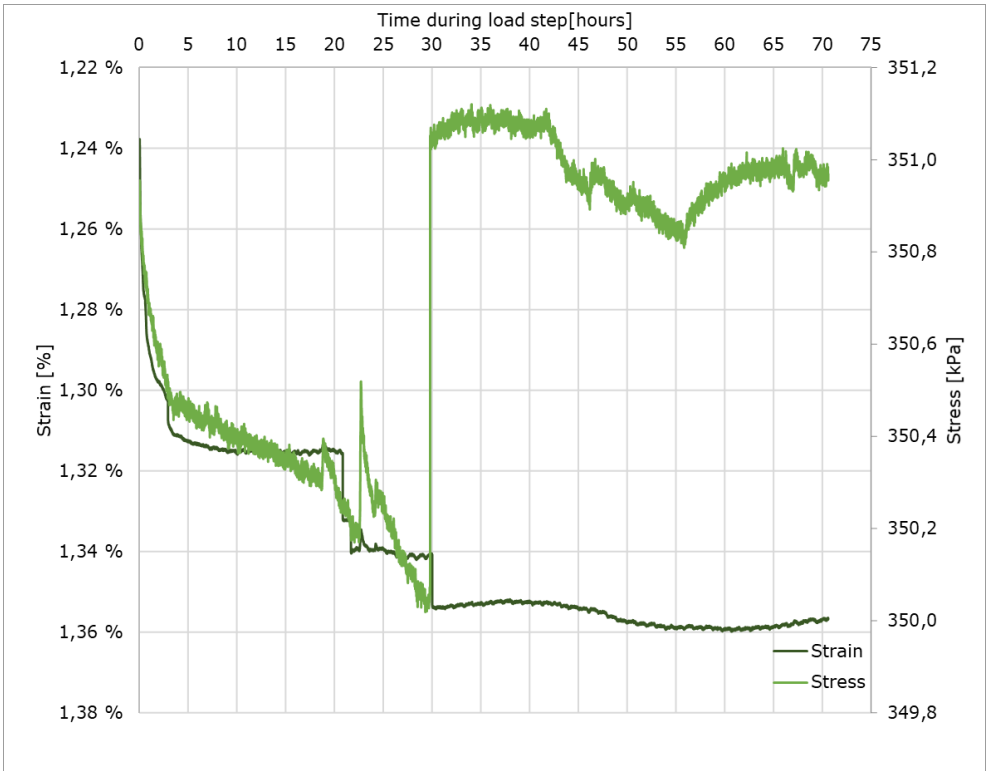

Figure 3.37 Time during the 70-hour load increment – strain and stress for CR 2

The strain and stress during the load step 350 kPa are shown in Figure 3.37. The strain, dark green line, indicates crushing at three points, after 21, 22 and 30 hours. The strain graph has an uneven surface, that can be caused by that the material is settling. The large leap in stress at 30 hours is due to adjustment of stress. The material does not fully adjust during the 70 hours of the load step where crushing of the material can be seen in two points. The time resistance for the crushed rock has a value of 4.86 million and a time resistance number of 1150, higher than the TBM spoil (418 828 and 98, 368 100 and 86).

Figure 3.38 shows the strain over time before and after the long increment. The time step of 350 kPa is not included since the scale made it difficult to see the inclination of the strain. The strain before the 70-hour time step can be seen at the upper axis, 0 to 3.5 hours. The time after can be seen at the lower axis, 72.5 to 75.5 hours. The load steps for test 2 last longer than for test 1, with 20 minutes steps before the 350 kPa and 30 minutes after. For the load steps lager than 350 kPa 30 minutes is not sufficient for the strain to settle.

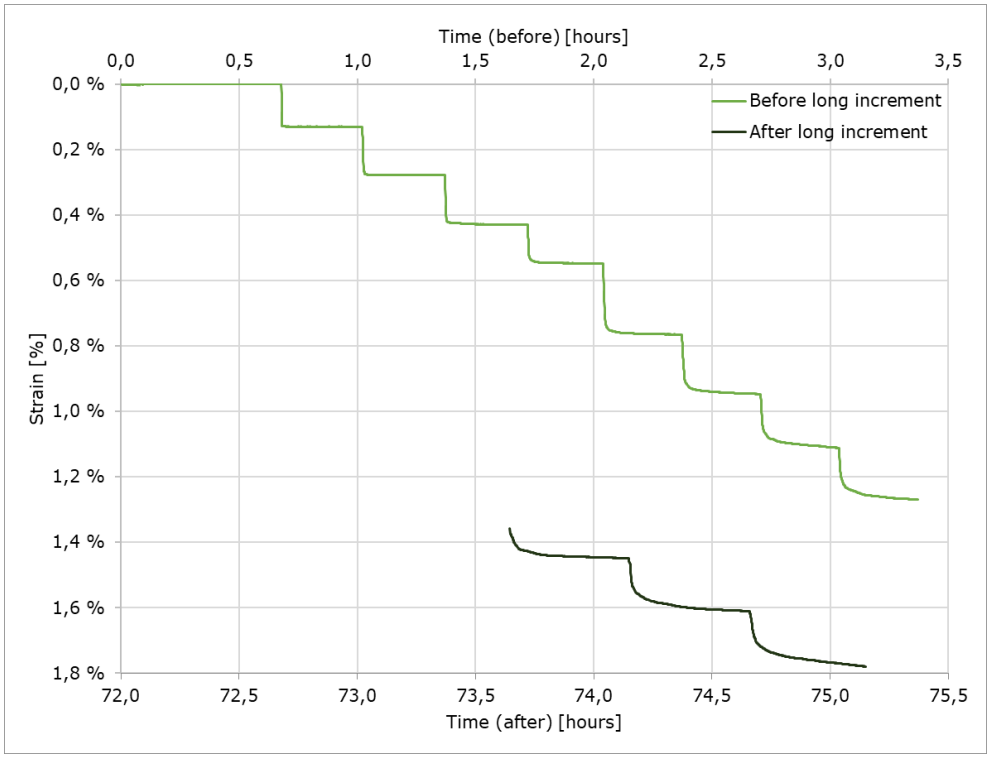

Figure 3.38 Time before long increment (upper x– axis) and after (lower x- axis) – strain for CR 2

3.3.8 Crushed rock, test 3

The material used for test 2 and 3 had a similarity in grain size distribution and had larger amount of fines than test 1. No water content sample was collected for this test, and the value 0.28 % is used for this sample. Figure 3.39 shows the similar results as for test 1 and 2, that there are little creep settlements until 350 kPa. The leap in stress at 250 kPa is due to imprudence increase when applying the load. There are small creep settlements in the material until the load step of 200 kPa, indicated by an almost smooth curve in Figure 3.39 and as straight lines in Figure 3.40.

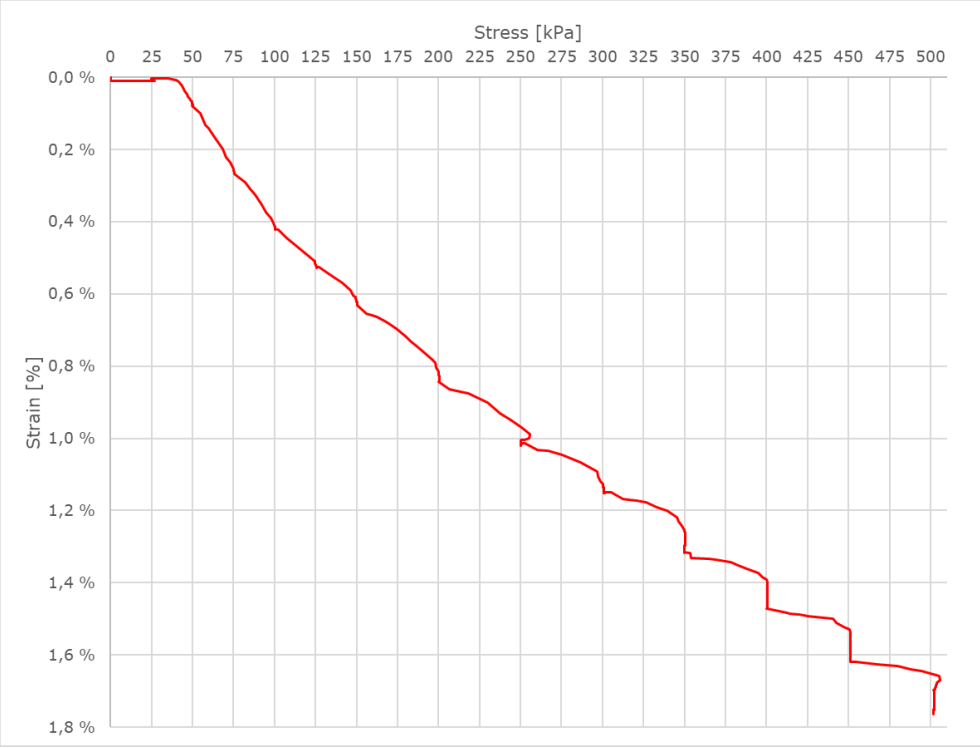

Figure 3.39 Stress – strain for CR 3

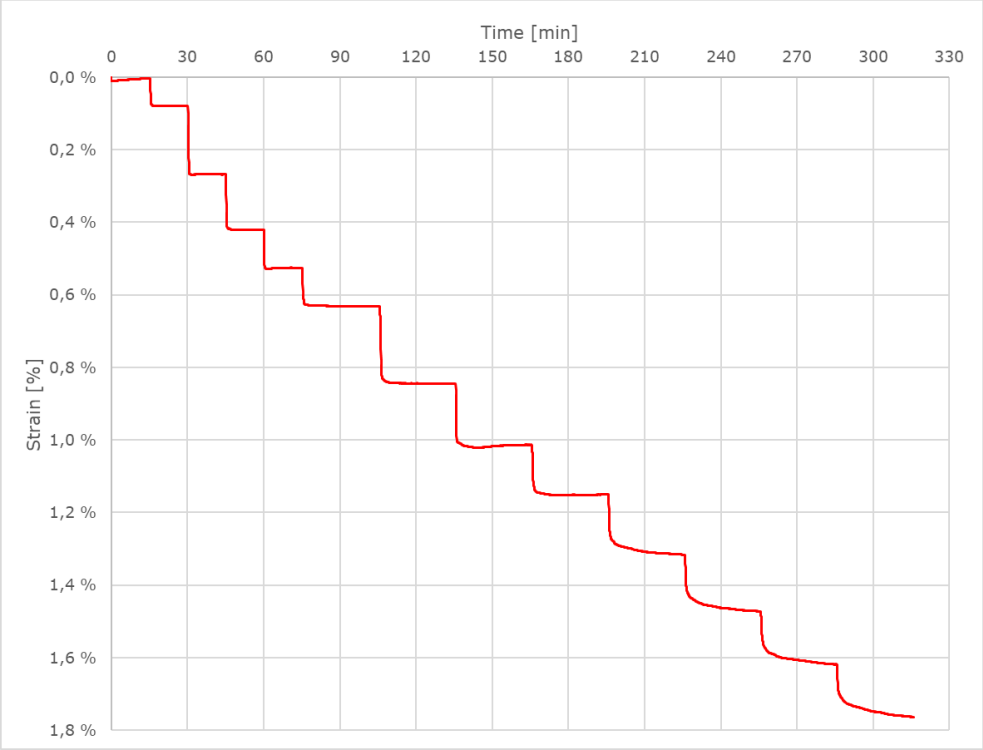

Figure 3.40 Time – strain for CR 3

Figure 3.40 shows that the strain is equalising during the load step until 350 kPa. At 250 and 300 kPa, 150 to 200 min. A small decrease in strain can be seen during the load steps. Some small crushing can be seen in the beginning in both Figure 3.39 and Figure 3.40.

4 Discussion and evaluation of material properties

4.1 Grain size distribution and grain shape

To comply with NS-EN standard, the grain size distribution of the TBM spoil is scaled down to not contain particles larger than 31.5 mm by using the parallel gradation method. Dorador and Villalobos (2020) has six recommendations when the method is used. 1) The gradation sample should not exceed a content of 10 % fines. 2) The parallelism between the scaled grain size distribution and the original should be kept. 3) The minimum and maximum density should be similar for the scaled material. 4) The particle shape must be maintained from the original. 5) Maintain the mineralogy and the compressive strength on the particles and 6) the balance for mixture of particles of different strength.

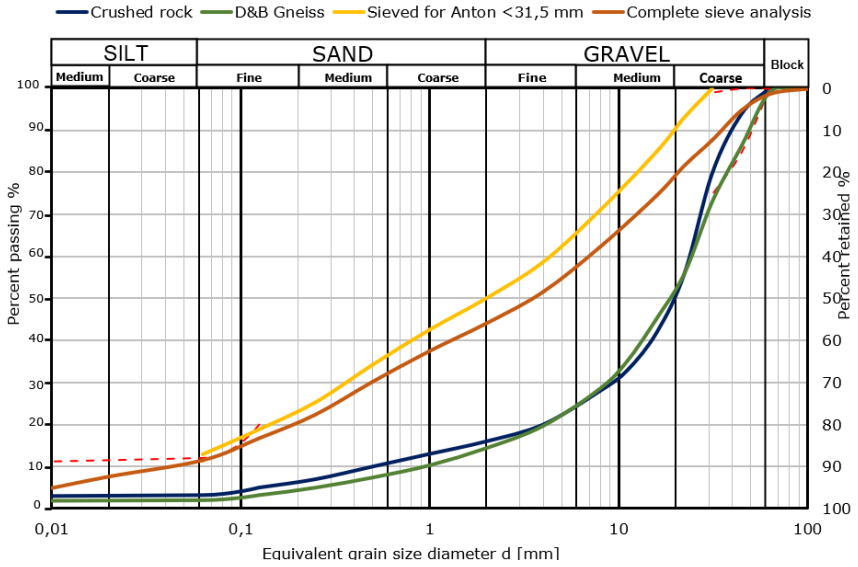

Figure 4.1 Collocation of grain size distributions from study

Figure 4.1 includes four different sieving curves, where the original TBM spoil contains 11.4 % fines and the gradation sample contain 13 %, exceeding the content of fines regarding the recommendations from Dorador and Villalobos. Some of the parallelism is lost between the curves, this to not exceed the content of fines. The minimum and maximum density of the sieved spoil and the spoil tested by Dahl, is in the same range, see Figure 4.9. It is worth nothing that Dahl's material has some variation in coarseness caused by separation in the barrels where the material was stored.

The crushed rock is not divided into 12.5 litres buckets and has a considerable variation in grain size distribution. This is noticeably in the laboratory investigation results, where the three results have considerable variation in the content of fines. Similar challenges occurred for Dahl's material. The scaling of the TBM spoil from the original curve constitutes in

general less than 10 %. When this material is divided in buckets and tested, the material has uniform oedometer results resulting in consistent properties for the material. This is favourable compared to the crushed rock and the TBM spoil tested by Dahl that has large variations in results, since the different tests were performed on materials with different grain size distribution.

The investigated TBM spoil is delivered from the Follo Line Project, earlier investigations indicates that the spoil is elongated and flaky. Pictures from the sieving analysis shown in Appendix B.3, indicates the same tendency for the material tested in the oedometer. It is particularly the larger particles in the TBM spoil that has a disadvantageous flaky and elongated shape. Removing the grain sizes exceeding 31.5 mm can therefore be incompatible with recommendation 4) and 5). Where in this case the requirements from *NS-EN ISO 17892-5:2017* are weighted over the recommendations from Dorador and Villalobos, since the scaled material are not far from the recommendations.

The grain size distributions shown in Figure 4.1 shows the TBM spoil compared to the crushed rock and a material produced from excavation with the D&B method. The grain size distribution of the crushed rock is chosen with the intention to be similar to the D&B spoil, but it will have some different properties due to the difference in origin. The crushed rock is produced with the intention to have favourable properties, such as grain shape and mechanical strength. Grain sizes and mechanical strength for D&B spoil varies, similar to TBM spoil, dependent on the geology along the tunnel alignment.

NGI investigated D&B spoil from Akershusstranda in Oslo in 2020. The largest cobbles measured was 89 cm, where the grain shape was variating in the material. Near a half of the particles had a cubic shape, the remaining material had shapes variating from elongated and flaky to very elongated and very flaky. The largest particles had a cubic shape (NGI, 2020).

The content of fines for both TBM spoil and blasted rock will be dependent on excavation method parameters. Where the thrust force of the TBM will influence the spoil, and the quality of explosives and further handling will influence the blasted rock. When comparing blasted rock from a tunnel with material from an open cut, the material from field site will have smaller content of fines. This due to lower amount of explosives (Ouchterlony *et al.*, 2006). Further crushing of both materials will increase the content of fines considerable, but it will also improve the grain shape. The most favourable grain shape is a cubic shape with rounded edges, like a natural material.

4.2 Water sensitivity and frost susceptibility

The water sensitivity of a material describes the material's ability to obtain its bearing capacity when the water content is increasing. The water sensitivity is dependent on the type and amount of fines. A material is considered water sensitive if it is containing more than 7 % fines smaller than 63µm. Thus, the crushed rock is not considered as water sensitive, since it has a content of 3.2 % of 63 µm and smaller (Aksnes et al., 2016). The TBM spoil can be considered as water sensitive since the tested material has a content of 13 % of 63 µm.

Problems with frost are dependent on three presumptions: frost temperatures, frost susceptible soil and presence of available water. The crushed rock has a larger frost depth than the TBM spoil, since the material has a lower content of fines. A frost susceptible material is a material with the ability to attract water by freezing. Available water is crucial and the water that is attracted to the freezing front is primarily capillary water. A material is considered frost susceptible if it contains more than 3 % of fines smaller than 20 µm (Aksnes *et al.*, 2016).

The sieving analysis of the crushed rock and the scaled TBM spoil do not contain a sieving smaller than 63 µm. Thus, the content of grain sizes smaller than 20 µm is unknown. The original and complete sieving analysis of the spoil contains 1 % of 20 µm. Sieving analysis of TBM spoil performed for the Follo Line project does not contain more than 3 % of 20 µm. According to Table 2.1 in chapter 2.2.2, the scaled TBM spoil is considered T2, medium frost susceptible. The original TBM spoil and the crushed rock is T1; little frost susceptible. NGI carried out laboratory investigations on the material from the Follo Line project, where the freezing and thawing properties of the spoil were tested. NGI concluded that the TBM spoil tested was not frost susceptible, since the material did not have enough capillary suction to form ice lenses (Bane NOR, 2020).

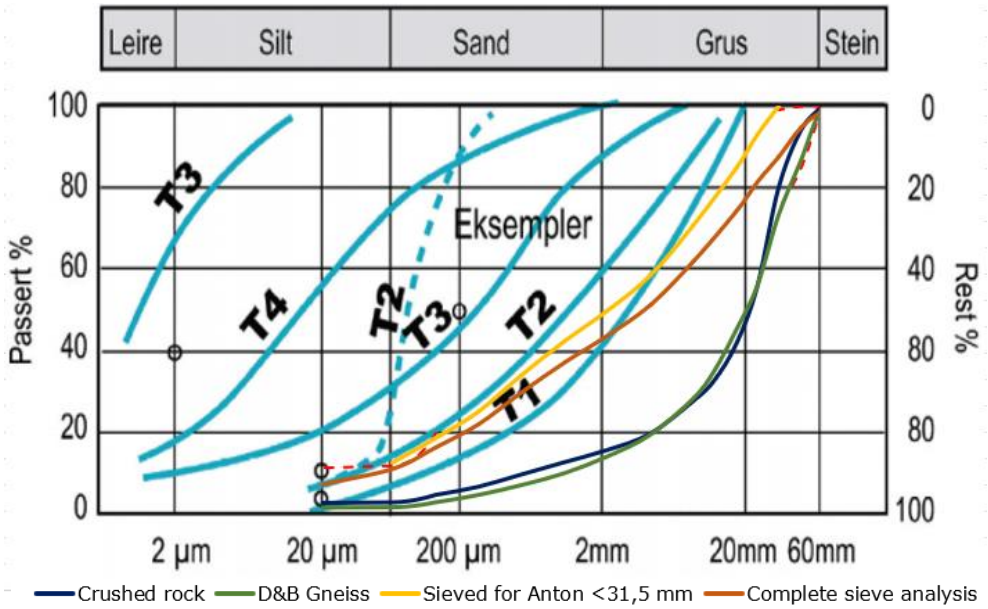

Figure 4.2 TBM spoil, crushed rock and D&B spoil plotted with examples of frost susceptible classes defined by NPRA (NPRA, 2010) (modified)

When considering the criteria for frost susceptibility used in Finland, the TBM spoil is considered to belong in group 2 or 3, and the crushed rock in group 4, see Figure 4.3. Where group 2 and 3 are considered as not frost susceptible but could have tendency to be frost susceptible since the original sieving curve falls slightly in the finer side of group 2. According to this classification the crushed rock needs further investigation to determine the frost susceptibility.

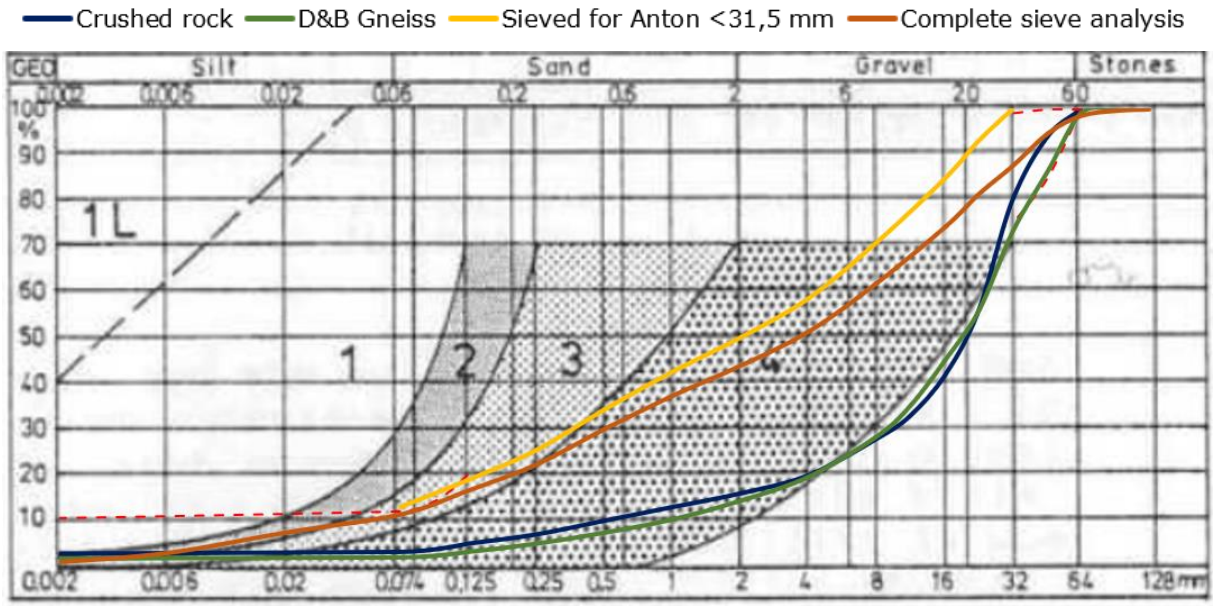

Figure 4.3 TBM spoil, crushed rock and D&B spoil plotted the determination of frost susceptibility of a soil on the basis of grain size distribution in Finland by ISSMFE (Slunga and Saarelainen, 2006) (modified)

4.3 Porosity, dry density and water content

The density of the material is dependent on the amount of pores and voids in the material. The density for a material is important for the evaluation of bearing capacity and the potential for settlements. The porosity at the start of the oedometer tests, at the end of the tests and the corresponding dry density are shown in Table 4.1.

Table 4.1 Change in porosity for the tests

	Test nr	Porosity [%]		Change in porosity	Dry density [t/m³]	
		(start)	(end)		(start)	(end)
TBM	1	34.9 %	26.8 %	8.1 %	1.74	1.96
	2	36.5 %	28.1 %	8.4 %	1.82	2.06
	3	34.6 %	28.2 %	6.4 %	1.86	2.08
	4	34.5 %	26.9 %	7.6 %	1.88	2.09
	Average	35.1 %	27.5 %	7.6 %	1.82	2.05
CR	1	37.5 %	36.1 %	1.5 %	1.68	1.72
	2	29.3 %	28.1 %	1.3 %	1.91	1.94
	3	31.8 %	30.6 %	1.2 %	1.84	1.87
	Average	32.9 %	31.6 %	1.3 %	1.81	1.85

From the investigations by NGI in 2020, the density and porosity were investigated in water and without water. The results indicates that the spoil had a porosity between 33 – 38 % under water and 38 – 39 % above (NGI, 2020). These tests were carried out by pouring the material into a cylinder and then measuring the density and porosity with no compaction. The porosity was measured under water with different content of salt, where the density increased with increasing content of salt. From the NGI report dated 1986, the porosity of layered and normally compacted TBM spoil varies between 20 – 25 % (Langford *et al.*, 2020).

These results show that the compaction of the material is of importance for the settlement potential of a construction fill. Meaning that the material could achieve a lower porosity when filled in layers and compacted in a larger scale. Higher amount of compaction work is needed to reduce the porosity when the water content is low. Whilst material with higher water content than the optimal can lead to less compaction. This because the water cannot be forced out of relatively impervious materials, independent on the amount of compaction (Kjærnsli, Valstad and Höeg, 1992).

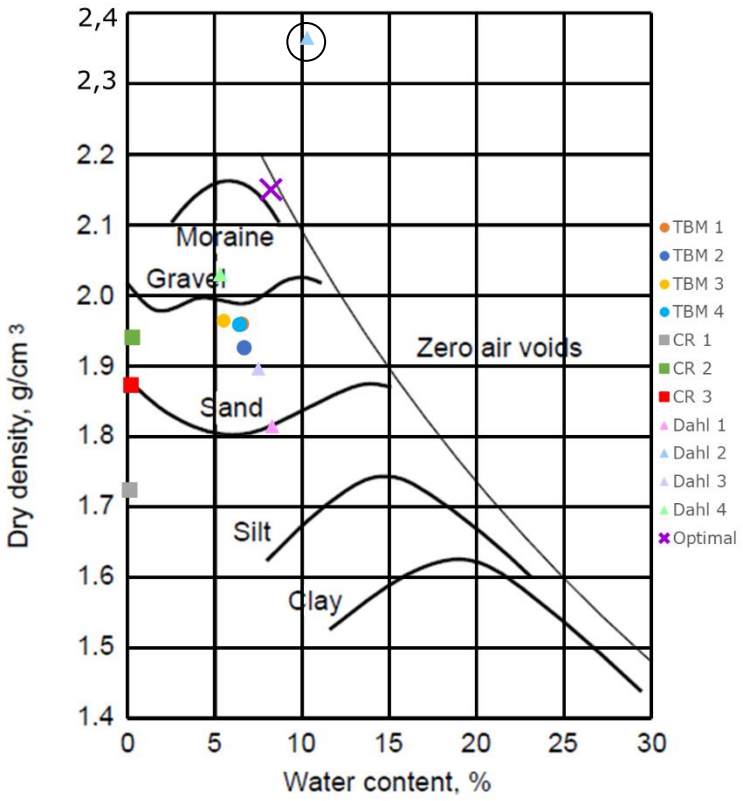

Figure 4.4 Water content – dry density for TBM spoil and crushed rock (Janbu, 1970)

Figure 4.4 shows typical optimal water contents and the optimal dry density for different materials. The water content and the dry density at the end of the tests are included as points, these are not the optimal values. The figure indicates that the main section of the TBM spoil is in the range between sand and gravel for this thesis. Dahl's result has some higher water content and dry density and are above the typical values for moraine marked in Figure 4.4. Note that test 2 by Dahl had excess pore pressure in the oedometer that lead to unlikely high values. The optimal water content and maximum dry density found by Dahl is marked in the figure by a cross.

The crushed rock is dry, has a large variation in dry density and shows no clear tendency. The water contents in the materials are not increased when tested in the oedometer, due to previous challenges to excess pore pressure in the cell. It is expected that the materials could reach an increased dry density if the water content is increased.

Table 4.2 compares the optimal values found in the literature survey. The results from the laboratory investigations in this thesis had a variation in dry density and water contents: 1.96 – 2.09 t/m^3 and 5.8 – 6.7 %. The dry density is in the range of the listed values, but has some lower water content, indicating that the material could achieve a higher density. Gertsch et al. (2020) has diverging values compared to the results from Dahl and NGI, this can indicate that the material tested in this study had a higher content of sand.

Table 4.2 Comparison of dry density and optimal water content from different studies

Dry density [t/m^3]	Optimal water content [%]	Study
2.15	8 – 10	(Dahl, 2018)
1.85 – 1.87	13.7 – 14.2	(Gertsch *et al.*, 2000)
2.18 – 2.27	6 – 8	(NGI, 1986)

4.4 Soil stiffness

The oedometer results are used to evaluate the deformation properties of the material by looking at the material's resistance to deformation. The oedometer modulus results from the laboratory investigations accomplished for both this thesis and the ones tested by Dahl are shown in Figure 4.5. The plots show that the results from this thesis are in the range of Dahls values, except from test 4 by Dahl, that has a somewhat higher stiffness.

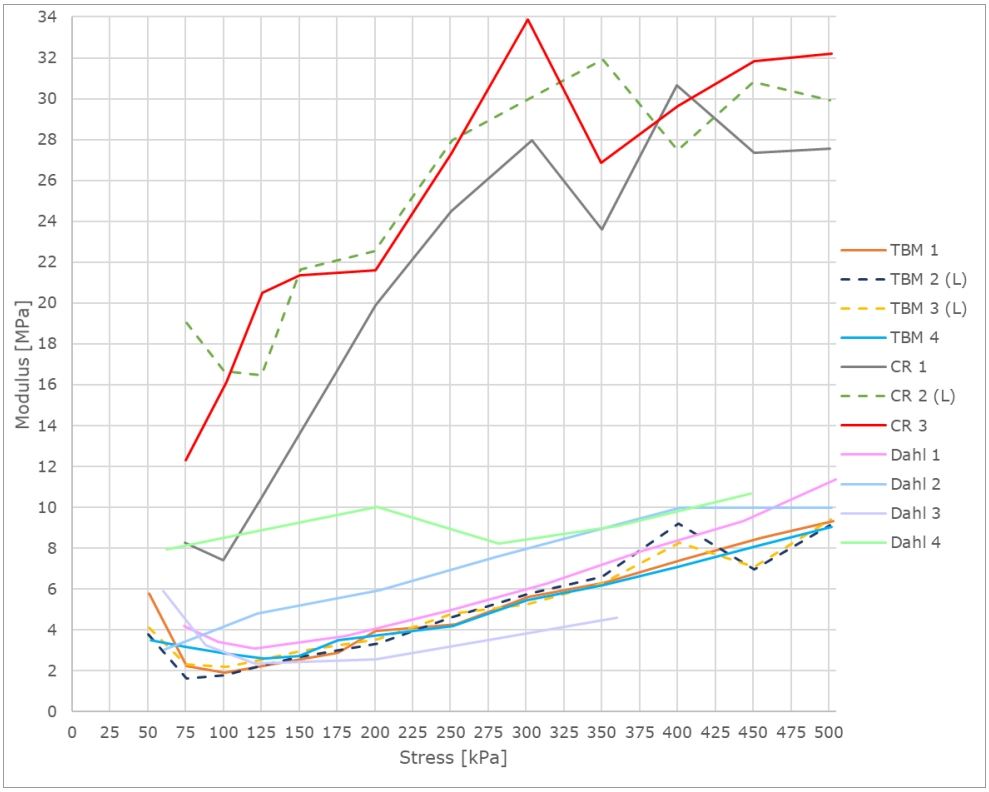

Figure 4.5 Stress – modulus from Dahl and this study

The scaled TBM spoil shows an equivalent plastic (PL) behaviour where the stiffness increases linearly with stress (Janbu, 1970). This behaviour can resemble the behaviour of normally consolidated clays and fine silt when Figure 4.5, Figure 4.7 and Figure 4.6 are compared. The stress and strain curves for TBM 1 to 4, see Figure 4.7, has a crack after 50 kPa, which indicates the preconsolidation stress (σ'_0), since the material behaves stiffer before this point, see Figure 4.5.

The stiffness of the crushed rock has an increase until 250 kPa before the curve is flattening. The stress-strain curve, see Figure 4.7, has first a higher increase in strain before the strain increases linearly. This can indicate that the crushed rock has an equivalent elastoplastic (EP) behaviour for stresses below 250 kPa, and an equivalent elastic (EE) behaviour for stresses over 250 kPa, see Figure 4.6.

The creep effects of the long-time increment at 350 kPa is small for these types of materials. Test 2 of crushed rock indicates that the material has a higher tendency of crushing or recompiling compared to the TBM spoil. Since the deformation plot for the crushed rock has more sudden increase than the TBM spoil plot. The deformation in the TBM spoil equalised during the first 28 – 30 hours, whilst the deformation did not equalise for the crushed rock.

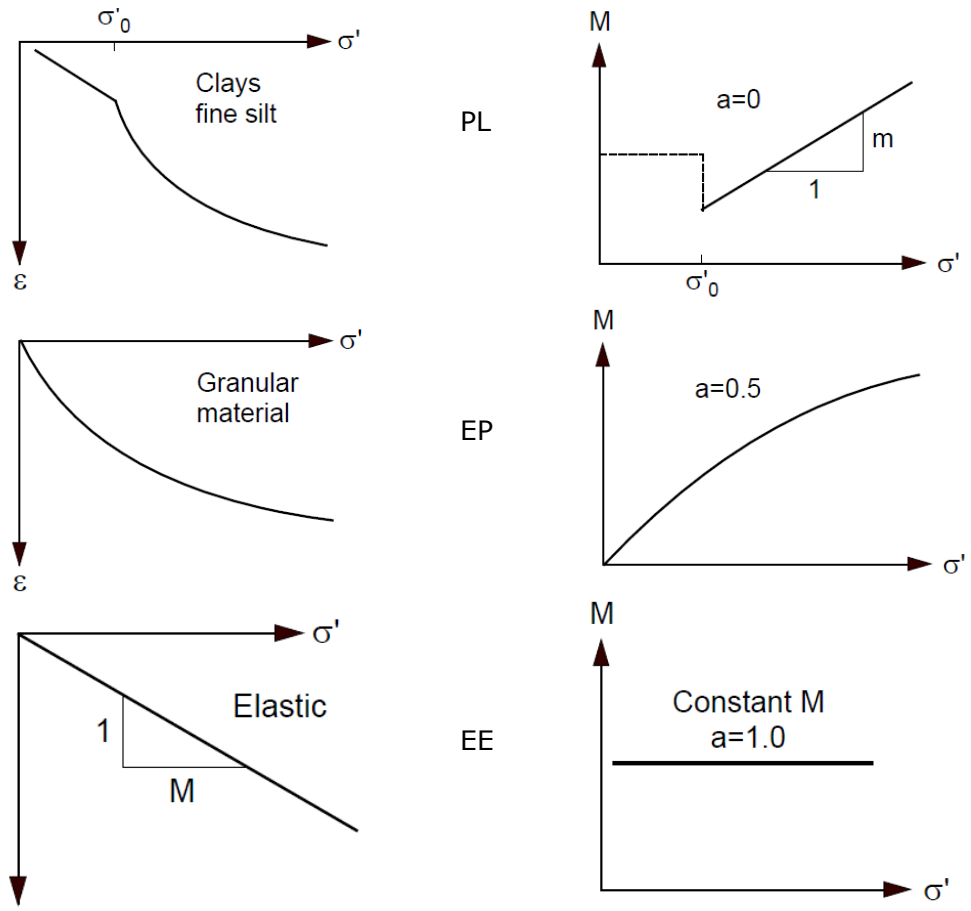

Figure 4.6 Oedometer results for granular material (Janbu, 1970)

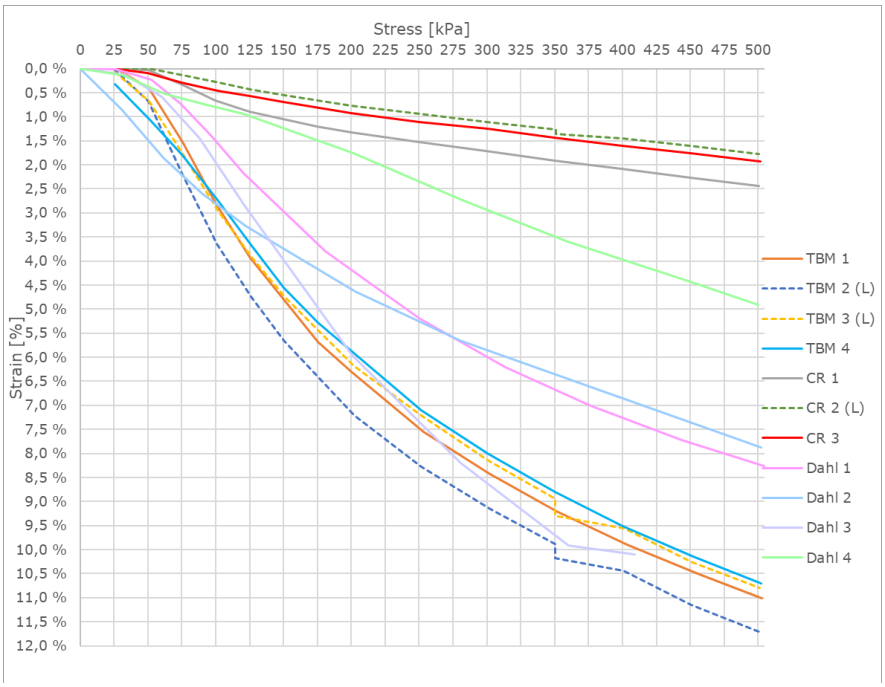

Figure 4.7 Stress – strain collocation of Dahl and this study

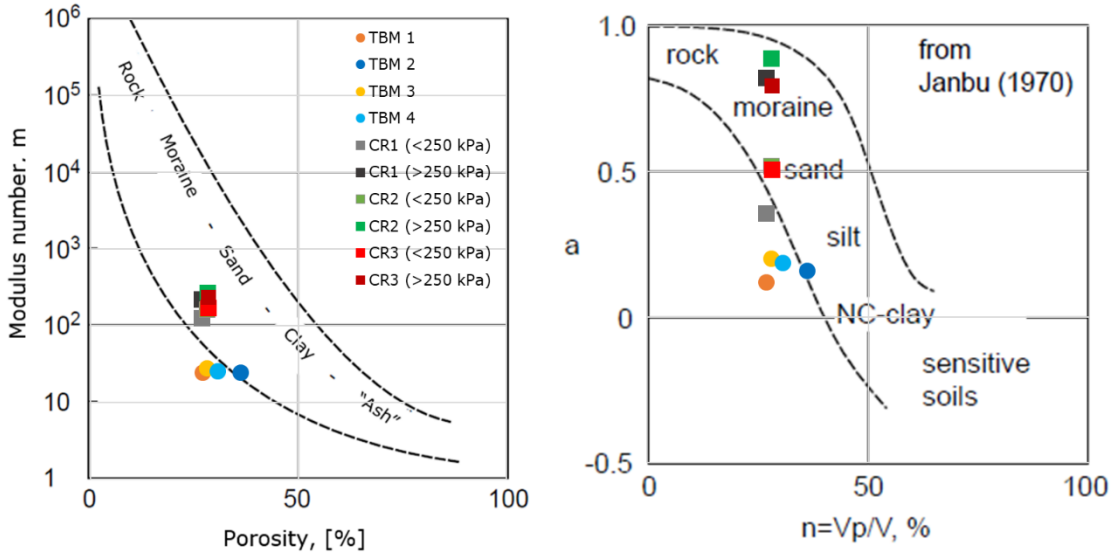

Figure 4.8 The stress exponent and modulus number for the tests (Janbu, 1970)

The stress exponent (a) and modulus number (m) for the materials is shown in Figure 4.8. These values are calculated as described in Chapter 3.1.4, where a and m are chosen to fit the oedometer modulus and stress curve. To fit the curve for the crushed rock, two graphs are generated; one for the stiffness < 250 kPa and one curve for > 250 kPa. These values are separated in Figure 4.8.

The chosen parameters are further used to estimate settlements in the material. These estimations are based on an example from Janbu (1970), where the method used is described in Chapter 3.1.4. To compare the settlement properties of the scaled TBM spoil to the original material tested by Dahl, the input parameters $\Delta\sigma$ (added load) and σ_0 (initial stress state) are the same as in Dahl's calculations. Where $\Delta\sigma$ = 50 kPa, roughly equal to the load of an eight-story building, and average σ_0 for a 30-meter drained fill is 15 m * 22 kN/m^3 = 330 kPa (Dahl, 2018).

Table 4.3 Estimation of settlements for compacted fill

	Test nr	a (<250 kPa)	a (>250 kPa)	m (<250 kPa)	m (>250 kPa)	n [%]	M [MPa]	ε [%]	δ [cm]
TBM	1	0.1		25		26.8 %	7.0	0.71 %	21
	2	0.2		24		28.1 %	6.7	0.75 %	22
	3	0.2		28		28.2 %	7.3	0.69 %	21
	4	0.2		26		26.9 %	6.9	0.73 %	22
CR	1	0.4	0.8*	127	225*	36.1 %	27.7	0.18 %	5
	2	0.5	0.9*	163	270*	28.1 %	30.8	0.16 %	5
	3	0.5	0.8*	170	237*	30.6 %	30.2	0.17 %	5

*Since the initial stress state is >200 kPa these values are used in the calculation.

Table 4.4 Estimation of settlements by Dahl (Dahl, 2018)

	Test nr	a	n [%]	M [MPa]	ε [%]	δ [cm]
Dahl	1	1	31.8 %	7	0.71 %	21
	2*	1	-	20	0.25 %	8
	3	1	29.2 %	4.5	1.10 %	33
	4	1	24.1 %	8	0.63 %	19

*The test had a high-water content (13%) and are separating from the other results in stiffness.

The average deformations calculated by Dahl is equal to 20.3 cm. The porosity of Dahl2 is very low compared to the other tests, caused by the hight content of water and are not included in the table. With Dahl2 excluded due to the high-water content, the average value is equal to 24.3 cm. Dahl4 has the lowest porosity and the closest to the porosity achieved in field by layered compaction.

The estimated deformations for a 30-metres fill of the tested TBM spoil is 21 – 22 cm, and 5 cm for the crushed rock. These results show that the estimated deformation does not increase much with less compaction, where Dahl4 with n= 24.1 % has δ= 19 cm and TBM 2 or 3 have n= 28 % and δ= 21 – 22 cm. The compaction of the tests is shown in Figure 4.9, where it is favourable to have a high dry density and modulus to reduce the possible future deformations. In comparison a NC-clay with medium stiffness, could for this load get deformations up to 1 meter. Whilst a sand can achieve nearly 0.5 meter. Compared to these materials, a deformation of 21 cm is considered small.

If the material is used in a construction fill, the total settlements will be dependent on the material properties during filling and compaction. Factors of importance are water content, layer thickness and compaction efffort, but also the underlying ground conditions and

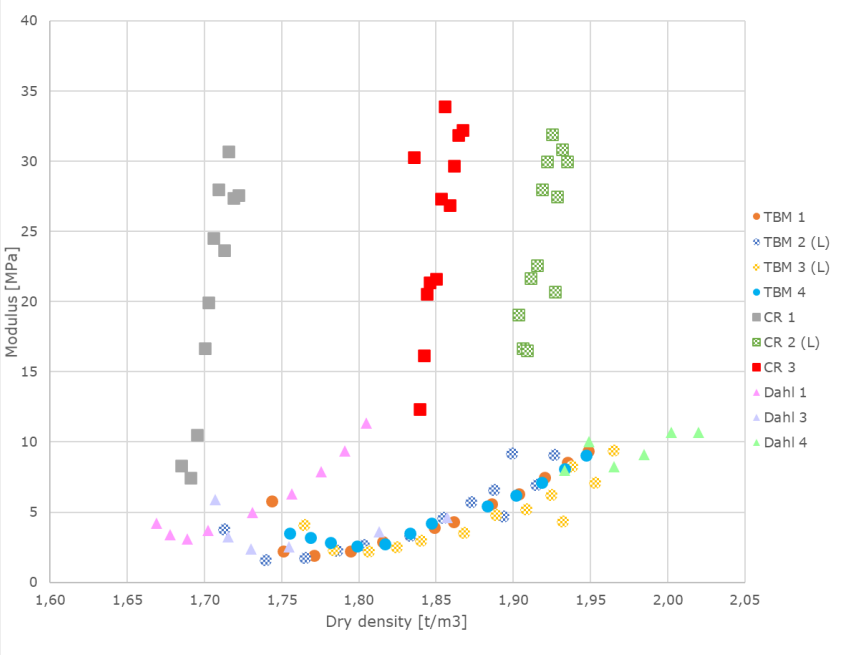

Figure 4.9 Dry density – modulus collocation of Dahl and this study

planned future loads. If the spoil is filled in layers, each layer will cause a load and compaction to the previous layers. The upper layers will have a higher potential for settlements due to a lower preload. The potential settlements are dependent on the weight of the prospective loads as well as the potential settlements in the subsurface under the fill (NGI, 2020).

When the stress strain curves for the TBM spoil and crushed rock are combined with the oedometer results carried out by (Kjærnsli, Valstad and Höeg, 1992), the TBM spoil is seen to have lower resistance towards deformation than the uniformly graded and loose material. The crushed rock has a higher resistance and are between the dense uniform and dense well graded gravel. The results correlate with their conclusion that the structure of compacted fills will primarily depend on the grain size distribution and the shape of the particles and how the material is placed and compacted.

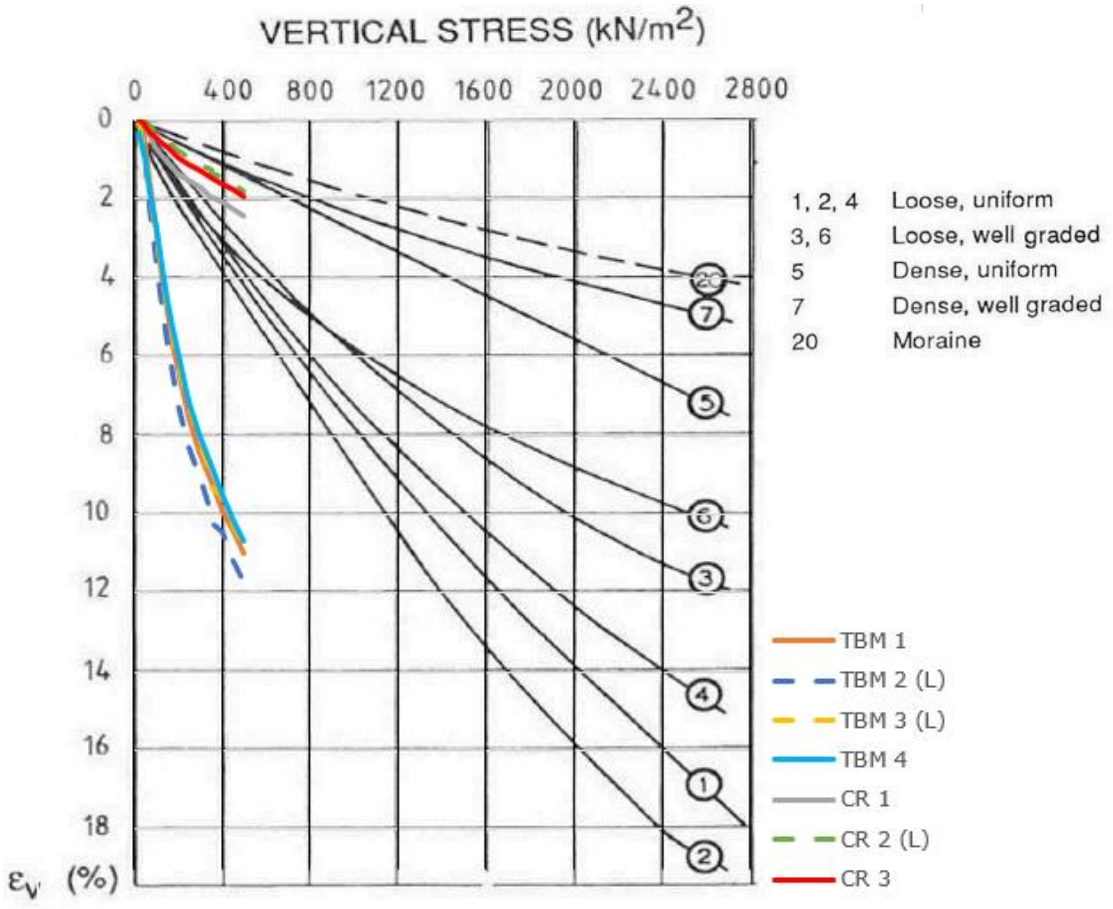

Figure 4.10 Oedometer results of tests on crust syenite, TBM spoil and crushed rock (Kjærnsli, Valstad and Höeg, 1992)

According to Kjærnsli (1968) the TBM spoil will be sensitive to the water content to achieve a better compaction. It will also have a higher resistance towards deformation than the crushed rock (Kjærnsli, 1968). According to Dahl's investigations in 2018, the TBM spoil has an optimal water content of 8.2 %, where the water content in the TBM spoil tested in this thesis has an average of 6.3 %. Water was not added to the spoil due to the risk of excess

pore pressure in the oedometer cell. Thus, it can be expected that the spoil can reach a higher compaction if the water content is closer to the optimal content.

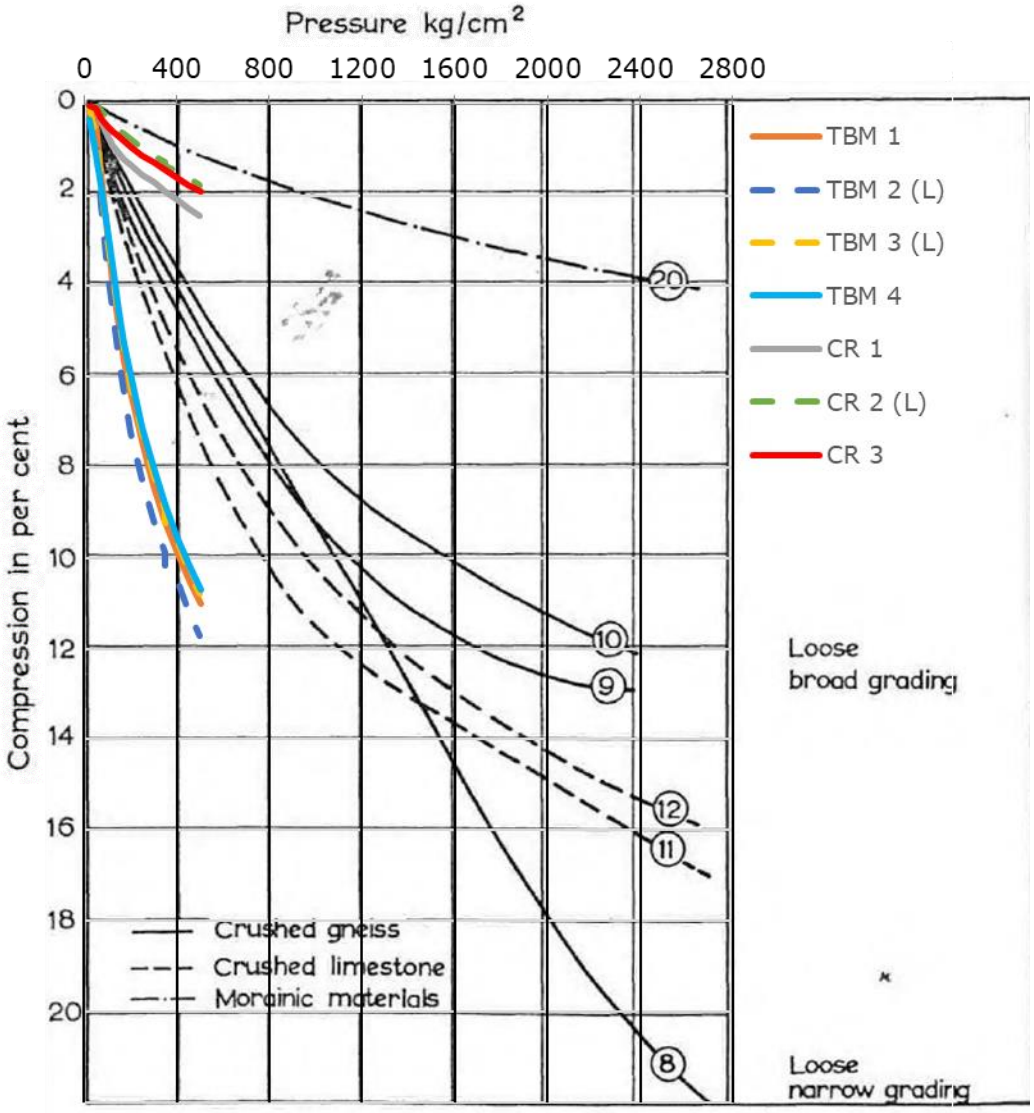

Figure 4.11 Pressure-compression curves of aggregates (Kjærnsli and Sande, 1966) (modified)

Figure 4.11 includes oedometer results by Kjærnsli and Sande (1966) with the results of this thesis added. Graph 8, 9 and 10 is tunnel spoil of crushed gneiss, 11 and 12 is flaky shaped crushed stone of limestone, and 11 and 12 is morainic materials. These results shows that the crushed rock tested in this thesis is stiffer than the D&B tunnel spoil from the same geological conditions tested by Kjærnsli and Sande, and closer to a morainic material. The TBM spoil has the same inclination as the crushed limestone, but with a lower stiffness. The further path for the spoil is challenging to determine, but the inclination from Figure 4.7 indicates that the deformation is decreasing and the shape could be simular to the tunnel spoil of crushed limestone.

4.5 Potential utilisation of TBM spoil

The results presented in this thesis reveal that TBM spoil can be utilised for several purposes. Reuse of TBM spoil reduces both the environmental footprint of the project and the costs related to spoil handling.

Tunnels excavated by TBMs are most often longer than 5 km due to the machine investment costs. Thus, considerable amounts of spoil are produced from these projects. This emphasises the need for knowledge about the geotechnical properties of TBM spoil and the options for utilisation. Among the factors determining the geotechnical properties of TBM spoil are the geology and the machine operation. Whilst the utilisation of spoil depends on several factors as the turnover in the market for tunnelling spoil, the project's capability of early planning and the geotechnical knowledge of the material. Geotechnical knowledge is crucial for the project in order to plan the methods for spoil processing for further utilisation.

Some of the TBM projects accomplished in the 1980s in Norway did not utilise the TBM spoil in a large scale. Most of the TBM spoil ended up as on-site depositions with no further utilisation. Most of these projects were located in rural areas and the transport costs would have exceeded the expenses for utilisations. Thus, on site deposition of material were the most cost-efficient way of spoil handling.

In the 21st century TBM projects like the Follo Line and the Ulriken tunnel have been constructed in urban areas in proximity to existing road infrastructure and there has been a market for using the material. In these projects the utilisation of TBM spoil has been in focus from an early project phase. This has resulted in extensive reuse of the spoil. The Follo Line project constructed a construction quality fill for future housing development of the municipality of Oslo. Whilst the Ulriken project capped the polluted seabed in Puddefjorden.

The range of TBM spoil application is dependent on the geotechnical and chemical properties of the material, as well as the spoil handling. From Table 2.3 on page 28, the utilisation is separated in classes that will be further discussed in the following chapters.

4.5.1 Concrete aggregates

In class 1 the TBM spoil can be utilised as a raw material on site, as aggregates for inner lining and segment concrete, shotcrete, asphalt mixes etc. Concrete aggregates require specific grain size distributions, grain shapes, mechanical strength, densities, water absorption abilities and chemical properties. To be utilised as aggregates in concrete the TBM spoil requires further treatment. The grains have a flaky shape which requires crushing to achieve the more favourable cubic shape.

The Follo Line project demonstrated that the requirements mentioned above can be accomplished with an in situ crushing plant. TBM spoil was successfully processed and reused as aggregates for on-site segment production for tunnel lining. Initially the project planned to utilise 10 – 15 % of the TBM spoil as aggregates for concrete- and segment production. However, this could not be achieved due to geochemical reasons. 20 % of the samples from the excavated material had presence of pyrrhotite. *NS-EN 12620* requires that aggregate containing pyrrhotite, cannot contain more than 0.1 % sulphur due to risk of

concrete spalling. Thus, to achieve the required quality of the concrete, the project had to import aggregates which fulfilled the requirements on geochemical content (Kalager and Gammelsæter, 2019).

From a geotechnical point of view the aggregates can be reused for concrete production. However, the geochemical requirements regarding the content of pyrrhotite is very strict. Detection of sulphur excludes the reuse of spoil if pyrrhotite is present. More research regarding limit values for content of both pyrrhotite and sulphur is needed as the requirements mentioned can be considered as conservative (NRPA, 2019).

4.5.2 Pea gravel for backfilling

Pea gravel is a segment backfill utilised to stabilise the segments when boring in rock with a double or single shield TBM. The pea gravel is utilised to the purpose due to its rounded shape (ITA, 2014). The TBM spoil could be utilised for this purpose if the material is sieved and scaled for the purpose. A hose diameter of 60 or 70 mm is often utilised for the purpose, and particles larger than this can clog the hose (Robbins, 2014). Although the grain shape of the spoil could make the pneumatically pumping more challenging, and further crushing of the material would be favourable to produce a more cubic shape. The Brenner Base Tunnel in Australia utilised approximately 15 % of the excavated spoil as a backfilling material (Voit and Kuschel, 2020).

4.5.3 Road construction

As for classification 3 the TBM spoil can be used for landscaping like embankment, backfilling, road sub-base etc. NRPA has defined requirements for materials used as asphalt aggregate, with values for flakiness index, Los Angeles-value, Micro-Deval- coefficient and degree of crushing.

For utilisation in both subbase and road base the grain size distribution from the results reveals that unprocessed TBM spoil is too frost susceptible. The requirements for the lower frost protection layer are related to maximum grain size (< 50 cm), the unit of fines and the coefficient of uniformity. Thus, reuse for these purposes requires further processing in terms of sieving and sorting.

Post sieving and sorting, the TBM spoil from favourable rock conditions can be utilised as both substructure and frost protection layer. It is emphasised that spoils produced from micaceous, foliated, or weathered rocks are not suitable for these purposes due to their mechanical properties in terms of low resistance against crushing.

However, if the TBM spoil is crushed and scaled to fulfil these requirements, or adjusted by adding other materials, the TBM spoil is suitable for reuse in road constructions (NRPA, 2018).

4.5.4 Railway construction

For use as aggregates for railway ballast in Norway the requirements in *NS-EN 13450:2002* must be complied. If TBM spoil should be utilised the grain sizes > 63 mm and < 32.5 mm must be removed and adapted to the maximum and minimum requirements. To fulfil the requirements for the shape index, further crushing of the material must be accomplished and the LA-value and Micro Deval- coefficient must be met (Standard Norge, 2002).

4.5.5 Construction fills

The results of this thesis reveal that TBM spoil has favourable geotechnical properties to be utilised as construction fills. Geotechnical testing of the material shows low inherent settlements. Thus, the settlements of the filling will mostly depend on the local ground conditions, the layer thicknesses and the compaction of material and the amount of future load.

The method for filling and compaction is dependent on the geotechnical knowledge of the material. By revealing the geotechnical properties, a tailormade procedure for filling and compaction of the material can be established. This in order to achieve high quality compaction and minimise future settlements. Such procedure should as a minimum include layer thicknesses, compaction method (e.g., Weight of vibrating roller, number of crossings) and water content, as well as the procedures for follow up and documentation.

It can be seen from the results from the water content samples from Dahl and this thesis, that extra attention should be paid to the water content as this seems to be on the dry side of the optimum water content. Improved results for compaction could be achieved by adding water to the material and optimising the water content. However, if the water content is too high, the level of compaction will decrease, see Figure 4.4 on page 82. Thus, to reduce the potential settlements, the project should be able to both add water before filling and avoid filling on days with heavy rainfall.

Since the procedure for filling and compaction of a construction quality fill is dependent on several geological, geotechnical and geochemical values, in addition to local factors of the landfill, it is recommended to perform a full-scale testing in terms of a test fill to optimise the procedure for filling and compaction of the material. This was accomplished for the Follo Line project and further discussed in Dahl's thesis (Dahl, 2018).

If large loads are planned on the construction fill, piled might be required. TBM spoil has the advantage to D&B spoil, in terms of excavation and piling, since the material does not contain boulders. When piles and sheet piles are installed in the TBM spoil, the porosity in the material will be reduced (and the compaction will be increased). Thus, the material will be favourable as a friction material and for the bearing capacity of the pile (NGI, 2020). A precaution when driving piles is that the piles can be pulled away from centre if stones or blocks are encountered, if the subgrade consists of more blocky material (as applied for D&B masses), predrilling could be necessary (NGF, 2019). Thus, TBM spoil with less boulders are favourable for landfills that will be further utilised as residential areas with building on top.

The Follo Line project utilised the material as a quality filling for a future residential area. The material was filled in 0.7 m thick layers where each layer was compressed with six passages with a vibrating roller. On days with heavy rainfall the filling was stopped. Documentation shows that the compaction of the material fulfils the requirements of 95 % maximal density from Standard Proctor test (NGI, 2019b).

4.5.6 Fillings on seabed

The TBM spoil could additionally be utilised as filling on the seabed to extend land areas or to cover polluted materials on the seabed. This was accomplished by the Ulriken project that covered polluted seabed in Puddefjorden in Bergen with a 40 cm thick layer of TBM spoil. The spoil was spread by a barge with an excavator and a downlead tube. The one-year control of the filling indicates that the TBM spoil is efficient as an isolating material and to secure erosion (COWI, 2020).

NGI has accomplished laboratory investigations regarding turbidity in water when spreading both TBM- and D&B spoil (NGI, 2020). These investigations focus on the turbidity with an increased salt content in the water. The conclusion is that the TBM spoil shows higher turbidity over an extended time period compared to D&B spoil. The turbidity of both types of material decreased with an increased salt content. The risk of high turbidity is reduced if it is accomplished with a downlead tube to place the material into a sea depth with higher salt content, or by installation of a silt curtain. NGI concluded that, despite the risk of high turbidity, with measures implemented, the TBM spoil can be utilised successfully as filling on the seabed. This is also confirmed with the experiences from spreading accomplished in Puddefjorden as this did not lead to turbidity values higher than the allowed values of +10 FNU for 20 minutes.

However, a filling on the seabed is more exposed to the risk of settlements compared to a landfill. There are less measures for compaction and facilitation of optimal water content. Thus, larger settlements must be expected, and further measures must be considered if a seabed filling should be utilised for further purposes in terms of buildings, infrastructure constructions etc. Pre-consolidation in terms of adding pre-loads (fill) that is removed at a later stage is an example of such a measure.

5 Summary and recommendations for further work

5.1 Summary and Conclusion

The aim of this study was to investigate the deformation properties of TBM spoil and compare test results from large scale oedometer tests on TBM spoil and crushed rock.

Several tunnels were excavated by use of TBMs in the 80s, before D&B replaced TBM as the main excavation method throughout the 90s. From the mid-2010s the TBM as excavation method increased again. The method was applied for large infrastructure projects as Røssåga (hydropower), the Follo Line (railway) and the Ulriken project (railway). In 2017 the Norwegian Tunnelling Society noted a record year for the Norwegian tunnelling industry; more than 7.8 million m^3 of rock were excavated. The Follo Line project topped the statistics with 1.5 million m^3 of excavated material (NFF, 2021).

These numbers demonstrate the potential for reduction of both the environmental footprint and project cost through reuse and utilisation of tunnelling spoil. Thorough knowledge regarding the geotechnical properties of the spoil is necessary for both planning for and implementing such reuse. Thus, several research projects have been performed. Most of them with focus on D&B spoil. Less research has been performed for TBM spoil and few projects were found that compared lab research from both TBM and D&B materials.

The TBM projects in the 80s were located in rural areas with little or no reuse of material. However, the TBM projects from 21st century are located in more urban areas, resulting in less available space for both construction rig and deposition of excess material. This increases the demand for reuse of material and thorough planning of the spoil handling.

Both the environmental impact and economical costs of the projects are dependent on the utilisation of the TBM spoil produced. The geotechnical properties provide the premises for reuse potential and the methods for processing the materials.

Previous experiences demonstrate that if the methods for spoil processing is tailor made based on the geotechnical properties, the utilisation of the material is efficient in the range of different applications. The utilisation of the material has not been optimal when the characteristics of the raw spoil has not been investigated and the material has been utilised without modifications or consideration.

Laboratory investigations with a large scale oedometer tests were conducted with both TBM spoil and crushed rock at the Geotechnical Laboratory at NTNU in Trondheim, Norway. The crushed rock is sieved and compiled with a grain size distribution with a maximum grain size comparable to the tested TBM spoil. However, it will represent a stronger material than D&B spoil from a tunnelling project. This because D&B spoil have less favourable grain shape and

mechanical properties than the crushed rock where the blasting and crushing can be optimised for the purpose of the material.

The grain size distribution of the TBM spoil is scaled with the parallel gradation method to fulfil the requirements regarding the ratio between the particle size and the size of the oedometer cell, given in *NS-EN ISO 17892-5:2017*. The natural water content in the TBM spoil is measured at 6.3 %, somewhat below the optimal water content for compaction at 8.23 % found by Dahl. No water was added to the material, due to the risk of excess pore pressure in the cell. The material is further built in to the oedometer in five to six layers, that is compacted with a vibrating plate for 60 seconds each.

Table 5.1 shows a summary of the geotechnical properties of the tested materials:

Table 5.1 Summary of material properties

Parameter	**Symbol**		**TBM spoil**	**Crushed rock**
Water content	w	%	5.5 – 6.7	0.13 – 0.28
Dry density	ρ_d	t/m^3	1.93 – 1.96	1.72 – 1.94
Porosity	n	%	26.8 – 28.2	28.1 – 36.1
Water sensitive			Yes	No
Frost susceptible			Yes. T2*	No. T1
Oedometer modulus	M	MPa	9.04 – 9.40	27.56 – 32.20
Stress exponent	a [σ<250 kPa]		0.1 – 0.2	0.4 – 0.5
	a [σ>250 kPa]			0.8 – 0.9
Modulus number	m [σ<250 kPa]		24 – 28	127 – 170
	m [σ>250 kPa]			228 – 270

*Do not have enough capillary suction to form ice lenses.

The tests on the TBM spoil resulted in an average strain of 11.1 % (and porosity of 27.5 %) with an IL-test up to a load of 500 kPa. The mean oedometer modulus at the end of the tests was 9.2 MPa, with an achieved dry density of 2.1 t/m^3. The tested material did not reach the porosity achieved when layered and compacted on the field site, 20 – 25 %. With an average porosity of 27.5 % and a load of 50 kPa on terrain level, the oedometer results indicates that the material could reach 21 – 22 cm of settlements for a 30 metres fill.

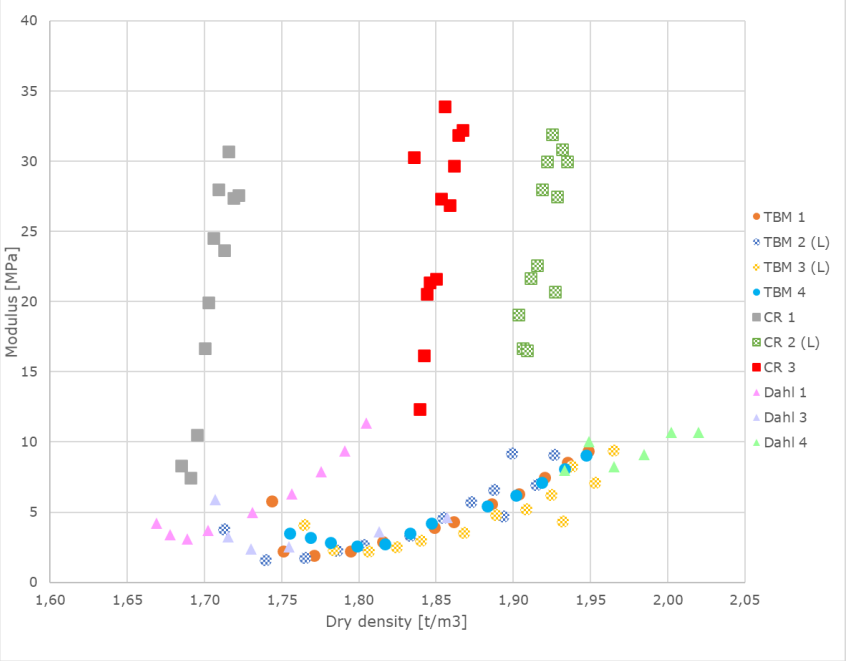

Figure 5.1 Dry density – modulus collocation of Dahl and this study

To simulate a "short-long" time simulation to investigate the creep effects in the material, two of the four TBM spoil tests and one of the crushed rock, had a load increment lasting for 70-hours. The deformation and stress were logged continuously where the material had small creep effects. The deformation stabilised after 28 – 30 hours. When compared to the crushed rock, the TBM spoil equalised quicker, and less crushing of material occurred, where the crushed rock did not equalise during the 70-hour load increment.

Based on the literature presented and the results from the laboratory investigations in this study, it is concluded that TBM spoil excavated from hard rock conditions can be utilised for establishing a good quality construction fill with success. It is demonstrated that the crushed material is stiffer than the TBM material, but the calculated level of settlements for a 30-metres filling is still low. The TBM spoil could be utilised with further processing as concrete aggregates, pea gravel, in road and railway constructions. Where the grain size distribution and the grain shape of the material could be optimised for these purposes with on-site equipment. Where utilisation of the material could ease the challenges with shortage of resources near urbanised areas, where cities like Oslo cannot comply with the local demand.

5.2 Recommendations for further work

Knowledge of the properties of the material is decisive for ensuring successful utilisation. There are several properties of the material that are still not investigated. Proposal for further investigations are listed below:

- The large scale oedometer used in this study does not have the H/D ratio according to the standard. It would be an advantage to develop an oedometer cell with an improved ratio.
- Other uncertainties which could be looked for the oedometer Anton is challenges when the TBM spoil has a water content close to the optimal.
- Degree of crushing in the contact zones in the top and bottom of the cell with wet sieving.
- Investigating the shear strength properties of the material in a large scale triaxial test or direct shear apparatus.
- Investigating the geotechnical properties of TBM spoil produced at other bedrock conditions. The rock conditions are variating from project to project, and the geotechnical properties of the TBM spoil must be regarded with consideration of local conditions.
- Further investigation of the water sensitivity and frost susceptibility for the material, like the capillarity rise in the spoil when frozen.
- Further full-scale test programs on TBM construction fills.
- Further testing of the quality of fills established under water.

Bibliography

AGJV (2020) An illustration of the TBM behind the cutterhead. Available at: https://www.banenor.no/globalassets/prosjekter/follobanen/pressebilder/orginalfiler_store/narbilde-av-tunnelboremaskinen-sett-bak-kutterhodet_-kilde-agjv.jpg (Accessed: 14.10.2020).

Aksnes, A. *et al.* (2016) *Lærebok vegteknologi*. Hamar: NPRA.

Alnæs, L. I. *et al.* (2019) *Produksjon og bruk av overskuddsmasser*. (Kortreist stein). Trondheim. Available at: https://www.sintef.no/globalassets/project/kortreist-stein/014-rapport-hovedfunn-h3-v2.0-endelig-med-vedlegg.pdf (Accessed: 12.05.2021).

Bane NOR (2020) *Vurdering av kvalitet av utført fylling ved Gjersrud - Stensrud* (The Follo Line Project UFB-31-A-70105). Oslo(Accessed: 11.12.2020).

Brown, T. H. (2015) Part 7 Geotechnical in Institute for Transportation Research and Education, N. C. S. U. and Contents (ed.) *Highway Engineering.* USA: Elsevier Inc.

Bruland, A. and Johannesen, O. (1991) *Fullprofilmasser - Materialegenskaper og anvendelser, Prosjektrapport 16-91*. Universitetet i Trondheim (Accessed: 30.10.2020).

COWI (2015) *TILTAKSPLAN FOR FORURENSET SJØBUNN I PUDDEFJORDEN, BERGEN*. Available at: https://www.miljodirektoratet.no/globalassets/tema/vann-hav-og-kyst/sjobunn---dumping-mudring-sandstrand/innhold-alle-fjorder-og-havner/bergen/tiltaksplan-puddefjorden.pdf/download (Accessed: 23.11.2020).

COWI (2020) *1-årskontroll etter tiltak mot forurenset sjøbunn i Puddefjorden*. Bergen. Available at: https://www.bergen.kommune.no/hvaskjer/tema/renere-havn-bergen/puddefjorden (Accessed: 27.05.2021).

Dahl, M. (2018) *Investigation of geotechnical properties of TBM spoil from the Follo Line Project*, NTNU. Available at: https://banenor.brage.unit.no/banenor-xmlui/handle/11250/2570668 (Accessed: 18.09.2020).

Dahlstrøm, O. *et al.* (2014) *Anbefalte retningslinjer for utarbeidelse av miljøbudsjett og miljøregnskap for tunneler*. NFF. Available at: https://nff.no/wp-content/uploads/sites/2/2020/04/Teknisk-rapport-nr-16.pdf (Accessed: 20.10.2020).

Dorador, L. and Villalobos, F. A. (2020) Analysis of the geomechanical characterization of coarse granular materials using the parallel gradation method, *Obras y Proyectos* 27, pp. 50-63. (Accessed: 30.04.2021).

Erben, H. and Galler, R. (2014) Tunnel spoil – New technologies on the way from waste to raw material, *Geomechanics and Tunnelling 7* No. 5, pp. 402-410. (Accessed: 11.05.2021).

European Commission (2017) *REPORT FROM THE COMMISSION TO THE EUROPEAN PARLIAMENT, THE COUNCIL, THE EUROPEAN ECONOMIC AND SOCIAL COMMITTEE AND THE COMMITTEE OF THE REGIONS*. Brussels. Available at: https://ec.europa.eu/environment/circular-economy/implementation_report.pdf (Accessed: 07.10.2020).

Gertsch, L. *et al.* (2000) Use of TBM Muck as Construction Material *Tunnelling and Underground Space Technology*, Vol. 15, pp. 379-402. Available at: https://doi.org/10.1016/S0886-7798(01)00007-4 (Accessed: 11.05.2021).

Glosli, C. (2020) *Nytt innovasjonssenter skal sørge for bærekraftig håndtering av jord og avfall*. Available at: https://www.nmbu.no/aktuelt/node/40577 (07.10.2020).

Hansen, L. *et al.* (1998) *Norwegian TBM Tunnelling*. Oslo: NFF.

Herrenknecht (2016) *"Magda Flåtestad" har nå satt i gang arbeidet med å drive tunnel i retning Ski*. Available at: https://www.banenor.no/Prosjekter/prosjekter/follobanen/tunnel-

ekeberg---langhus/innhold/2016/full-tbm-produksjon-pa-follobanen/ (Accessed: 11.12.2020).
ITA (2014) ITAtech Guidelines on Best Practices For Segment Backfilling, *ITAtech*, No. 4. Available at: https://about.ita-aites.org/media/k2/attachments/ITAtech/ITA-AITES-Report_4-HD.pdf (Accessed: 28.05.2021).
ITA (2019) *Handling, Treatment and Disposal of Tunnel Spoil Materials*. Available at: https://about.ita-aites.org/publications/search-for-a-publication (Accessed: 23.11.2020).
Janbu, N. (1970) *Grunnlag i geoteknikk*. Trondheim: Tapir akademiske forlag.
Kalager, A. K. and Gammelsæter, B. (2019) Did the selection of TBMs for the excavation of the Follo Line project tunnels satisfy the expectations? , *WTC*. Available at: https://www.banenor.no/globalassets/prosjekter/follobanen/stian-nett/did-the-selection-of-tbms-for-the-excavation-of-the-follo-line-tunnels-satisfy-the-expectations-1.pdf (Accessed: 29.11.2020).
Kjærnsli, B. and Sande, A. (1966) Compressibility of some Coarse-Grained Materials, *Proceedings of European Conference on soil mehanics and foundation engineering*, Vol. I, pp. 245-251. (Accessed: 16.05.2021).
Kjærnsli, B. (1968) Publication nr. 73, in NGI (ed.) *Fundamentering på grus- og steinfyllinger.* Oslo: NGI.
Kjærnsli, B., Valstad, T. and Höeg, K. (1992) *Rockfill dams* Trondheim: Tapir.
Langford, J. *et al.* (2020) TBM-KAKS – KARAKTERISERING OG POTENSIALE FOR NYTTIGGJØRING, PÅ LAND OG I SJØ, *FJELLSPRENGNINGSTEKNIKK BERGMEKANIKK/ GEOTEKNIKK 2020*, pp. 6.1-6.21. (Accessed: 11.02.2021).
Leps, T. M. (1970) Review of shearing strength of rock ll in Journal of soil mechanics and foundation Vol.96, *ASCE*. (Accessed: 28.11.2020).
Macias, J. and Bruland, A. (2014) D&B versus TBM: Review of the parameters for a right choice of the excavation method. Available at: https://www.researchgate.net/publication/264942493_DB_versus_TBM_Review_of_the_parameters_for_a_right_choice_of_the_excavation_method (Accessed: 19.10.2020).
Maidl, B. *et al.* (2008) *Hardrock tunnel boring machine*. Berlin: Ernst & Sohn.
Mathiesen, S. (2020) Fjellandet Norge kan gå tom for god sand og grus *Teknisk Ukeblad*. TU.no. Available at: https://www.tu.no/artikler/fjellandet-norge-kan-ga-tom-for-god-sand-og-grus/495664 (Accessed: 28.05.2021).
Miljødirektoratet (2018) Problemer med plast ved utfylling av sprengstein i sjø. Available at: https://www.miljodirektoratet.no/Documents/publikasjoner/M1085/M1085.pdf (Accessed: 11.11.2020).
Motzfeldt, E. (1975) *Bæreevnen av fundamenter på sand bestemt ved modellforøk i kjempeødometer*, NTNU. (Accessed: 20.04.2021).
NFF (2009) *Behandling og utslipp av driftsvann fra tunnelanlegg*. (Teknisk rapport 09). Available at: https://nff.no/wp-content/uploads/sites/2/2020/04/Teknisk-rapport-nr-9.pdf (Accessed: 12.05.2021).
NFF (2021) *Tunnelstatistikken*. Available at: https://nff.no/publikasjoner/tall-og-statistikk/ (Accessed: 28.05.2021).
NGF (2019) *Peleveiledningen*. Oslo: NGF.
NGI (1986) *Prosjekt fullprofilmasser materialegenskaper*. Oslo(Accessed: 13.11.2020).
NGI (2019a) WP 2.6: Vurdering av nyttiggjøring av TBM-kaks. Available at: https://www.ngi.no/download/file/15522 (Accessed: 04.11.2020).
NGI (2019b) *WP 2.6: Vurdering av TBM-kaks*. (GEOreCIRC). Available at: https://www.ngi.no/download/file/15522 (Accessed: 10.05.2021).
NGI (2020) *Vurdering av sedimentasjon av TBM-kaks ved utfylling i sjø. Laboratorie- og modellforsøk*. (Accessed: 04.05.2021).

NGU (1985) *Grusdatabasen*. Available at: http://geo.ngu.no/kart/grus_pukk_mobil/ (Accessed: 21.04.21).

Nielsen, K., Hansen, S. E. and Myrvang, A. (1994) Kostnadseffektiv og miljøvennlig pukkproduksjon under jord, *Fjellsprengningkonferansen*, 1994, pp. 122-137. Available at: https://nff.no/wp-content/uploads/sites/2/2020/04/Fjellsprengningsdagen-1994.pdf (Accessed: 14.05.2021).

Nilsen, B. and Tidemann, A. (1993) *Rock Engineering*. Trondheim: Tapir.

NPRA (2010) *Geoteknikk i vegbygging*. Vegdirektoratet. Available at: https://www.vegvesen.no/_attachment/70057/binary/1305835?fast_title=H%C3%A5ndbok+V220+Geoteknikk+i+vegbygging+%2818+MB%29.pdf (Accessed: 15.04.2021).

NPRA (2014) *R210 Laboratorieundersøkelser*. Statens Vegvesen. Available at: https://www.vegvesen.no/_attachment/185231/binary/1276518?fast_title=H%C3%A5ndbok+R210+Laboratorieunders%C3%B8kelser+%2811+MB%29.pdf (Accessed: 13.11.2020).

NRPA (2015) *Bergarters potensielle effekter på vannmiljøet ved anleggsvirksomhet*. Hamar. Available at: https://vegvesen.brage.unit.no/vegvesen-xmlui/bitstream/handle/11250/2659778/Rapport%20389%20Bergarters%20potensielle%20effekter%20p%c3%a5%20vannmilj%c3%b8et%20ved%20anleggsvirksomhet.pdf?sequence=1&isAllowed=y (Accessed: 13.05.2021).

NRPA (2018) *Håndbok N200*. Statens Vegvesen. Available at: https://www.vegvesen.no/_attachment/2364236/binary/1269980?fast_title=H%C3%A5ndbok+N200+Vegbygging+%2810+MB%29.pdf (Accessed: 27.05.2021).

NRPA (2019) *Pyrrhotite in concrete aggregates*. (Impact on concrete durability). Available at: https://vegvesen.brage.unit.no/vegvesen-xmlui/bitstream/handle/11250/2626353/Magnetkis%20komplett%20SVV%20rapport%20463%2017MB_.pdf?sequence=4&isAllowed=y (Accessed: 27.05.2021).

Ofstad, C. S. *et al.* (2018) GEOreCIRC - utilization of TBM spoil. Available at: https://www.ngi.no/download/file/13111 (Accessed: 21.10.2020).

Ouchterlony, F. *et al.* (2006) Constructing the fragment size distribution of a bench blasting round, using the new Swebrec function, *Fraglast* No. 8, pp. 332-344. (Accessed: 14.05.2021).

PEAB (2018) *Sanering av forurenset sjøbunn. Sluttrapport.* . (Renere Puddefjord). Available at: https://www.bergen.kommune.no/publisering/api/filer/T541922111 (Accessed: 28.11.2020).

railsystem.net (2015) Drill and Blast Method. Available at: http://www.railsystem.net/drill-and-blast-method/ (Accessed: 14.10.2020).

Robbins (2014) *Tunnel Segment Backfilling with Double Shield TBMs*. Available at: http://www.robbinstbm.com/wp-content/uploads/2014/01/Tunnel-Segment-Backfilling-DS-TBMs_View-Only.pdf (Accessed: 28.05.2021).

Robertson, J. *et al.* (1984) Paticle size analysis of soils - A comparson of dry and wet sieving, *Forensic Science International*, 24(Elsevier Scientific Publisher Ireland LTD.), pp. 209. doi: 0379-0738/84/$03.00.

Sandven, R. *et al.* (2017) *Geotechnics Field and Laboratory Investigations*. NTNU. (Accessed: 29.04.2021).

Slunga, E. and Saarelainen, S. (2006) *Determination of frost-susceptibility of soils* Available at: https://www.issmge.org/uploads/publications/1/22/STAL9781614996569-3577.pdf (Accessed: 24.11.2020).

Standard Norge (2002) NS-EN 13450:2002+NA:2009 Aggregates for railway ballast: European Committee for Standardization, . (Accessed: 10.05.2021).

Standard Norge (2012) *NS-EN 933-1:2012 Tests for geometrical properties of aggregates Part 1: Determination of particle size distribution Sieving method*

Available at: https://www.standard.no/nettbutikk/sokeresultater/?search=NS-EN+933-1 (Accessed: 07.04.2021).

Standard Norge (2017) *NS-EN ISO 17892-5:2017 Geotechnical investigation and testing*. Available at: https://www.standard.no/nettbutikk/sokeresultater/?search=NS-EN+ISO+17892-5%3a2017+Geotechnical+investigation+and+testing (Accessed: 23.02.2021).

Syversen, I. L. G. (2020) Geotechnical properties of TBM spoil (pp. 50). (Accessed: 19.12.2020).

The Royal Norwegian Council for Scientific and Industrial Research and The Public Roads Administration's Committee (1973) *Frost i jord*. (Sikring mot teleskade)(Accessed: 14.05.2021).

Voit, K. and Kuschel, E. (2020) Rock Material Recycling in Tunnel Engineering, *Applied sciences*, No. 10. Available at: https://www.mdpi.com/2076-3417/10/8/2722/pdf (Accessed: 28.05.2021).

Appendix

Appendix A: Results from laboratory investigations

A.1 Specialisation project

The oedometer tests for the specialisation project was accomplished in November 2020, the intention of these tests was to prepare the equipment and to test the method as a preparation for this master thesis. Two tests were accomplished, where the first test failed due to that the plate in the oedometer got jammed in the duct tape and the plastic sheet. For the second test the plastic sheet was cut down to the height of the material, but then an error with the equipment caused that the air leaked out of the cell between the plastic sheet and the walls in the oedometer. The error occurred at 244 kPa, and the test was stopped. As a consequence, the lid of the oedometer was removed and an extra layer of material was added. The material was preloaded with 244 kPa at the beginning of the second trial.

The TBM spoil utilised for these tests were not sieved to a grading curve optimised for Anton, meaning that the material contained particles larger than 31.5 mm, the sieving curve for this material is shown in Figure 3.12 as the complete sieving analysis. The spoil was stored in a large barrel for three years, and the material was splitted. The material from the test shown in Figure 0.2, was from the top of the barrel, and had a large amount of coarser material. The matter of fact that the material is preloaded and consists of a coarser sort, result in a stiff material with little strain.

The built-in sample contains of six compacted layers where layer five and six contains 15 kg. The test is mostly following the method described in Chapter 3.1.1, with some exceptions. The load steps in this test lasts for 30 minutes and the weight of the test is considerably lower than the tests in this thesis with 150 kg. The test result for this test has a considerably lower strain value than the tests carried out on split and sieved spoil. The coarse and preloaded TBM spoil are closer in strain values to the crushed rock than the sieved and split TBM spoil.

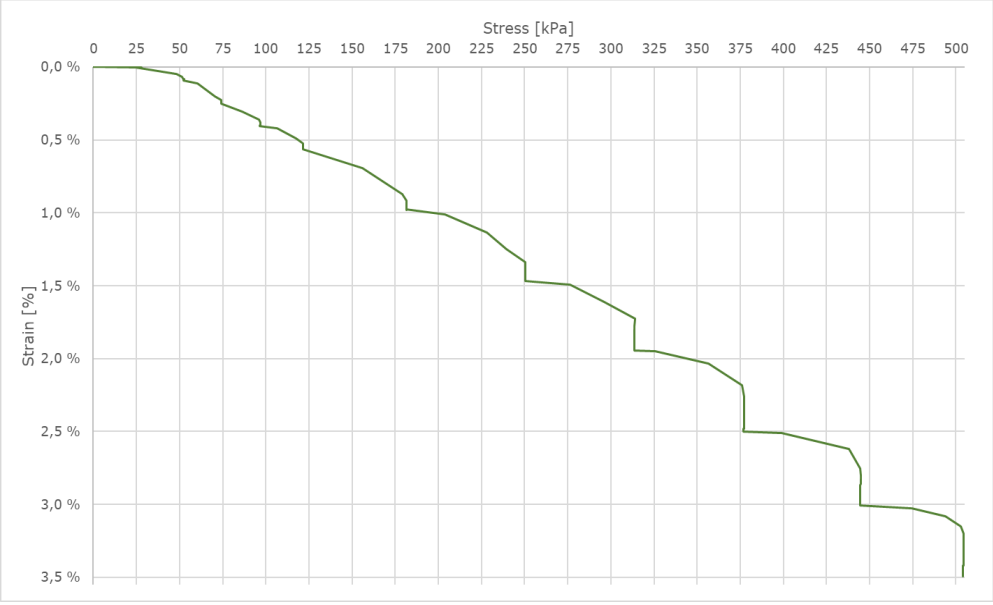

Figure 0.1 Stress and strain curve for oedometer test 2020

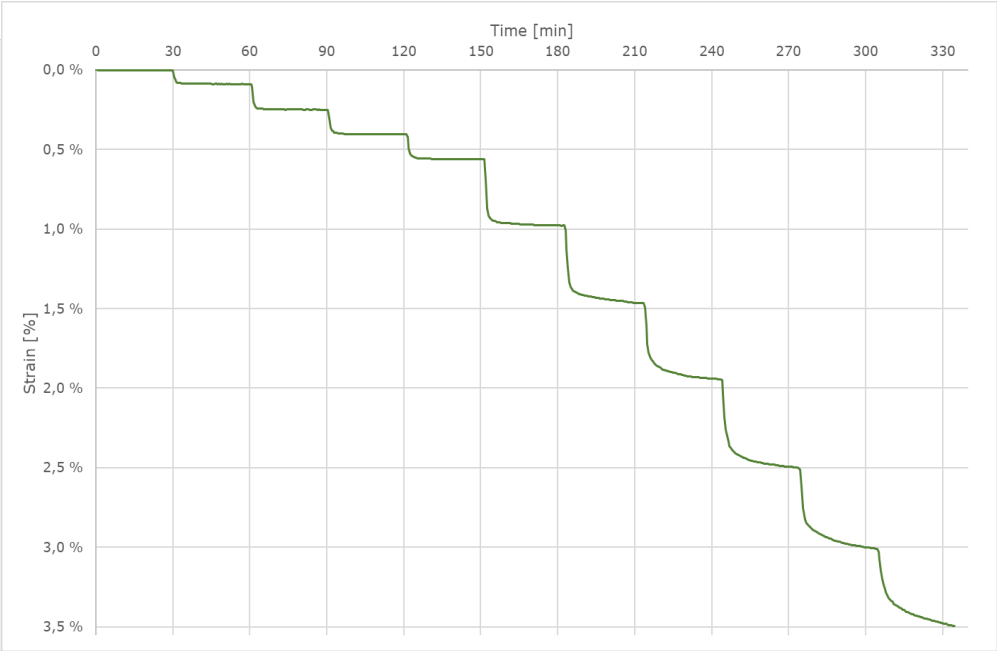

Figure 0.2 Stress and time curve for oedometer test 2020

Figure 0.3 shows the strain values at the end of the 13 load steps for the oedometer test carried out in the specialisation project and in this master thesis. From this figure it is clearer that the material behaves more like the crushed rock when the strain values are considered. The test from 2020 has lower strain values than test 1 and 3 with blasted rock

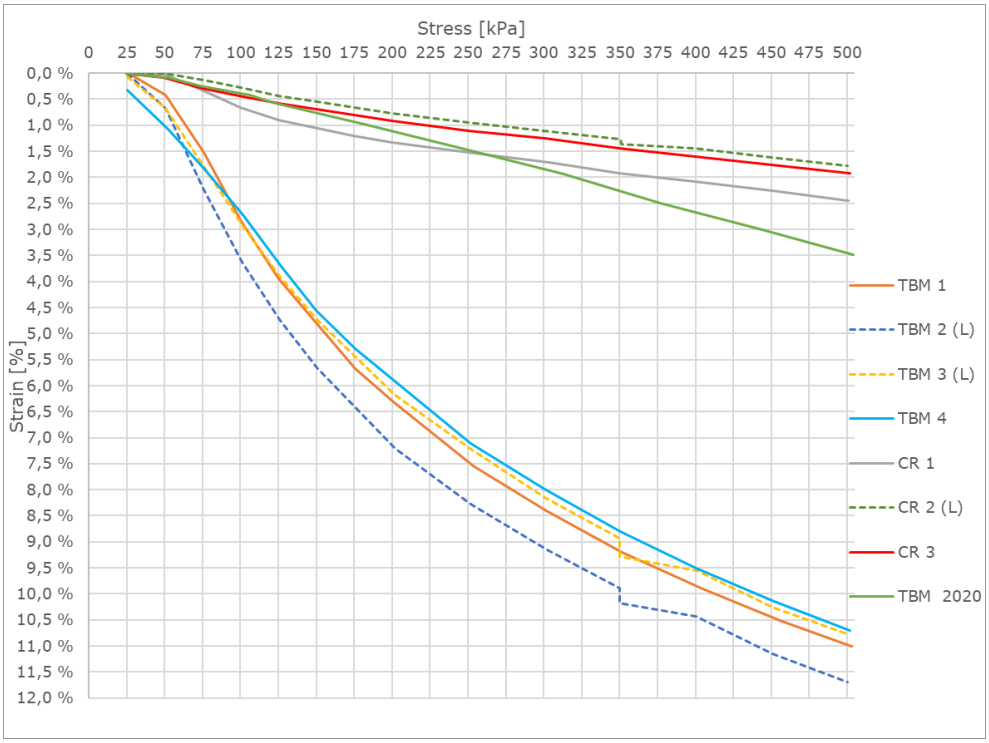

Figure 0.3 Collocation of stress and strain curves for the 2020 and 2021 tests

until the value of the preload. When considering the oedometer modulus in Figure 0.4 the 2020 test has lower oedometer modulus than the crushed rock but has more similar values to the TBM spoil.

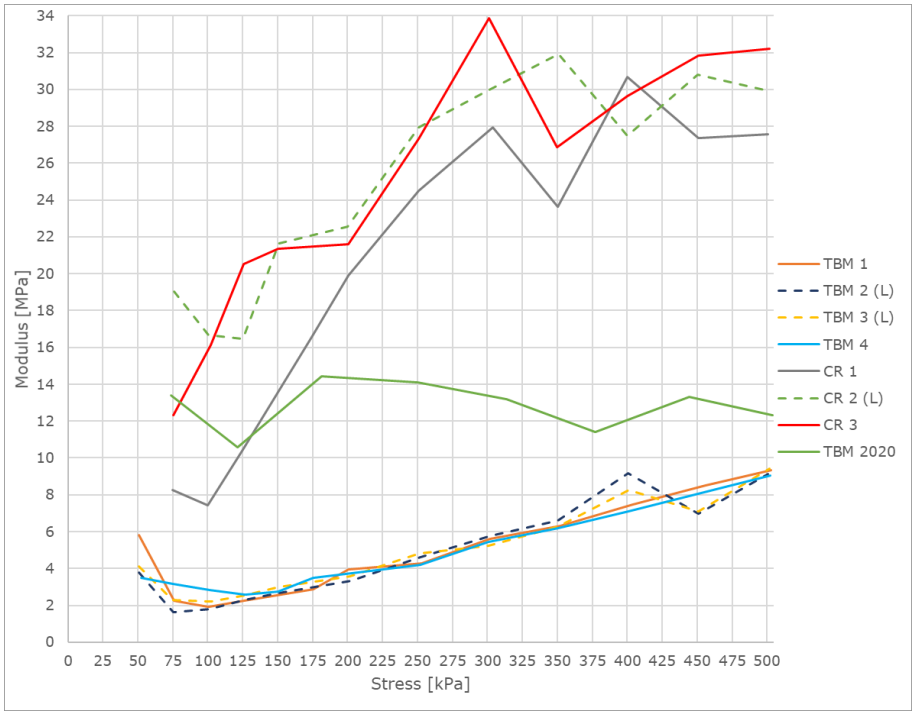

Figure 0.4 Collocation of stress and modulus curves for the 2020 and 2021 tests

Figure 0.5 indicates that the 2020 spoil has a modulus and a dry density similar to CR 3. Most likely caused by the preload, the thin layers on top and the coarse material. Since this test is meant as a preliminary test for the master thesis, and has incongruous method and material, the results will not be included in the discussion of material properties.

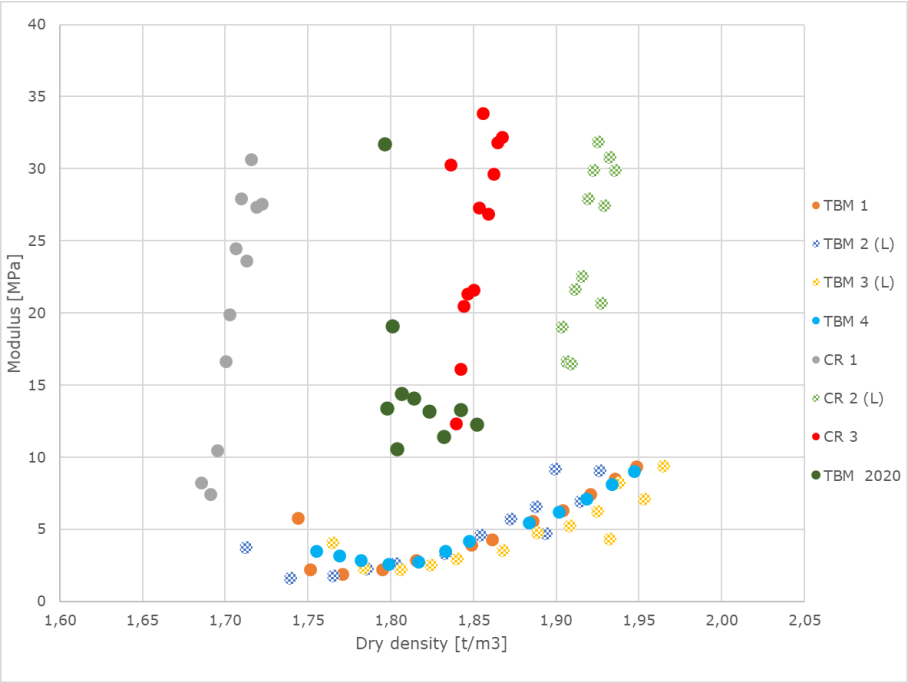

Figure 0.5 Collocation of dry density and modulus curves for the 2020 and 2021 tests

A.2 Collocation of tests

Table 0.2 Stress and time of load increment for TBM spoil

	TBM 1		TBM 2		TBM 3		TBM 4	
	Stress	Load increment	Stress	Load increment	Stress	Load increment	Stress	Load increment
	[kPa]	[min]	[kPa]	[min]	[kPa]	[min]	[kPa]	[min]
1	26.7	16.4	25.4	20.5	25.7	30.3	25.7	14.4
2	51.0	16.2	50.6	20.4	50.7	30.3	52.3	14.9
3	75.7	15.8	75.6	20.5	75.1	30.5	75.4	15.0
4	100.7	21.2	100.9	20.6	102.2	31.2	101.5	14.8
5	125.5	20.6	126.0	20.6	126.5	30.1	127.0	30.2
6	175.6	21.7	150.3	21.2	151.0	31.4	150.1	30.0
7	200.7	18.9	202.3	21.2	201.7	30.3	175.6	30.2
8	253.3	21.4	251.8	21.1	251.5	29.9	251.8	29.9
9	301.7	21.5	302.4	20.3	300.5	30.6	300.5	30.5
10	351.7	20.8	350.3	21.4	350.2	30.0	350.6	29.6
			350.3	4248.6	350.2	4216.5		
11	403.8	21.5	400.7	30.4	401.2	29.9	400.4	29.9
12	455.7	22.3	451.0	30.9	450.9	30.2	452.3	30.2
13	503.1	18.5	500.6	30.4	501.5	32.0	502.1	31.5

Table 0.1 Stress and strain results for TBM spoil

	TBM 1		TBM 2		TBM 3		TBM 4	
	Stress	Strain	Stress	Strain	Stress	Strain	Stress	Strain
	[kPa]	[%]	[kPa]	[%]	[kPa]	[%]	[kPa]	[%]
1	26.7	0.00 %	25.4	0.01 %	25.7	0.07 %	25.7	0.32 %
2	51.0	0.42 %	50.6	0.67 %	50.7	0.68 %	52.3	1.08 %
3	75.7	1.52 %	75.6	2.21 %	75.1	1.74 %	75.4	1.81 %
4	100.7	2.84 %	100.9	3.64 %	102.2	2.97 %	101.5	2.72 %
5	125.5	3.94 %	126.0	4.74 %	126.5	3.92 %	127.0	3.71 %
6	175.6	5.68 %	150.3	5.65 %	151.0	4.74 %	150.1	4.55 %
7	200.7	6.32 %	202.3	7.21 %	201.7	6.17 %	175.6	5.28 %
8	253.3	7.54 %	251.8	8.28 %	251.5	7.21 %	251.8	7.10 %
9	301.7	8.41 %	302.4	9.16 %	300.5	8.15 %	300.5	8.00 %
10	351.7	9.20 %	350.3	9.88 %	350.2	8.94 %	350.6	8.80 %
			350.3	10.17 %	350.2	9.29 %		
11	403.8	9.90 %	400.7	10.43 %	401.2	9.55 %	400.4	9.51 %
12	455.7	10.51 %	451.0	11.16 %	450.9	10.25 %	452.3	10.15 %
13	503.1	11.01 %	500.6	11.70 %	501.5	10.79 %	502.1	10.70 %

Table 0.4 Stress and load increment time for crushed rock

	CR 1		CR 2		CR 3	
	Stress	Load increment	Stress	Load increment	Stress	Load increment
	[kPa]	[min]	[kPa]	[min]	[kPa]	[min]
1	25.3	12.5	25.9	20.2	24.9	15.1
2	50.4	16.7	50.9	20.5	49.9	15.2
3	74.8	15.9	75.9	20.5	75.3	14.9
4	99.9	16.1	100.4	21.0	102.2	15.0
5	125.1	16.4	125.4	21.0	125.7	15.2
6	174.8	17.7	151.1	19.1	150.3	30.6
7	200.6	15.4	200.2	20.0	200.3	29.9
8	250.6	17.0	251.0	20.0	250.7	30.0
9	303.9	16.9	300.3	20.0	301.1	30.0
10	350.1	17.3	350.8	20.2	349.8	30.1
			351.0	4216.4		
11	399.8	17.3	400.2	30.2	400.3	30.1
12	450.9	16.7	450.3	30.7	450.9	29.9
13	500.7	16.6	500.5	29.4	501.9	30.4

Table 0.3 Stress and strain results for crushed rock

	CR 1		CR 2		CR 3	
	Stress	Strain	Stress	Strain	Stress	Strain
	[kPa]	[%]	[kPa]	[%]	[kPa]	[%]
1	25.3	0.01 %	25.9	0.00 %	24.9	0.00 %
2	50.4	0.02 %	50.9	0.00 %	49.9	0.09 %
3	74.8	0.32 %	75.9	0.13 %	75.3	0.29 %
4	99.9	0.66 %	100.4	0.28 %	102.2	0.46 %
5	125.1	0.90 %	125.4	0.43 %	125.7	0.57 %
6	174.8	1.20 %	151.1	0.55 %	150.3	0.69 %
7	200.6	1.33 %	200.2	0.77 %	200.3	0.92 %
8	250.6	1.53 %	251.0	0.95 %	250.7	1.11 %
9	303.9	1.72 %	300.3	1.11 %	301.1	1.25 %
10	350.1	1.92 %	350.8	1.27 %	349.8	1.44 %
			351.0	1.36 %		
11	399.8	2.08 %	400.2	1.45 %	400.3	1.61 %
12	450.9	2.26 %	450.3	1.61 %	450.9	1.76 %
13	500.7	2.45 %	500.5	1.78 %	501.9	1.92 %

Table 0.6 Detailed weight of each layer [kg]

	TBM 1	TBM 2	TBM 3	TBM 4	CR 1	CR 2	CR 3
Layer 1	16.6	17.2	19.2	17.1	17.3	16.0	16.0
	16.4	16.0	18.8	17.1	17.5	16.0	17.0
Layer 2	17.7	17.8	19.7	18.0	17.5	16.0	16.0
	17.5	18.1	19.4	18.6	17.0	16.0	16.0
Layer 3	15.6	17.6	18.9	17.3	17.5	16.0	16.0
	16.6	18.4	20	16.6	17.0	16.0	16.0
Layer 4	17.1	17.9	20.05	18.4	17.7	16.0	17.0
	16.5	17.5	19.2	17.8	17.0	16.0	16.0
Layer 5	16.0	18.4	19.1	18.0	17.0	16.0	16.0
	16.5	17.4	20.6	17.8	-	16.0	16.0
Layer 6	17.0	13.2		17.4	-	16.0	16.0
	-	-	-	-	-	10	8.8

Table 0.5 Weight of each layer for the tests [kg]

	TBM 1	TBM 2	TBM 3	TBM 4	CR 1	CR 2	CR 3
Layer 1	33	33.2	38	34.2	34.8	32	33
Layer 2	35.2	35.9	39.1	36.6	34.5	32	32
Layer 3	32.2	36	38.9	33.9	34.5	32	32
Layer 4	33.6	35.4	39.25	36.2	34.7	32	33
Layer 5	32.5	35.8	39.7	35.8	17	32	32
Layer 6	17	13.2	0	17.4	0	26	24.8
Sand layers	8	8	-	8	8	8.6	8.2
Weight buckets	4.76	4.32	4.17	4.75	-	-	-
Total weight of test	186.74	193.18	190.78	197.35	163.5	194.6	195

A.3 TBM spoil

Table 0.8 Test values for test 1 (TBM spoil)

Load step	Time	Load increment	Stress	Deformation	Strain
	[min]	[min]	[kPa]	[mm]	[%]
1	16	16	26.7	0.0	0.00 %
2	33	16	51.0	2.1	0.42 %
3	48	16	75.7	7.8	1.52 %
4	70	21	100.7	14.5	2.84 %
5	90	21	125.5	20.2	3.94 %
6	112	22	175.6	29.1	5.68 %
7	131	19	200.7	32.3	6.32 %
8	152	21	253.3	38.6	7.54 %
9	174	21	301.7	43.1	8.41 %
10	195	21	351.7	47.1	9.20 %
11	216	21	403.8	50.7	9.90 %
12	238	22	455.7	53.8	10.51 %
13	257	18	503.1	56.4	11.01 %

Table 0.7 Test values for test 2 (TBM spoil)

Load step	Time	Load increment	Stress	Deformation	Strain
	[min]	[min]	[kPa]	[mm]	[%]
1	20.5	20.5	25.4	0.0	0.01 %
2	40.9	20.4	50.6	3.7	0.67 %
3	61.4	20.5	75.6	12.0	2.21 %
4	82.0	20.6	100.9	19.7	3.64 %
5	102.6	20.6	126.0	25.7	4.74 %
6	123.8	21.2	150.3	30.6	5.65 %
7	145.0	21.2	202.3	39.1	7.21 %
8	166.0	21.1	251.8	44.9	8.28 %
9	186.3	20.3	302.4	49.6	9.16 %
10	207.7	21.4	350.6	53.6	9.88 %
	4456.4	70.8 hours	350.3	55.1	10.17 %
11	4486.8	30.4	400.7	56.5	10.43 %
12	4517.7	30.9	451.0	60.5	11.16 %
13	4548.1	30.4	500.6	63.4	11.70 %

Table 0.10 Test values for test 3 (TBM spoil)

Load step	Time	Load increment	Stress	Deformation	Strain
	[min]	[min]	[kPa]	[mm]	[%]
1	30.3	30.3	25.7	0.4	0.07 %
2	60.7	30.3	50.7	3.6	0.68 %
3	91.2	30.5	75.8	9.1	1.74 %
4	122.4	31.2	102.2	15.6	2.97 %
5	152.6	30.1	126.5	20.6	3.92 %
6	184.0	31.4	151.0	25.0	4.74 %
7	214.2	30.3	201.7	32.5	6.17 %
8	244.2	29.9	251.5	37.9	7.21 %
9	274.8	30.6	300.5	42.8	8.15 %
10	304.8	30.0	351.6	47.0	8.93 %
	4521.3	70.3 hours	350.2	48.9	9.29 %
11	4551.1	29.9	401.2	50.2	9.55 %
12	4581.3	30.2	450.9	53.9	10.25 %
13	4613.3	32.0	501.5	56.8	10.79 %

Table 0.9 Test values for test 4 (TBM spoil)

Load step	Time	Load increment	Stress	Deformation	Strain
	[min]	[min]	[kPa]	[mm]	[%]
1	14	14.4	25.7	1.7	0.32 %
2	29	14.9	52.3	5.8	1.08 %
3	44	15.0	75.4	9.8	1.81 %
4	59	14.8	101.5	14.7	2.72 %
5	89	30.2	127.0	20.0	3.71 %
6	119	30.0	150.1	24.6	4.55 %
7	149	30.2	175.6	28.5	5.28 %
8	179	29.9	251.8	38.4	7.10 %
9	210	30.5	300.5	43.2	8.00 %
10	239	29.6	350.6	47.5	8.80 %
11	269	29.9	400.4	51.3	9.51 %
12	299	30.2	452.3	54.8	10.15 %
13	331	31.5	502.1	57.8	10.70 %

A.4 Crushed rock

Table 0.11 Test values for test 1 (Crushed rock)

Load step	Time	Load increment	Stress	Deformation	Strain
	[min]	[min]	[kPa]	[mm]	[%]
1	12.5	12.5	25.3	0.05	0.01 %
2	29.1	16.7	50.4	0.11	0.02 %
3	45.1	15.9	74.8	1.58	0.32 %
4	61.1	16.1	99.9	3.26	0.66 %
5	77.5	16.4	125.1	4.46	0.90 %
6	95.2	17.7	174.8	5.94	1.20 %
7	110.6	15.4	200.6	6.59	1.33 %
8	127.6	17.0	250.6	7.60	1.53 %
9	144.5	16.9	303.9	8.55	1.72 %
10	161.8	17.3	350.1	9.52	1.92 %
11	179.1	17.3	399.8	10.33	2.08 %
12	195.8	16.7	450.9	11.26	2.26 %
13	212.5	16.6	500.7	12.15	2.45 %

Table 0.12 Test values for test 2 (Crushed rock)

Load step	Time	Load increment	Stress	Deformation	Strain
	[min]	[min]	[kPa]	[mm]	[%]
1	20.2	20.2	25.9	-0.01	0.00 %
2	40.7	20.5	50.9	-0.01	0.00 %
3	61.2	20.5	75.8	0.68	0.13 %
4	82.2	21.0	100.4	1.45	0.28 %
5	103.2	21.0	125.4	2.24	0.43 %
6	122.3	19.1	151.1	2.86	0.55 %
7	142.3	20.0	200.2	3.99	0.77 %
8	162.3	20.0	250.9	4.94	0.95 %
9	182.2	20.0	300.3	5.80	1.11 %
10	202.4	20.2	350.8	6.63	1.27 %
	4418.7	70.3 hours	351.0	7.08	1.36 %
11	4448.9	30.2	400.2	7.56	1.45 %
12	4479.6	30.7	450.3	8.41	1.61 %
13	4509.1	29.4	500.5	9.29	1.78 %

Table 0.13 Test values for test 3 (Crushed rock)

Load step	Time	Load increment	Stress	Deformation	Strain
	[min]	[min]	[kPa]	[mm]	[%]
1	15.05	15.1	24.9	0.02	0.00 %
2	30.2	15.2	49.9	0.43	0.08 %
3	45.1	14.9	75.3	1.45	0.27 %
4	60.1	15.0	102.2	2.28	0.42 %
5	75.25	15.2	125.7	2.85	0.53 %
6	105.8	30.6	150.3	3.43	0.63 %
7	135.65	29.9	200.3	4.58	0.84 %
8	165.65	30.0	250.7	5.49	1.01 %
9	195.65	30.0	301.1	6.23	1.15 %
10	225.7	30.1	349.8	7.13	1.32 %
11	255.75	30.1	400.3	7.98	1.47 %
12	285.65	29.9	450.9	8.77	1.62 %
13	316.05	30.4	501.9	9.56	1.76 %

Appendix B: Pictures from the laboratory investigations

B.1 TBM spoil, test 1

Figure 0.9 TBM 1, Sand layer

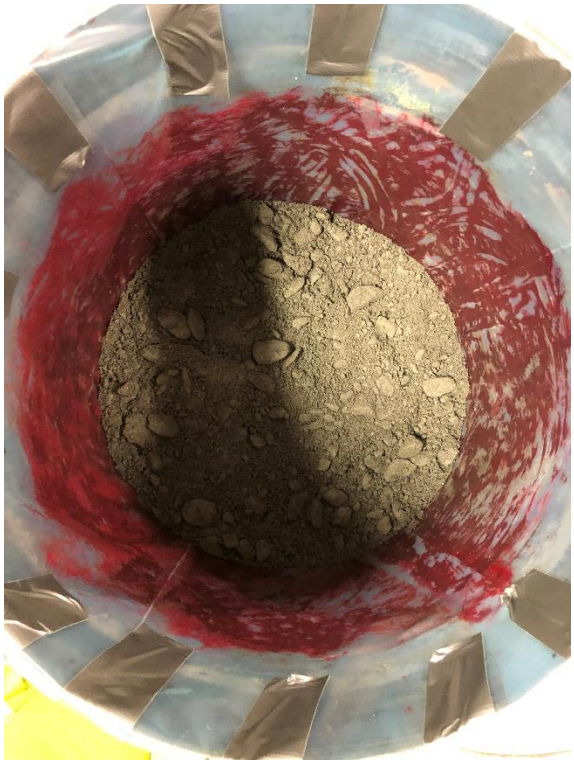

Figure 0.6 TBM 1, First layer, not compacted

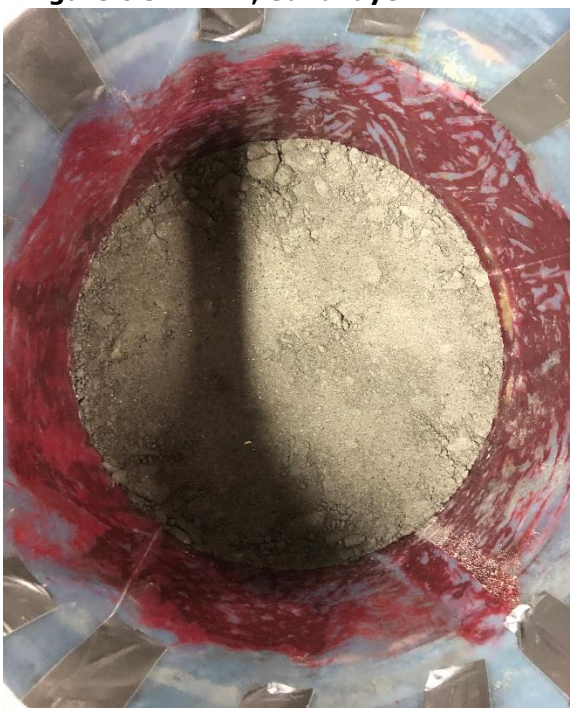

Figure 0.7 TBM 1, second layer, compacted

Figure 0.8 TBM 1, third layer, compacted

Figure 0.12 TBM 1, fourth layer, compacted

Figure 0.11 TBM 1, fifth layer, compacted

Figure 0.10 TBM 1, upper sand layer

B.2 TBM spoil, test 2

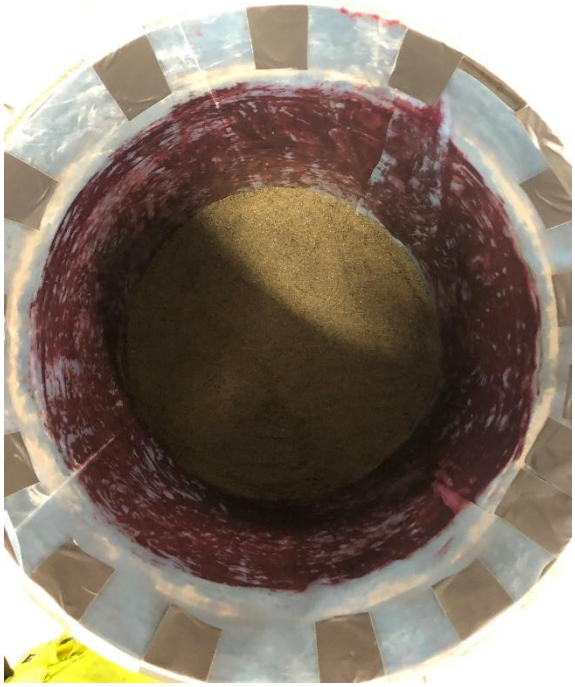

Figure 0.16 TBM 2, lower sand layer

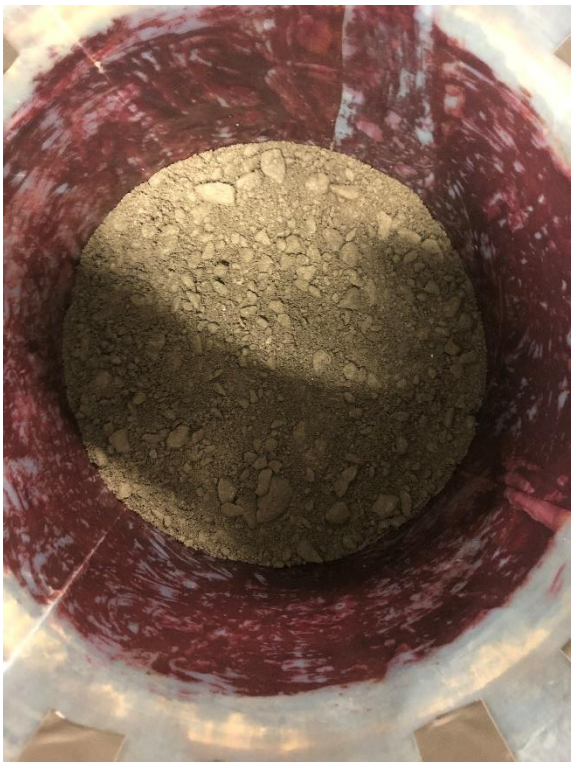

Figure 0.14 TBM 2, first layer, not compacted

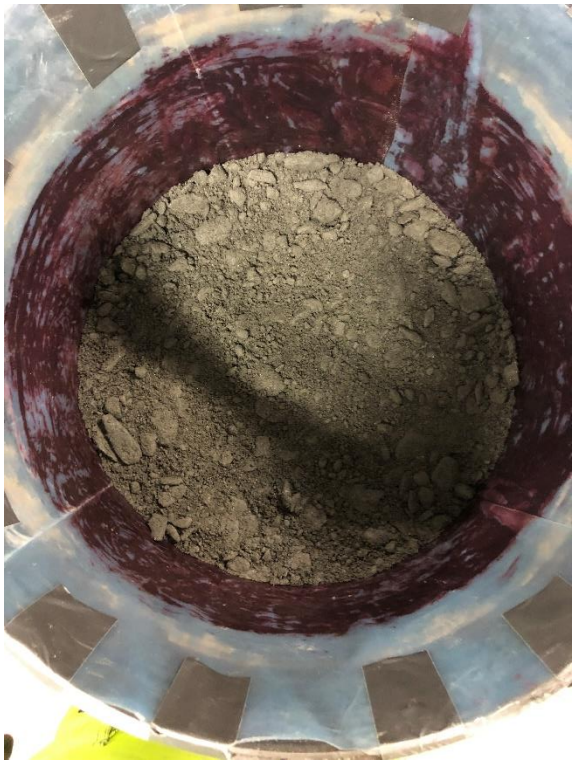

Figure 0.15 TBM 2, second layer, not compacted

Figure 0.13 TBM 2, third layer, not compacted

Figure 0.20 TBM 2, fourth layer, not compacted

Figure 0.19 TBM 2, fifth layer, not compacted

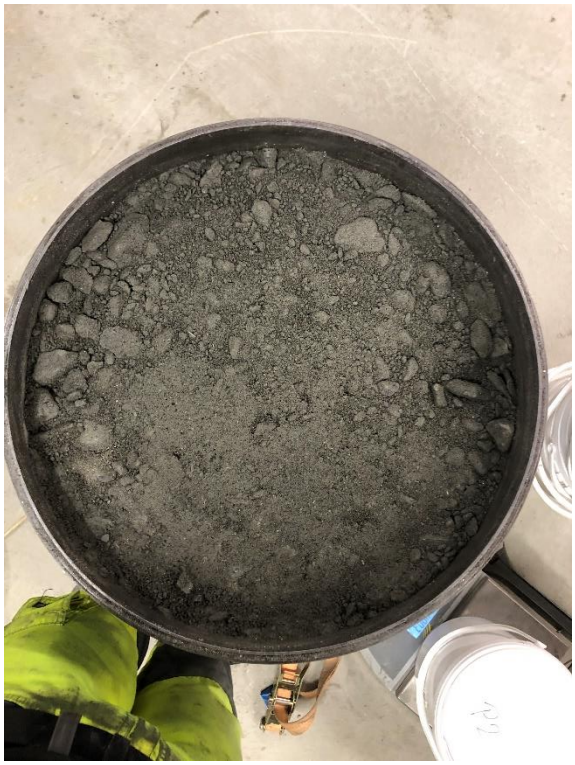

Figure 0.18 TBM 2, sixth layer, compacted

Figure 0.17 TBM 2, upper sand layer

B.3 TBM spoil, test 3

Figure 0.24 TBM 3, first layer, not compacted

Figure 0.23 TBM 3, second layer, not compacted

Figure 0.22 TBM 3, third layer, not compacted

Figure 0.21 TBM 3, fourth layer, not compacted

Figure 0.25 TBM 3, fifth layer, not compacted

Figure 0.29 TBM 3, sieving analysis, 22.4 mm

Figure 0.28 TBM 3, sieving analysis, 19 mm

Figure 0.27 TBM 3, sieving analysis, 16 mm

Figure 0.26 TBM 3, sieving analysis, 11.2 mm

Figure 0.32 TBM 3, sieving analysis, 8 mm

Figure 0.33 TBM 3, sieving analysis, 4 mm

Figure 0.30 TBM 3, sieving analysis, 2 mm

Figure 0.31 TBM 3, sieving analysis, 1 mm

Figure 0.37 TBM 3, sieving analysis, 0.5 mm

Figure 0.36 TBM 3, sieving analysis, 0.25 mm

Figure 0.35 TBM 3, sieving analysis, 0.125 mm

Figure 0.34 TBM 3, sieving analysis, 63 µm

Figure 0.38 TBM 3, sieving analysis, <63 µm

B.4 TBM spoil, test 4

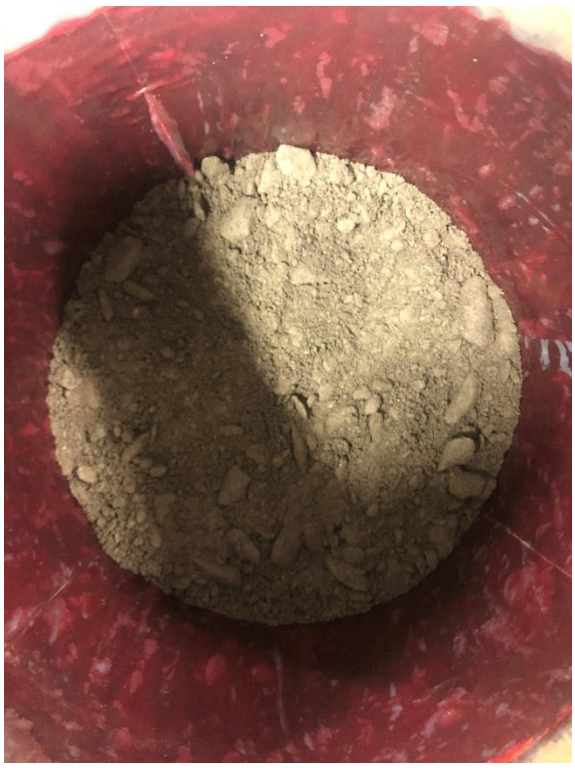

Figure 0.39 TBM 4, first layer, not compacted

Figure 0.40 TBM 4, second layer, not compacted

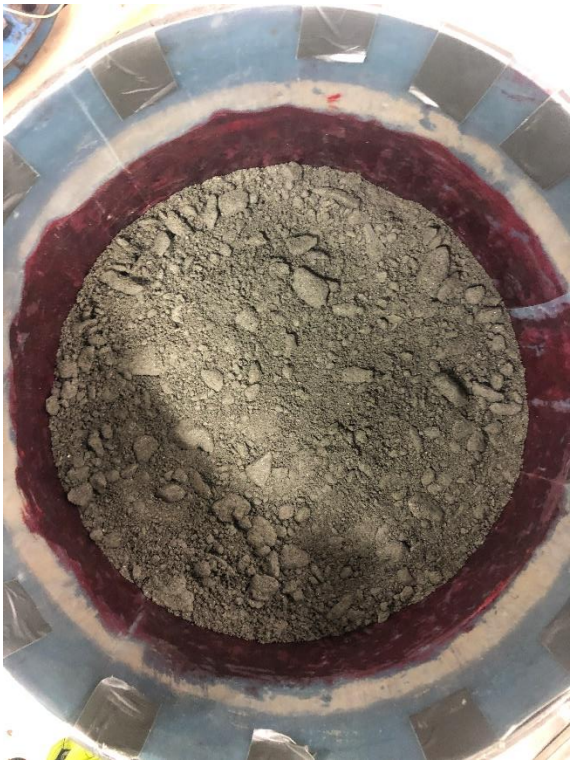

Figure 0.42 TBM 4, third layer, not compacted

Figure 0.41 TBM 4, fourth layer, not compacted

Figure 0.45 TBM 4, fifth layer, compacted

Figure 0.43 TBM 4, sixth layer, compacted

Figure 0.44 TBM 4, upper sand layer

B.5 Crushed rock, test 1

Figure 0.49 CR 1, first layer, compacted

Figure 0.46 CR 1, second layer, compacted

Figure 0.48 CR 1, third layer, compacted

Figure 0.47 CR 1, fourth layer, compacted

Figure 0.51 CR 1, fifth layer, compacted

Figure 0.50 CR 1, upper sand layer

B.6 Crushed rock, test 2

Figure 0.55 CR 2, first layer, compacted

Figure 0.54 CR 2, second layer, not compacted

Figure 0.52 CR 2, third layer, compacted

Figure 0.53 CR 2, fourth layer, compacted

Figure 0.58 CR 2, fifth layer, compacted

Figure 0.57 CR 2, sixth layer, compacted

Figure 0.56 CR 2, upper sand layer after test

B.7 Crushed rock, test 3

Figure 0.62 CR 3, first layer, compacted

Figure 0.61 CR 3, second layer, compacted

Figure 0.60 CR 3, third layer, compacted

Figure 0.59 CR 3, fourth layer, not compacted

Figure 0.65 CR 3, fifth layer, compacted

Figure 0.64 CR 3, sixth layer, compacted

Figure 0.63 CR 3, upper sand layer

Isolde Louise Grønlund Syversen

Deformation properties of hard rock TBM spoil

NTNU
Norwegian University of
Science and Technology